

AN EXPERIMENTAL STUDY OF MECHANICAL PROPERTIES OF
NON ENZYMATICALLY GLYCATED BOVINE FEMUR CORTICAL BONE

A THESIS SUBMITTED TO
THE GRADUATE SCHOOL OF NATURAL AND APPLIED SCIENCES
OF
MIDDLE EAST TECHNICAL UNIVERSITY

BY

GÜLİN FINDIKOĞLU

IN PARTIAL FULFILLMENT OF THE REQUIREMENTS
FOR
THE DEGREE OF DOCTOR OF PHILOSOPHY
IN
ENGINEERING SCIENCES

JULY 2012

Approval of the thesis

**AN EXPERIMENTAL STUDY OF MECHANICAL PROPERTIES OF
NON ENZYMATICALLY GLYCATED BOVINE FEMUR CORTICAL BONE**

submitted by **GÜLİN FINDIKOĞLU** in partial fulfillment of the requirements for
the degree of **Doctor of Philosophy in Engineering Sciences Department, Middle
East Technical University** by,

Prof. Dr. Canan ÖZGEN
Dean, Graduate School of **Natural and Applied Sciences**

Prof. Dr. Murat DİCLELİ
Head of Department, **Engineering Sciences**

Assoc. Prof. Dr. ZAFER EVİS
Supervisor, Engineering Sciences Dept., METU

Examining Committee Members:

Prof. Dr. Turgut Tokdemir
Engineering Sciences Dept., METU

Assoc. Prof. Dr. Zafer Evis
Engineering Sciences Dept., METU

Assoc. Prof. Dr. Dilek Keskin
Engineering Sciences Dept., METU

Assoc. Prof. Dr. Hasan Okuyucu
Materials Engineering Dept., YBU

Assoc. Prof. Dr. Ayşen Tezcaner
Engineering Sciences Dept., METU

Date: 12.07.2012

I hereby declare that all information in this document has been obtained and presented in accordance with academic rules and ethical conduct. I also declare that, as required by these rules and conduct, I have fully cited and referenced all material and results that are not original to this work.

Name, Last Name : Glin FINDIKOĐLU
Signature :

To my family

ABSTRACT

AN EXPERIMENTAL STUDY OF MECHANICAL PROPERTIES OF NON ENZYMATICALLY GLYCATED BOVINE FEMUR CORTICAL BONE

Fındıkoğlu, Gülin

Ph.D., Department of Engineering Sciences

Supervisor: Assoc. Prof. Dr. Zafer Evis

July 2012, 142 Pages

The aim of this study is to investigate the deterioration in mechanical integrity of the collagen network in bovine bone with aging, which are related to fracture toughness. Age-related changes in collagen molecular structures formed by non-enzymatic glycation were examined and indentation fracture technique was used as a method for measuring the microstructural toughness of cortical bone. Microcrack propagation characteristics of bone for fragility were also studied.

Young and old group of bovine cortical bone specimens were grouped into 2 as ribosylated and non-ribosylated which were rested in solutions for four weeks. Series of indentations were made on bone specimen groups for each of five masses 10g, 25g, 50g, 100g and 200g for 10 sec to detect the effect of applied indentation load. The applied load was increased to 300g, 500g, 1000g and 2000g for 10 sec to be able to make microcracks. Series of indentations were made on bone specimen groups for each of five durations 5sec, 10sec, 20sec, 30sec for 100g to study the effect of indentation duration. Specimens were examined in the wet and dry state while studying the factors effecting microhardness measurement.

Microhardness values measured by 10g of load for 10sec were indifferent between the ribosylated and non-ribosylated groups in the young and old bovine bone pointing that this load is not indicative of the structural collagen changes. Loads

of 25g, 50g, 100g and 200g for 10 sec were able to differ ribosylated bone from non-ribosylated bone for the young and old bovine bones. Degree of microhardness increased with increased incubation period. Microhardness of dry specimens being either ribosylated or non-ribosylated were found to be statistically higher than wet specimens in young and old bone except for 10g for 10sec.

It has been shown that the calculated fracture toughness measured by the indentation method is a function of indentation load. Additionally, effect of indentation size might have resulted in a higher toughness measurement for higher indent loads with longer cracks even if the toughness is not actually higher. Methods using indentation technique has difficulty in relating the resistance to crack growth to the Mode I fracture toughness definition. Indentation fracture toughness allows sampling only one point on the *R*-curve methods and was not considered as successful for assessing materials with rising *R*-curve. Toughness is ranked incorrectly among ribosylated and non-ribosylated bovine bone by this technique.

Presence of extrinsic toughening mechanisms including crack bridging due to uncracked ligaments and collagen fibers were directly observed by scanning electron microscope. Ribosylated bone was found to have lower number of collagen bridging compared to non-ribosylated bovine bone. As a summary, indentation fracture method by Vickers indentation in bone is a method for measuring the fracture toughness.

Keywords: Non-enzymatic glycation; Microindentation; Toughness; Bone; Fracture

ÖZ

ENZİMATİK OLMAYAN YOLLA GLİKİZE EDİLEN İNEK FEMUR KORTİKAL KEMİĞİNİN MEKANİK ÖZELLİKLERİNİN DENEYSEL ÇALIŞMASI

Fındıkoğlu, Gülin

Ph.D., Mühendislik Bilimleri Bölümü

Tez Yöneticisi: Doç. Dr. Zafer Evis

Temmuz 2012, 142 Sayfa

Bu çalışmanın amacı inek kemiğinde kırılma tokluğuyla ilgili olan kollajen ağının mekanik bütünlüğünde yaşa bağlı bozulmayı araştırmaktır. Kollajenin moleküler yapısında enzimatik olmayan glikasyon yöntemiyle oluşturulan yaşlanmaya bağlı değişiklikler incelenmiştir ve kortikal kemikteki mikroyapıya ait tokluğun ölçümü için indentasyona bağlı kırılma yöntemi kullanılmıştır. Kemiğin mikrokırığın ilerleme özellikleri de kırılma için çalışılmıştır.

Solüsyonlarda dört hafta bekletilen genç ve yaşlı ineklere ait kortikal kemik örnekleri ribozillenmiş ve ribozillenmemiş olmak üzere 2 gruba ayrılmıştır. İndentasyon ağırlığının etkisini tespit etmek için kemik örneği gruplarında 10 sn boyunca 10 g, 25 g, 50 g, 100 g ve 200 g'lık 5 ayrı yük seri indentasyonlar halinde uygulanmıştır. Mikrokırık oluşturabilmek için uygulanan yük 10 sn boyunca 300 g, 500 g, 1000 g ve 2000 g'a kadar çıkartılmıştır. İndentasyon süresinin etkisini çalışmak için 100 g 5 sn, 10 sn, 20 sn ve 30 sn boyunca 5 sürenin herbiri kemik örnekleri üzerinde seri indentasyonlar halinde uygulanmıştır. Mikrosertlik ölçümünü etkileyen faktörleri çalışırken örnekler kuru ve ıslak halde incelenmiştir.

10g 10sn ile ölçülen mikrosertlik değerleri bu yükün kolajen yapısındaki değişiklikleri gösteremeyeceğine işaret ederek genç ve yaşlı kemiğin ribozillenmiş ve ribozillenmemiş grupları arasında farksız bulunmuştur. 10 sn boyunca uygulanan 25 g, 50 g, 100 g and 200 g yükleri ribozillenmiş kemiği ve ribozillenmemiş kemikten genç, yaşlı inek kemiklerinde ayırt etmiştir. Mikrosertliğin derecesi uzayan inkübasyon süresi ile artmıştır. Genç ve yaşlı kemiklerde ribozillenmiş veya ribozillenmemiş kuru örneklerin mikrosertlikleri ıslak örneklerden 10 gr 10 sn hariç istatistiksel olarak daha yüksek bulunmuştur.

İndentasyon metodu ile ölçülen hesaplanmış kırılma tokluğunun indentasyon yükünün bir fonksiyonu olduğu gösterilmiştir. İlâveten, indentasyon boyutunun etkisi uzun kırıkları olan yüksek yüklerde tokluk ölçümünün gerçekte olmasa da fazla çıkmasına neden olabilir. İndentasyon tokluğunu kullanan yöntemler kırık büyüme direncini Mod I kırılma tokluğu tanımına ilişkilendirmekte zorluk çeker. İndentasyon kırılma tokluğu R eğrisi yöntemlerindeki tek bir noktanın örneklenmesine izin verir ve yükselen R eğrisi olan materyallerin değerlendirilmesinde başarılı olarak kabul edilmez.

Kırılmamış ligamentler ve kollajen liflerine bağlı kırık köprüleşmesi de dahil olmak üzere dışsal tokluk mekanizmaları direk olarak tarayıcı elektron mikroskobu ile gözlenmiştir. Ribozillenmiş kemiğin ribozillenmemiş inek kemiğine göre daha az sayıda kollajen köprüleşmesi yaptığı bulunmuştur. Özet olarak, Vickers indentasyon yöntemiyle yapılan indentasyon tokluğu ölçümü kırılma tokluğunun ölçülmesinde bir yöntem olarak kullanılabilir.

Anahtar Kelimeler: Enzimatik Olmayan Glikasyon; Mikroindentasyon; Tokluk; Kemik; Kırılma

ACKNOWLEDGEMENTS

I wish to express my deepest gratitude to my supervisor Assoc. Prof. Dr. Zafer Evis for his guidance, advice, criticism, encouragements and insight throughout the research.

I would also like to thank Prof. Dr. Turgut Tokdemir and Assoc. Prof. Dr. Hasan Okuyucu for their suggestions and comments. I would like to thank gratefully to Prof. Dr. Ruşen Geçit for his efforts, encouragements, support and insight from the very beginning. I would like to make a special thank to Dr. Rezan Yorgancıođlu who was the first guide for the inspiration.

I gratefully acknowledge my friend Dr. Semih Erhan who helped and supported and, İdil Uysal who worked and guided me for the lab work. I also wish to thank all of my class mates and lab friends who were always understanding and helpful towards me. I thank to Assoc. Prof. Dr. Fahrettin Öztürk and Prof. Dr. Erol Arcaklıođlu for the technical support. I also thank to all people involved in acquiring and processing of samples some of whom are Osman Yeşilyurt, Assist. Prof. Dr. Çetin Karataş, Erol Mobilya and Sabanođlu Kasap.

I acknowledge my greatest thank and gratitude to my father Ziya Fındıkođlu and my mother Semahat Fındıkođlu and my sister Renin Fındıkođlu who are always considering, caring, loving, supporting, financing, encouraging me throughout my life. I am proud of you.

This study was supported by METU BAP Project No: BAP BAP-03-10-2010-02

TABLE OF CONTENTS

ABSTRACT	V
ÖZ	VII
ACKNOWLEDGEMENTS	IX
TABLE OF CONTENTS	X
LIST OF TABLES	XIV
LIST OF FIGURES	XVI
CHAPTERS	
1.INTRODUCTION	1
2.REVIEW OF LITERATURE	3
2.1. EPIDEMIOLOGY OF OSTEOPOROSIS.....	3
2.2.BONE.....	5
2.2.1. <i>Bone Cells</i>	6
2.2.1.1. Osteoblasts	6
2.2.1.2. Osteoclasts	7
2.2.2. <i>Bone Matrix</i>	7
2.2.3. <i>Types Of Bone</i>	8
2.3. COLLAGEN	10
2.3.1. <i>COLLAGEN BIOSYNTHESIS</i>	10
2.4. BONE MODELLING AND REMODELLING	14
2.4.1. <i>Age-Related Alterations in Modelling and Remodelling Adulthood</i>	17
2.5. MECHANICAL PROPERTIES OF BONE	17
2.5.1. <i>The Hierarchical Structure of Bone</i>	18
2.5.2. <i>The Graded Structure of Bone Material</i>	20
2.5.3. <i>Anisotropy of Bone</i>	20
2.5.4. <i>Role of Bone Composition and Microstructure</i>	21

2.6. AGE-RELATED CHANGES IN THE MATERIAL PROPERTIES OF BONE	25
.....
2.7. MECHANISMS OF BONE FRACTURE	26
2.8. MICRO INDENTATION	27
2.8.1. <i>Structural Organization and Mechanical Properties of Bone</i>	27
2.8.2. <i>Microindentation</i>	28
2.8.3. <i>Hardness</i>	29
2.8.4. <i>Factors Effecting Microindentation Test Results in Bone</i>	29
2.9. TOUGHNESS	30
2.9.1. <i>Strength vs. Toughness</i>	30
2.9.2. <i>K_{1c} and G_{1c} Fracture Toughness Measurements</i>	31
2.9.3. <i>Crack-Resistance Curve</i>	33
2.9.4. <i>Nonlinear-Elastic Fracture Mechanics</i>	34
2.9.5. <i>Calculation of Toughness from Crack Length Measurements Directly</i>	35
2.9.6. <i>Factors Effecting Toughness</i>	38
2.9.6.1. <i>Effect of Loading Mode</i>	38
2.9.6.2. <i>Plane Stress versus Plane Strain</i>	38
2.9.6.3. <i>Effect of Anatomical Location and Microstructural Orientation</i>	39
2.9.6.4. <i>Effects of Microstructural Factors</i>	40
2.9.6.5. <i>Effect of Age</i>	41
2.10. MICROFRACTURE MECHANISMS OF BONE	42
2.10.1. <i>How Fracture Occurs?</i>	42
2.10.2. <i>Microdamage as a Manifestation of Bone Fragility</i>	43
2.10.3. <i>Mechanistic Aspects of Microfracture</i>	44
2.10.3.1. <i>Microindentation Induced Microcracking</i>	45
2.10.3.2. <i>Microdamage Analysis utilizing SEM</i>	46
2.10.3.3. <i>Compositional Parameters Affecting Bone Quality</i>	48
2.10.3.4. <i>R-curve Analysis</i>	49
2.10.3.5. <i>Intrinsic-Extrinsic Mechanisms of Fracture</i>	49
2.10.3.6. <i>Aging Effects on Crack Bridging</i>	53

2.11 MECHANISMS OF BONE AGING	55
2.11.1 <i>Effects of Aging on Bone Ultrastructure</i>	55
2.11.2. <i>Effect of Cross-Links to the Mechanical Properties of Bone</i>	56
2.11.3. <i>Age-Related Changes in Biochemical Properties of Collagen</i>	61
2.11.3.1. Collagen Biosynthesis and Fibril Formation.....	61
2.11.3.2. Enzymatically Formed Intermolecular Cross-Linking.....	63
2.11.3.3. Non-Enzymatic Cross-Linking (Glycation).....	63
3.MATERIALS AND METHODS	68
3.1. PREPARATION OF SPECIMENS.....	68
3.2. POLISHING	68
3.3. DENSITY	69
3.4. NON-ENZYMATIC GLYCATION PROCESS	69
3.5. MICROMECHANICAL TESTING BY MICROINDENTATION	70
3.5.1. <i>Variation of Hardness with Applied Load</i>	71
3.5.2. <i>Hardness Variation with Duration</i>	71
3.5.3. <i>Calculation of Microhardness</i>	71
3.5.4. <i>Calculation of Fracture Toughness by Micro-Hardness Test</i>	72
3.6. MACROMECHANICAL TESTING	72
3 POINT BENDING TEST	72
3.7. SCANNING ELECTRON MICROSCOPY	74
3.8. STATISTICAL ANALYSIS	74
4.RESULTS	75
4.1. MICROHARDNESS.....	75
4.2. TOUGHNESS AND MICROCRACKS.....	86
4.3. CHARACTERIZATION OF FRACTURE SURFACES BY MICROSCOPY	103
5.DISCUSSION	110
5.1. VARIABLES THAT EFFECT MICROHARDNESS.....	110
5.2. MICROCRACK FORMATION BY MICROINDENTATION	113

5.3. MICROINDENTATION TOUGHNESS	115
5.4. EFFECT OF AGING ON TOUGHNESS.....	118
5.5. TOUGHENING MECHANISMS	121
6.CONCLUSIONS	124
7.REFERENCES.....	126
CURRICULUM VITAE.....	136

LIST OF TABLES

TABLES

- Table 2.1:** The number of discharges and deaths due to extremity or trunk/vertebra fractures in Turkey with respect to statistical data of Turkish Statistical Institute. The distribution of fractures to ages or sexes and etiology (traumatic or non-traumatic) is not specified [9]. 4
- Table 2.2:** Amino acid composition of collagens from different species [19]. 11
- Table 2.3:** Some physical and chemical characteristics of bone that may influence biomechanical bone quality are shown, categorized by physical scale [24]. 18
- Table 2.4:** Range of single value K and G (mode I) for cortical bone to demonstrate toughness, comparing with some widely used materials [34]. 33
- Table 4.1:** Microhardness values expressed as mean \pm SD measured by 10 g of applied force for 10 sec on transverse sections of R and NR young and old bovine bone with respect to duration of NEG in wet and dry state. 76
- Table 4.2:** Microhardness values expressed as mean \pm SD measured by 25 g of applied force for 10 sec on transverse sections of R- and NR- young and old bovine bone with respect to duration of NEG in wet and dry state. 77
- Table 4.3:** Microhardness values expressed as mean \pm SD measured by 50 g of applied force for 10 sec on transverse sections of R- and NR- young and old bovine bone with respect to duration of NEG in wet and dry state. 78
- Table 4.4:** Microhardness values expressed as mean \pm SD measured by 100 g of applied force for 10 sec on transverse sections of R- and NR- young and old bovine bone with respect to duration of NEG in wet and dry state. 79
- Table 4.5:** Microhardness values expressed as mean \pm SD measured by 200 g of applied force for 10 sec on transverse sections of R and NR young and old bovine bone with respect to duration of NEG in wet and dry state. 80
- Table 4.6:** Microhardness values expressed as mean \pm SD measured by 100 g of applied force for 5 sec on transverse sections of R and NR young and old bovine bone with respect to duration of NEG in wet and dry state. 81
- Table 4.7:** Microhardness values expressed as mean \pm SD measured by 100 g of applied force for 20 sec on transverse sections of R- and NR- young and old bovine bone with respect to duration of NEG in wet and dry state. 82

Table 4.8: Microhardness values expressed as mean±SD measured by 100 g of applied force for 30 sec on transverse sections of R and NR young and old bovine bone with respect to duration of NEG in wet and dry state.	83
Table 4.9: Microhardness values expressed as mean±SD measured by 300 g of applied force for 10 sec on transverse sections of ribosylated young and old bovine bone with respect to duration of NEG in dry state.	84
Table 4.10: Microhardness values expressed as mean±SD measured by 500 g of applied force for 10 sec on transverse sections of R- young and old bovine bone with respect to duration of NEG in dry state.	85
Table 4.11: Microhardness values expressed as mean±SD measured by 1000 g of applied force for 10 sec on transverse sections of R- young and old bovine bone with respect to duration of NEG in wet and dry state.	85
Table 4.12: Microhardness values expressed as mean±SD measured by 2000 g of applied force for 10 sec on transverse sections of R- young and old bovine bone with respect to duration of NEG in wet and dry state.	86
Table 4.13: Comparison of density measurement expressed as mean±SD for young and old non ribosylated bovine bone transverse section specimens and their correlation with microhardness measurement made by 100 g of load for 10 sec.	86
Table 4.14: Average values for modulus of elasticity determined by 3 point bending test in young and old bovine bone with respect to duration of ribosylation (NEG).	87
Table 4.15: K_{Ic} values expressed as mean±SD and measured by microcrack length in young and old dry bovine bone with respect to various applied load and duration of ribosylation (NEG).	89

LIST OF FIGURES

FIGURES

- Figure 2.1:** Photomicrograph of osteoblasts. Two spicules of bone developing in the mesenchyme are shown. Numerous osteoblasts form an almost continuous row in relation to the surface of the bony trabecula. Three large osteoclasts (arrows) also occur in relation to the developing bone [16]. 6
- Figure 2.2:** A: Photomicrograph of a bone section showing osteoclasts (arrows); B: Higher magnification of osteoclasts and the erosion of bone matrix close to it [15]. 7
- Figure 2.3:** Thick section of bone illustrating the cortical compact bone and the lattice of trabeculae of cancellous bone [15]. 8
- Figure 2.4:** Schematic drawing of the wall of a long bone: haversian system and outer and inner circumferential lamellae. The protruding haversian system on the left shows the orientation of collagen fibers in each lamellae at the right is a haversian system showing lamellae, a central blood capillary, and many osteocytes with their processes [15]. 9
- Figure 2.5:** Schematic diagram showing the different posttranslational modifications and assembly of type I collagen into fibrils [22]. 13
- Figure 2.6:** Remodelling cycle. (1) Osteocytes are connected to each other and to lining cells on the endosteal surface adjacent to the marrow; (2) Damage to osteocytic processes by a microcrack produces osteocyte apoptosis. (3) The distribution of apoptotic osteocytes provides the topographical information needed to target osteoclasts to the damage. (3) Lining cells secrete collagenase to break down unmineralized collagen revealing mineralized bone and creating remodelling cavity in which progenitors for osteoblastogenesis and osteoclastogenesis are brought by blood or marrow locally. (4) Osteoclasts (Oc) make bone resorbption and clean damage as well as phagocytose osteocytes by its cytoplasmic extensions between osteocyte and lacunar wall. (5) The reversal phase and cement line formation comes after. (6) Osteoid is produced by osteoblasts and (7) Some osteoblasts are embedded in osteoid in which they stay and differentiate into osteocytes making reconstruction of the canalicular network of osteocytes [7]. 16
- Figure 2.7:** The hierarchical levels of structure found in secondary osteonal bone [25]. 19

Figure 2.8: Variation in the modulus and strength of trabecular bone with respect to bone density. (a) Modulus of elasticity studied in power law relation as a function of BMD for trabecular bone. (b) Yield stress under compression was studied as a function of BMD in specimens of human trabecular type of bone [7].	22
Figure 2.9: Strains for tension, compression and at yield strains of human trabecular type of bone bone in human considering BMD. Error bars show one standard deviation [7].	23
Figure 2.10: Stress versus strain graph for specimens taken from the diaphysis of cortical bone oriented transversely (T) and longitudinally (L). Anisotropic character of bone is shown in specimens tested longitudinally and transversely [7].	24
Figure 2.11: A) Image of a microindentation by Vickers technique from bovine bone in wet state, B) Knoop microindentation image obtained from bovine bone in wet state [30].	28
Figure 2.12: Illustrations for different modes of loading. Mode I loading was shown in the first figure to demonstrate tensile-opening type, mode II loading was shown in the second figure to demonstrate for shear type and mode III loading was shown in the third figure for anti-plane shear or tearing. Loading in vivo can be related with one or more than one of the modes [34].	32
Figure 2.13: Schematic diagram for indentation fracture. Development of a radial crack of length a after loading. After loading and unloading cracks with overall size of c grows.	35
Figure 2.14: Fracture toughness standard suggested by ASTM E399 for the orientation code is shown by the illustration. The first letter represents normal direction to the crack plane whereas second letter denotes direction of crack propagation [37].	39
Figure 2.15: Variation in fracture toughness by aging in bone obtained from human cortex. Crack growth in L-C direction in femur (top) and for crack growth in C-L direction in tibia (bottom) are shown [33].	41
Figure 2.16: A) Stages of fracture behaviour: the elastic range E: the continuum damage mechanics range (CDM), and B) the fracture mechanics [39, 40].	42
Figure 2.17: Illustrations for some types of toughening mechanisms in cortical bone: A) Crack deflection; B) crack bridging; C) uncracked ligament bridging; D) diffuse microcracking [2].	45
Figure 2.18: A) An image from a crack in cortical bone of 61-year-old human obtained by optical micrography. Notice the development of uncracked	

ligaments and daughter cracks. B) Collagen fibrils making up bridging in a crack wake in bone from human cortex [44]. 47

Figure 2.19: Fracture surface details from bovine bone: (a) intra-lamellar bundles of fibers (dots) represent lamellae which are pulled apart (L), lamellae are linked by inter-lamellar fibers (arrows), and; (b) pulled-out bundles of fibers (c). Transverse fracture surface image of an osteon by SEM. Rupture of cement line and interlamellar interfaces shows concentric shape of lamellae and the outer borders of “pulled out” osteons [42,45,46]. 48

Figure 2.20: (a) Comparison of theoretical (microcrack-free and bridge-free) and experimental curves for compliance. Notice that the measured compliance is lower than the theoretical compliance, that gives an important clue about the function of crack bridging in the mechanism of toughening in cortical bone of human. (b) Change in compliance of a sample with a crack working with the mechanism of toughening [44,47]. 52

Figure 2.21: KR(Δa) resistance curves in vitro in cortical bone of human for extension of stable crack with respect to age. Notice rising R-curve behavior is linear [52]. 54

Figure 2.22: Change in the (a) crack-initiation toughness (K_{Ic}), and (b) crack growth toughness (R-curve gradient) in cortical bone from human being by aging [43,51]. 55

Figure 2.23: Graphs for age vs (E , K_{Ic} , s_f , J , W_f). L, A, P show lateral, anterior and posterior aspects, respectively. The filled dots show the mean of three values at an age group. The lines represent linear regressions of least squares by confidence intervals of 95% [33]. (A) Results of Zioupos et al. for modulus of elasticity. (B) Dotted line shows the study results of Yamada on a bone from human femur that is relatively wet at RT [62]. In (C), the dotted data and lines are results from wet specimens of human tibia obtained at RT on CT specimens longitudinally by Bonfield and Behiri [63]. (D) Results of Zioupos et al. for work of fracture. (E) dotted line represents results for a rate of critical strain energy release in mode-I from tibia at RT on CT specimens in the longitudinal direction, by Norman et al.[64]. 59

Figure 2.24: Collagen molecule biosynthesis. Collagen synthesis steps are schematized. (A) and (B) occurs intracellularly while (C) and (D) occur extracellularly. 62

Figure 2.25: Formation of Schiff base and AGE. A) Reaction of glucose and lysine bound to peptide to make up a Schiff base that undergoes rearrangement of Amadori spontaneously to give the Amadori product, an aminodeoxyketose. Both ketose and Schiff base are supposed to undergo further reaction to form

AGEs. B) Break down of glucose to glyoxal and glucosone oxidatively, which react later with side-chains of protein to form AGEs [67].....	64
Figure 2.26: Formation of pentosidine [67].....	65
Figure 2.27: Cross-linking location. Mature,() ; Immature, (I); and (↓) cross-links of the collagen fibre by aging [67].....	67
Figure 3.1: Microhardness tester.....	70
Figure 3.2: Microindentations were made on 3 samples belonging to 8 groups at varying indentation loads and durations both in wet and dry state.....	71
Figure 3.3: Scheme for specimens obtained from the cortical wall thickness of long bones.	73
Figure 4.1: Alteration of colour from white tone in the control group towards a yellow tone in the ribosylated group as a subjective indicator of NEG.....	87
Figure 4.2: Graph for change in elastic modulus measured by 3 point bending test in young and old bovine bone with respect to duration of ribosylation (NEG). (a) young NR-bovine bone; b) old NR-bovine bone; c) young R-bovine bone; d) old NR-old bovine bone).....	88
Figure 4.3: Mean microcrack length vs indentation load graph A) for young ribosylated dry bovine bone, B) for old ribosylated dry bovine bone, C) for comparison of young and old bovine bone: a) 300 g for 10 sec; b) 500 g for 10 sec; c) 100 g for 10 sec; d) 2000 g for 10 sec; e) 300 g in young bovine bone for 10 sec; f) 300 g in old bovine bone for 10 sec; g) 500 g in young bovine bone for 10 sec; h) 500 g in old bovine bone for 10 sec; i) 1000 g in young bovine bone for 10 sec; j) 1000 g in old bovine bone for 10 sec; k) 2000 g in young bovine bone for 10 sec; l) 2000 g in old bovine bone for 10 sec.	90
Figure 4.4: Mean K_{Ic} values measured by different microindentation loads with respect to duration of ribosylation A) in young bovine bone B) in old bovine bone C) both: a)300 g for 10 sec; b) 500 g for 10 sec; c) 100 g for 10 sec; d) 2000 g for 10 sec; e) 300 g in young bovine bone for 10 sec; f) 300 g in old bovine bone for 10 sec; g) 500 g in young bovine bone for 10 sec; h) 500 g in old bovine bone for 10 sec; i) 1000 g in young bovine bone for 10 sec; j) 1000 g in old bovine bone for 10 sec; k) 2000 g in young bovine bone for 10 sec; l) 2000 g in old bovine bone for 10 sec.....	92
Figure 4.5: Mean microcrack length values measured by different microindentation loads with respect to duration of ribosylation: A) in young ribosylated dry bovine bone; B) in old ribosylated dry bovine bone; C) both: a) 300 g for 10 sec; b) 500 g for 10 sec; c) 100 g for 10 sec; d) 2000 g for 10 sec; e) 300 g in young bovine bone for 10 sec; f) 300 g in old bovine bone for 10 sec; g) 500 g	

in young bovine bone for 10 sec; h) 500 g in old bovine bone for 10 sec; i) 1000 g in young bovine bone for 10 sec; j) 1000 g in old bovine bone for 10 sec; k) 2000 g in young bovine bone for 10 sec; l) 2000 g in old bovine bone for 10 sec.
 93

Figure 4.6: Mean K_{1c} vs mean microcrack length by 300 g for 10 sec microindentation load A) for young ribosylated dry bovine bone; B) for old ribosylated dry bovine bone; C) for comparison of young and old bovine bone with respect to duration of ribosylation (NEG): a) week 1; b) week 2; c) week 3; d) young bovine bone in week 1; e) old bovine bone in week 1; f) young bovine bone in week 2; g) young bovine bone in week 3; h) old bovine bone in week 3.
 94

Figure 4.7: Mean K_{1c} vs mean microcrack length by 500 g for 10 sec microindentation load: A) for young ribosylated dry bovine bone, B) for old ribosylated dry bovine bone, C) for comparison of young and old bovine bone with respect to duration of ribosylation (NEG): a) week 1, b) week 2, c) week 3, d) young bovine bone in week, 1 e) old bovine bone in week 1, f) young bovine bone in week 2, g) old bovine bone in week 2, h) young bovine bone in week 3, i) old bovine bone week in 3.
 95

Figure 4.8: Mean K_{1c} vs mean microcrack length by 1000 g for 10 sec microindentation load: A) for young ribosylated dry bovine bone; B) for old ribosylated dry bovine bone; C) for comparison of young and old bovine bone with respect to duration of ribosylation (NEG): a) week 1; b) week 2; c) week 3; d) young bovine bone in week 1; e) old bovine bone in week 1; f) young bovine bone in week 2; g) old bovine bone in week 2; h) young bovine bone in week 3; i) old bovine bone in week 3.
 97

Figure 4.9: Mean K_{1c} vs mean microcrack length by 2000 g for 10 sec microindentation load: A) for young ribosylated dry bovine bone; B) for old ribosylated dry bovine bone; C) for comparison of young and old bovine bone with respect to duration of ribosylation (NEG): a) week 1; b) week 2; c) week 3; d) young bovine bone in week 1; e) old bovine bone in week 1; f) young bovine bone in week 2; g) old bovine bone in week 2; h) young bovine bone in week 3; i) old bovine bone week in 3.
 98

Figure 4.10: K_{1c} vs microcrack length at various indentation loads in A) young ribosylated dry bovine bone B) old ribosylated dry bovine bone C) for comparison of young and old bovine bone after 1 week of ribosylation (NEG): a) 300 g; b) 500 g; c) 1000 g; d) 2000 g of indentation load; e) 300 g in young bovine bone for 10 sec; f) 300 g in old bovine bone for 10 sec; g) 500 g in young bovine bone for 10 sec; h) 500 g in old bovine bone for 10 sec; i) 1000 g in young bovine bone for 10 sec; j) 1000 g in old bovine bone for 10 sec; k) 2000 g in young bovine bone for 10 sec; l) 2000 g in old bovine bone for 10 sec.
 99

- Figure 4.11:** K_{Ic} vs microcrack length at various indentation loads in A) young ribosylated dry bovine bone; B) old ribosylated dry bovine bone; C) for comparison of young and old bovine bone after 2 weeks of ribosylation (NEG): a) 300 g; b) 500 g; c) 1000 g; d) 2000 g of indentation load; e) 300 g in young bovine bone for 10 sec; f) 500 g in young bovine bone for 10 sec; g) 500 g in old bovine bone for 10 sec; h) 1000 g in young bovine bone for 10 sec; i) 1000 g in old bovine bone for 10 sec; j) 2000 g in young bovine bone for 10sec; k) 2000 g in old bovine bone for 10 sec..... 100
- Figure 4.12:** K_{Ic} vs microcrack length at various indentation loads in A) young ribosylated dry bovine bone; B) old ribosylated dry bovine bone; C) for comparison of young and old bovine bone after 3 week of ribosylation (NEG): a) 300 g; b) 500 g; c) 1000 g; d) 2000 g of indentation load; e) 300 g in young bovine bone for 10 sec; f) 300 g in old bovine bone for 10 sec; g) 500 g in young bovine bone for 10 sec; h) 500 g in old bovine bone for 10 sec; i) 1000 g in young bovine bone for 10 sec; j) 1000 g in old bovine bone for 10 sec; k) 2000 g in young bovine bone for 10 sec; l) 2000 g in old bovine bone for 10 sec..... 101
- Figure 4.13:** K_{Ic} vs microcrack length at 1000 g indentation loads in young and old dry bovine bone after A) 2 weeks of ribosylation; B) 3 weeks of ribosylation (NEG): a) young bovine bone; b) old bovine bone..... 102
- Figure 4.14:** K_{Ic} vs microcrack length at 2000 g indentation loads in young and old dry bovine bone after A) 2 weeks of ribosylation; B) 3 weeks of ribosylation (NEG): a) young bovine bone; b) old bovine bone..... 103
- Figure 4.15:** SEM images from fracture surface of cylindrical shaped cortical bone specimens after 3 point bending test from different specimens in A,B,C,D.... 104
- Figure 4.16:** Indentations without microcracks at load lower than 200 g A) x600, B) x400 times of magnification. Canals that belong to Haversian system and a line of non-indentation induced crack are also visible..... 104
- Figure 4.17:** SEM images of A) a microcrack originating from the corner of a microcrack formed by microindentation testing in young ribosylated bovine bone 1 week after ribosylation B) and C) closer view of microcrack tip and wake in the same fracture, D) in a different specimen..... 105
- Figure 4.18:** SEM image of a microcrack from young bovine bone 2 weeks after ribosylation in views getting closer to the wake zone: (A, B), (C, D), and (E, F, G, H) pairs of images belong to 3 different specimens..... 107
- Figure 4.19:** SEM images of microindentation induced microcracking from young bovine bone 3 weeks after ribosylation. A, B and C, D and E, F, G and H, I, J, K belong to different specimens or different microcracks..... 108

LIST OF ABBREVIATIONS

<i>AGE</i>	:Advanced Glycation End Products
<i>ASTM</i>	:American Society for Testing and Materials
<i>BMD</i>	:Bone Mineral Density
<i>BMU</i>	:Basic Multicellular Unit
<i>BSU</i>	:Bone Structural Unit
<i>DXA</i>	:Dual X-Ray Absorbsiometry
<i>E</i>	:Modulus of Elasticity
G_c	:Critical Strain Release Energy Rate
<i>H</i>	:Microhardness
<i>HA</i>	:Hydroxyapatite
K_{Ic}	:Critical Stress Intensity Factor in Mode I (tensile opening)
<i>LEFM</i>	:Linear Elastic Fracture Mechanics
NEG	:Non-enzymatic Glycation
<i>NR</i>	:Non-Ribosylated
<i>R</i>	:Ribosylated
<i>RT</i>	:Room Temperature
<i>SD</i>	:Standard Deviation
<i>SEM</i>	:Scanning Electron Microscopy
<i>VIF</i>	:Vicker's Indentation Fracture Test

CHAPTER 1

INTRODUCTION

The structural integrity of mineralized tissues such as cortical bone is clinically important, since bone forms the load-bearing and protective frame for the body. Age-related derangement of the bone fracture features, together with increased expectancy of life causes increased incidence of fracture of bone in the older people. Understanding the underlying fracture mechanisms and how these are effected by extrinsic (e.g. mechanical loading) as well as intrinsic (e.g. disease, aging) factors might help to define risk of fracture and develop preventive measures.

Increase in the risk of bone to fracture might be caused by age-related changes in the skeleton. Alterations occur in the bone constituents, such as the organic and mineral phases, or in their arrangement in space such as microstructure and orientation. Bone loss in bone mineral density (BMD) has been proposed to be the major factor contributing to fracture risk. Measurements of bone quantity is useful in predicting fracture risk. On the other hand it cannot explain incidence of fracture totally due to the fact that the risk of bone fracture for older women is higher than younger women, although the risk of fracture for both groups are the same [1]. It was shown that about 10-fold rise in risk of fracture occurs with aging that is BMD independent [2]. Besides BMD, qualitative factors such as bone microstructure and porosity, alterations in the network of collagen could also cause significant changes in bone fracture characteristics. Results of the studies show that features of bone fracture are effected by multiple factors [3].

Bone quality and strength were commonly measured by elastic modulus and ultimate tensile strength. Since fractures of bone in vivo are often started and/or promoted by cracks, it is questionable whether they provide enough information. Some studies investigating the effects of these factors found that even without

important alterations in BMD, the tensile strength could decay with age because of the increased porosity [3].

One measure of quality that is directly related to the fracture of materials is fracture toughness [1]. Fracture toughness test measures the stress intensity or energy necessary for a crack to propagate in a material. It may give a more meaningful way of evaluation. Although bone is neither isotropic nor homogeneous, it was found that linear elastic fracture mechanics (LEFM) approaches are still valid for evaluating the bone's fracture toughness on the condition that same bone type is compared [3].

Since bone is a composite material consisting of mineral and organic phases, alterations in its constituents modify its biomechanical behavior. Collagen, which composes 90% of the organic phase in bone, is susceptible to posttranslational modifications, including non-enzymatic glycation (NEG). It was reported that alterations in microstructure of bone and morphology of osteons causes important alterations in fracture toughness of bone. Additionally, alterations in structural properties of network of collagen was reported to correlate with fracture toughness of bone [3].

Cyclic loading application on cortical bone causes microdamage formation. In vivo, accumulation of microdamage is related with the imbalance between microdamage formation and remodeling which repairs damage due to fatigue. Morphology of damage (diffuse damage or linear microcracks) is a function of tissue properties and local strain together [4].

The aim of this study is that the mechanical integrity of the collagen network in human bone deteriorates with age, and such adverse changes correlate with the decreased toughness of aged bone. Age-related changes in collagen molecular structures by NEG and indentation fracture as a method of measuring the microstructural toughness of cortical bone were examined and microcrack propagation characteristics of bone for fragility were studied.

CHAPTER 2

REVIEW OF LITERATURE

2.1. EPIDEMIOLOGY OF OSTEOPOROSIS

Fractures caused by osteoporosis have been becoming a global public health problem. In the United States of America (USA) alone, there are 1.5 million fractures, including 300,000 hip fractures and 300,000 clinical vertebral fractures in each year [5]. Osteoporosis is important because it causes substantial morbidity and costs \$13.8 billion a year (1995 dollars) in the USA alone [6].

The number of hip fractures that occur each year in the world has been estimated by Cooper et al. to be 1.66 million in 1990 and is predicted to rise to 6.26 million by the year 2050 [7]. In the US alone, age-related fractures of spine, hip and wrist costed more than \$17 billion in 2001. Another estimate has been done by Gullberg et al., who found similar figures to those of Cooper et al., for 1990 it was estimated that 1.25 million hip fractures (338,000 in men and 917,000 in women) occurred worldwide and that the number of hip fractures will increase by 310% in men and 240% in women by 2025, due to the aging of the population [8]. With modest assumptions concerning secular trends (by increasing incidence of hip fractures), the number of hip fractures could range between 7.3 million and 21.3 million by 2050.

Today only the number of fractures without any specifications is available on web page of Turkish Statistical Institute (Table 2.1) [9].

Table 2.1: The number of discharges and deaths due to extremity or trunk/vertebra fractures in Turkey with respect to statistical data of Turkish Statistical Institute. The distribution of fractures to ages or sexes and etiology (traumatic or non-traumatic) is not specified [9].

YEARS	NUMBER OF HOSPITALIZATION DUE TO EXTREMITY FRACTURES	NUMBER OF HOSPITALIZATION DUE TO TRUNK OR VERTEBRA FRACTURES	NUMBER OF DEATHS DUE TO EXTREMITY FRACTURES	NUMBER OF DEATHS DUE TO TRUNK OR VERTEBRA FRACTURES
1997	3648	450	6	2
1998	3529	375	2	6
1999	3076	270	8	1
2000	2628	314	4	3
2001	2301	471	8	3
2002	1853	410	2	2
2003	3232	6258	16	71
2004	2533	464	8	4

It is needed to establish database concerning the prevalence, outcomes and treatment of osteoporosis and fractures in Turkey. It is stated in web page of Turkish Osteoporosis Association that it is planned to cooperate with Turkish Statistical Institute about formation of multi-centric data base with relevant updates and corrections [10].

Fractures due to osteoporosis causes occasional disability and pain. Several osteoporotic fractures such as hip fractures have a very high morbidity and mortality, and there are similar new findings for vertebral fractures [11]. Rates of mortality after hip fracture are 4-times higher in men compared to women. A fracture in vertebra might be considered as a risk factor for long-term morbidity, particularly in women, and for mortality both in women and men [12].

Osteoporosis is a systemic disease characterized by a low bone mass and deterioration of microarchitectural structure of bone tissue, which increases skeletal fragility and susceptibility of bone to fracture [13]. Osteoporosis is happening as a

result of any imbalance between the activity of the bone cells (osteoblasts and osteoclasts), which leads to bone degradation [12]. It is one of the most common situations related with aging. Many risk factors play a role in the pathogenesis of osteoporosis.

Low bone mass is not the only factor effecting the occurrence of bone fractures in the elderly. The fractures risk increases with age for a given bone mass. Moreover, the overall composition (i.e. ratio of mineral, water, collagen and matrix proteins), the biochemical and physical characteristics of these constituents (i.e. degree of mineralization, collagen nature), the architecture and morphology (i.e. bone size, trabecular microarchitecture, geometry), and the nature and severity of pre-existing microcracks are the factors which effect the bone resistance to fracture [12].

Two independent risk factors for osteoporotic fracture are advanced age and low BMD. Each standard deviation (SD) decrease in BMD or each 5 year increment in age is related with an ~2 (1.5-3)-fold increase in the risk of fracture [6],[12]. It is reported that each decrease of 1 SD of BMD measured by dual-energy X-ray absorptiometry (DXA) is associated with an age adjusted 50%-150% increase in the risk of osteoporotic fractures in postmenopausal women [13].

In a retrospective study by Cankurtaran et al. conducted from February 2002 through July 2003 with 783 female and 464 male participants aged 65 years and older in Turkey, BMD measures were performed using DXA at femoral neck and lumbar spine [14]. 29.5% of cases of osteoporosis were found in males; 45.9% of female patients had osteoporosis, 36.6% had osteopenia [14].

2.2.BONE

Bone is a specialized connective tissue composed of intercellular calcified material, the bone matrix, and three cell types: osteocytes, osteoblasts and osteoclasts.

2.2.1. Bone Cells

2.2.1.1. Osteoblasts

Osteoblasts are responsible for the synthesis of the organic components of bone matrix (type I collagen, proteoglycans and glycoproteins). Deposition of the inorganic components of the bone also depends on the presence of viable osteoblasts. Some osteoblasts are gradually surrounded by newly formed matrix and become osteocytes (Figure 2.1). During this process, a space called lacuna is formed. Lacuna are occupied by osteocytes and their extensions, along with a small amount of extracellular noncalcified matrix. Matrix components are secreted at the cell surface, which is in contact with older bone matrix, producing a layer of new (but not yet calcified) matrix, called osteoid, between the osteoblast layer and the previously formed bone. This process, bone apposition, is completed by subsequent deposition of calcium salts into the newly formed matrix [15].

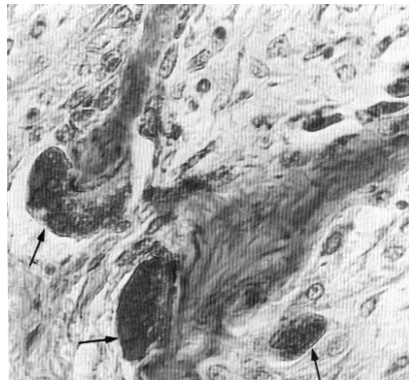


Figure 2.1: Photomicrograph of osteoblasts. Two spicules of bone developing in the mesenchyme are shown. Numerous osteoblasts form an almost continuous row in relation to the surface of the bony trabecula. Three large osteoclasts (arrows) also occur in relation to the developing bone [16].

2.2.1.2. Osteoclasts

Osteoclasts are very large, branched motile cells. Dilated portions of the cell body (Figure 2.2) contain 5 to 50 or more nuclei. In areas of bone resorption, osteoclasts lie within enzymatically etched depressions in the matrix known as Howship's lacunae. Osteoclasts are derived from the fusion of bone marrow derived cell, and belong to the mononuclear phagocyte system. The osteoclasts secrete collagenase and other enzymes and pumps protons into a subcellular pocket, promoting the localized digestion of collagen and dissolving calcium salt crystals [15].

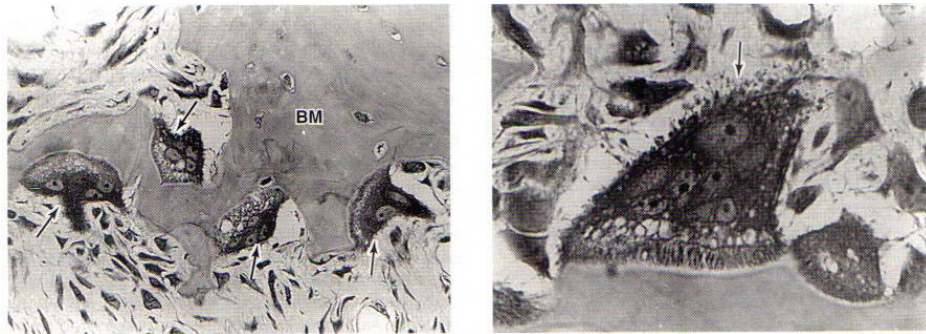


Figure 2.2: A: Photomicrograph of a bone section showing osteoclasts (arrows); B: Higher magnification of osteoclasts and the erosion of bone matrix close to it [15].

2.2.2. Bone Matrix

Inorganic matter represents about 50% of the dry weight of bone matrix. Calcium and phosphorus are especially abundant. X-ray diffraction studies have shown that calcium and phosphorus form hydroxyapatite (HA) crystals with the composition of $\text{Ca}_{10}(\text{PO}_4)_6(\text{OH})_2$. Significant quantities of amorphous (noncrystalline) calcium phosphates are also present. In electron micrographs, bone minerals appear as plates that lie alongside the collagen fibrils but are surrounded by

ground substance. The surface ions of HA are hydrated, and a layer of water and ions forms around the crystal and the body fluids.

The organic matrix of bone is type I collagen and ground substance, which contain proteoglycan aggregates and several specific structural glycoproteins. Some of the glycoproteins are produced by osteoblasts and demonstrate affinity for both HA and the cell membrane; they might be involved in binding osteoblasts and osteoclasts to bone matrix. Bone glycoproteins may also be responsible for promoting calcification of bone matrix.

The association of HA with collagen fibers is responsible for the hardness and resistance of bone tissue. After bone is decalcified, its shape is preserved, but it becomes as flexible as a tendon. Removal of the organic part of the matrix which is mainly collagenous also leaves the bone with its original shape; however it becomes fragile, breaking and crumbling easily when handled [15].

2.2.3. Types Of Bone

Gross observation of bone cross section shows dense areas without cavities, corresponding to compact bone and areas with interconnecting cavities corresponding to cancellous (spongy) bone (Figure 2.3). Both compact and the trabeculae separating the cavities of cancellous bone have the same histologic structures.

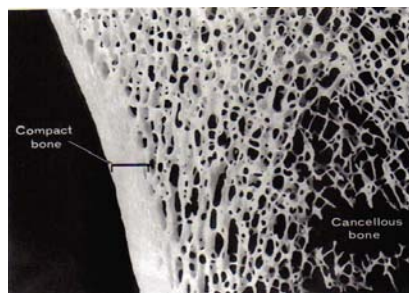


Figure 2.3: Thick section of bone illustrating the cortical compact bone and the lattice of trabeculae of cancellous bone [15].

In long bones, the ends called epiphysis are composed of spongy bone covered by a thin layer of compact bone, with a small component of spongy bone on its inner surface around the bone marrow cavity. The cylindrical part, diaphysis is almost totally composed of compact bone, with a small component of spongy bone completely surrounded by compact bone.

In sites where compact bone is found, such as the diaphysis of long bones, the lamella shows a typical organization made up of haversian systems, outer circumferential lamella, inner circumferential lamellae and interstitial lamellae (Figure 2.4).

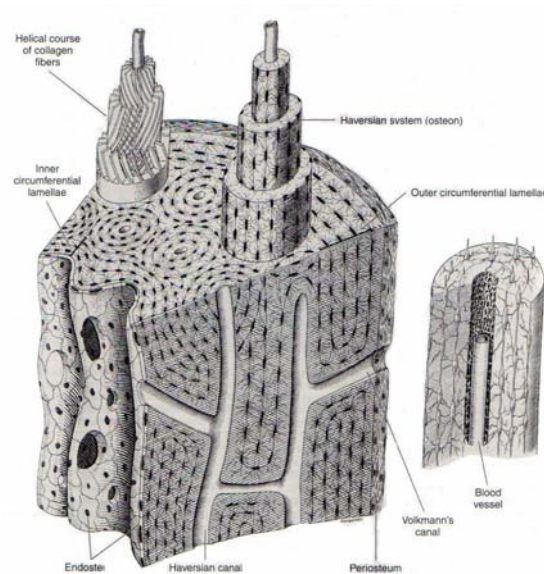


Figure 2.4: Schematic drawing of the wall of a long bone: haversian system and outer and inner circumferential lamellae. The protruding haversian system on the left shows the orientation of collagen fibers in each lamellae at the right is a haversian system showing lamellae, a central blood capillary, and many osteocytes with their processes [15].

2.3. COLLAGEN

2.3.1. COLLAGEN BIOSYNTHESIS

Collagen is the most abundant protein of the body [17]. In living organisms, collagen is the principle load carrying component of blood vessels, tendons, bone, muscle, etc [18]. Its structure is specially fitted for its structural role. It is a fibrillar protein. The basic structural unit of collagen is tropocollagen. Tropocollagen is composed of three polypeptide chains. Each polypeptide chain has the same general formula $(-\text{Gly-X-Y-})_{333}$. The glycine is at the first position. Some of the amino acid residues at the positions of X and Y are lysine, proline, alanine and hydroxylysine. Collagen is a glycoprotein that is composed of only two kinds of carbohydrate residues, that are galactose and glucose. These are linked in O-glycosidic bonds to hydroxylysyl residues.

In collagen, each chain of polypeptide fits into a special kind of helix that is left handed, kinked, rigid with three amino acids per turn. Next, the three helical polypeptides enfold around one another to make triple stranded, right handed superhelix. The superhelix is stabilized by hydrogen bonds. The collagen molecules aggregate in an ordered chain to form microfibrils, which then come together to make fibers. Covalent cross linkages form at various levels of organization of fibers and these provide greater strength to collagen fiber mechanically. Biosynthesis of collagen is related with many posttranslational modifications. Biosynthesis of collagen contains these differing posttranslational reactions: 1. Some prolyl and lysyl residues' hydroxylation. 2. Some hydroxylysyl residues' glycosylation. 3. Folding of polypeptides of procollagen into triple helix. 4. Transformation of procollagen to collagen. 5. Self building into fibrils. 6. Strategically located hydroxylysyl and lysyl residues' oxidative deamination to form cross-linkages between polypeptide chains of the same molecule and also among the neighbour molecules that provide stability and strength to the fibrils.

The first three steps occur within the cell, on the other hand the last three take place out of the cell. The unique feature of each type of connective tissue such as the rigidity of the bone, flexibility of the skin, elasticity of the arteries and strength of the tendon is determined by the organization and composition of collagen as well as other components of matrix. However amino acid composition of collagen might slightly differ between species (Table 2.2).

Table 2.2: Amino acid composition of collagens from different species [19].

COLLAGEN SOURCES AMINO ACIDS	AMINO ACID (%)					
	STURGEON SWIM-BLADDER	SHARK	FEMUR OF OX	PORCINE SKIN	HUMAN TENDON	HUMAN BONE
Aspartic acid	6.9	6.4	4.3	5.1	3.9	3.8
Threonine	3.8	2.4	1.9	1.7	1.5	1.5
Serine	5.8	3.3	3.5	3.5	3.0	2.9
Glutamic acid	11.4	11.0	6.5	11.4	9.5	9.0
Proline	12.8	13.3	11.8	13.3	10.3	10.1
Hydroxyproline	11.8	8.8	10.3	12.6	7.5	8.2
Glycine	27.7	25.4	31.7	22.1	26.4	26.2
Alanine	11.6	11.4	10.8	8.7	9.0	9.3
Valine	2.3	2.7	2.4	2.1	2.1	1.9
Methionine	1.4	1.8	0.5	0.5	0.5	0.4
Isoleucine	1.7	2.7	1.3	1.1	0.9	1.1
Leucine	2.6	2.6	3.0	2.9	2.1	2.1
Tyrosine	0.5	7.2	0.7	0.5	0.3	0.4
Phenylalanine	2.5	2.1	1.9	1.9	1.2	1.2
Histidine	0.8	1.7	0.6	0.7	1.4	1.4
Hydroxylysine	1.9	0.9	0.8	-	1.5	0.6
Lysine	3.5	3.7	3	3.5	3.5	4.6
Arginine	10	8.6	5.0	8.4	16.0	15.4

The glycine residue that is located at every third position contains the smallest side chain (R-group) and therefore it is able to occupy a limited space where the three chains of polypeptides are nearest to one another. Hydroxyproline and proline residues inhibit the free rotation around N-C terminal bond. The chain of polypeptides has a kinked and rigid conformation. Above mentioned stereochemical features causes the formation of the superhelix shape. Formation of hydrogen bond between the glycy residue's NH group in one chain and prolyl or other amino acid residue's OH group in the X-position of a chain next to it causes stabilization of triple helix. If prolyl residue is replaced by any other amino acid, the interchain hydrogen bond take place by the way of a water bridged structure. These bonds are further stabilized by hydrogen bonding between hydroxyl group of the trans-4-hydroxyprolyl residue, which is located at the Y position. Additionally the chains are held together by covalent linkages associated with lysine residues.

Polypeptide chains made up of only glycine, proline and hydroxyproline residues with this order form a very stable helix. Furthermore the thermal stability of the triple helix decreases in the order of the repeated sequences of the chain: Gly-Pro-Hyp>Gly-Pro-Y>Gly-X-Pro>Gly-X-Y. In polypeptide chain of tropocollagen, approximately one third of the chain has Gly-Pro-Hyp order and two thirds has Gly-X-Y, for this reason triple helix stability is reduced. Amino acid residues except for hydroxy proline and proline that fit the X and Y positions decrease stability of the helix on the other hand they are necessary for the organization of collagen at the next level, i.e. microfibril formation. Hydroxylysine glycosides occur at the Y position and may determine the diameter of the fibril. The side chains of the amino acids protrude from the center of the helix towards outside. This allows hydrophobic and ionic interactions between tropocollagen molecules. These interactions effect the way by which individual molecules come together and form microfibrils first, then larger fibrils and eventually fibers [17].

All fibrillar collagens are synthesized and secreted from the cell into the extracellular matrix as precursors called procollagens (Figure 2.5). The ends of each rod have short extensions that are not in the form of triple-helix. These end-regions

or telopeptides that are different at the amino and carboxyl termini of each rod are necessary in the formation of the intermolecular cross-linkages. Intermolecular cross-linkages stabilize the fibrils and increase their tensile strength. The covalent cross-linkages between N- and C- telopeptides and their corresponding helix region on neighbouring molecules effects formation of the mature fibril [20]. Proteolytic cleavage of N- and C-terminal of propeptides by specific procollagen N- and C- proteinases ends up with the production of mature collagen molecules. These spontaneously assemble into fibrils [21].

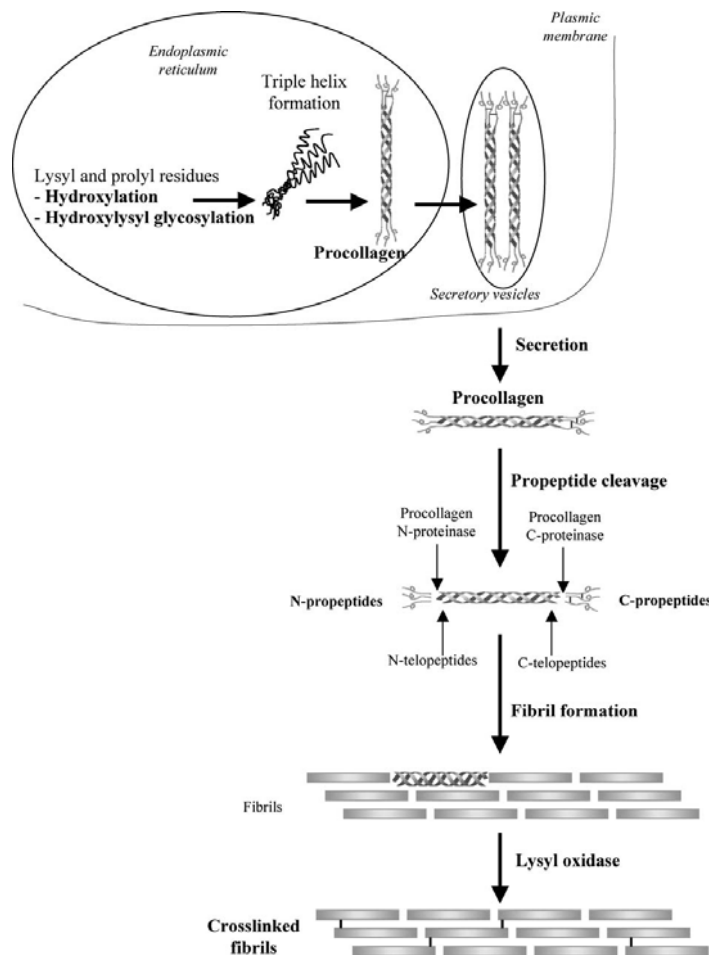


Figure 2.5: Schematic diagram showing the different posttranslational modifications and assembly of type I collagen into fibrils [22].

The microfibril, about 4nm wide, is made up of four to eight tropocollagen molecules that align in a highly ordered and specific way. This could occur due to the interactions of amino acid residues at X and Y position. In this arrangement, each molecule is placed by about one fourth of its length away from the neighbours longitudinally. The longitudinally displaced tropocollagen molecules are not linked. There is a gap of about 40 nm between the end of one triple helix and the beginning of the next. These holes may provide sites for deposition of HA crystals in the formation of bone.

The tensile strength of collagen fibril is determined by covalent cross links related with lysly and hydroxylysyl side chains. The packing arrangement of tropocollagen molecules provides tensile strength and prevents sliding of molecule over another. The properties and extend of cross linking depend on physiological function as well as the age of the tissue. With age, the density of cross linkages increases, making connective tissue rigid and brittle [17].

2.4. BONE MODELLING and REMODELLING

Bone is continuously being turned over by modelling and remodelling processes. This allows maintenance of the biomechanical integrity of the skeleton. In addition, it supports the maintenance of ionic balance of plasma and mechanical support of the body. Bone remodelling allows the removal of old bone and replacement with the new bone tissue [23]. In this way, bone modelling and remodelling achieve strength for loading and lightness for mobility; by depositing bone in locations where it is needed to modify bone size and shape, and by removing bone from where it is not needed to avoid bulk [7].

Bone remodelling has five phases. 1. Activation: Osteoclasts are activated; 2. Resorption: Osteoclasts erode and form a bone cavity; 3. Reversal: Osteoblasts are activated; 4. Formation: Osteoblast fill the cavity with the new bone; 5. Quiescence: Bone tissue stays inactive until the next cycle begins (Figure 2.6).

The aim of modelling and remodelling processes while growth is to attain the maximum strength for skeleton whereas the aim of bone remodelling in period of adulthood is to provide strength of bone by damaged bone removal. Bone acquires fatigue damage at the time of repeated loading like roads, buildings and bridges, but only bone has a mechanism for damage detection, removal and replacement with newly formed bone. Therefore, bone can restore composition of material, macro and micro architecture. However, in osteoporosis, there is a disequilibrium between the resorption and formation in the favor of bone resorption.

The formation phase of the remodelling cycle must restore the damaged bone by normal bone with a same volume. This event is based on the normal work, production and life span of osteoblasts and osteoclasts which play a role in Basic Metabolism Unit or Basic Multicellular Unit (BMU), but the BMU is a multicellular unit and a lot of types of cells take place in the cascade of remodelling [7].

The number of active remodelling units in the trabecular bone is about three times higher than that in the cortical bone. Because of the significant amount of surface area, trabecular bone is more active metabolically than the cortical bone [7].

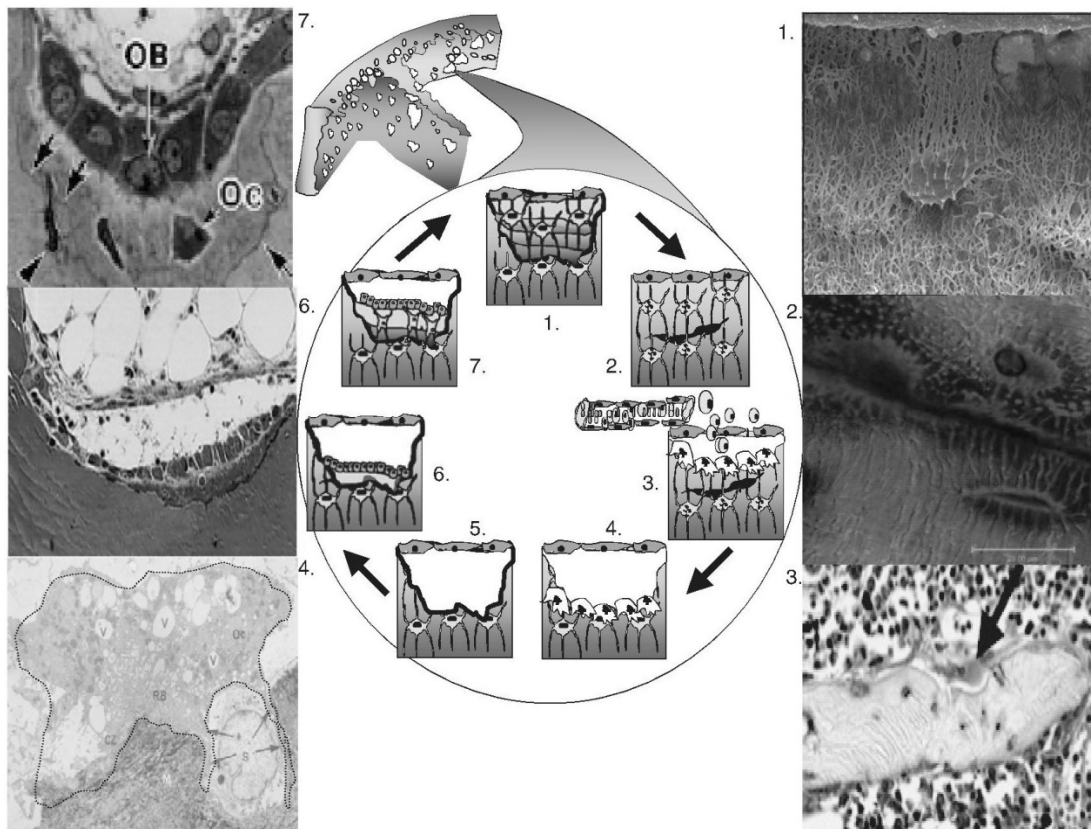


Figure 2.6: Remodelling cycle. (1) Osteocytes are connected to each other and to lining cells on the endosteal surface adjacent to the marrow; (2) Damage to osteocytic processes by a microcrack produces osteocyte apoptosis. (3) The distribution of apoptotic osteocytes provides the topographical information needed to target osteoclasts to the damage. (3) Lining cells secrete collagenase to break down unmineralized collagen revealing mineralized bone and creating remodelling cavity in which progenitors for osteoblastogenesis and osteoclastogenesis are brought by blood or marrow locally. (4) Osteoclasts (Oc) make bone resorption and clean damage as well as phagocytose osteocytes by its cytoplasmic extensions between osteocyte and lacunar wall. (5) The reversal phase and cement line formation comes after. (6) Osteoid is produced by osteoblasts and (7) Some osteoblasts are embedded in osteoid in which they stay and differentiate into osteocytes making reconstruction of the canalicular network of osteocytes [7].

2.4.1. Age-Related Alterations in Modelling and Remodelling Adulthood

Bone capacity for modelling and remodelling decreases since there are four changes in age-related the cellular machinery. Adaption capacity of bone to loading is damaged because as remodelling works each time, bone is lost. Therefore, age-related alteration in the machinery for the first time is a decrease in formation of bone at the level of cells effecting BMU [7]. The second problem is a decrease in formation of bone at tissue level. The third abnormality in remodelling is an elevation of resorbed bone volume by the BMU, which could be due to a period of deficiency of sex hormone [7]. The fourth abnormality due to aging in the cellular machinery is an elevation in bone remodelling rate after menopause. This goes together with by the negative bone balance in BMU as resorbed bone volume increases and newly formed volume of bone decreases [7].

2.5. MECHANICAL PROPERTIES OF BONE

The mechanical properties of bone can be examined at two levels which are structural and material behaviour. The tissue level or material features of bone are studied by making standardized mechanical tests on uniform bone tissue samples. Testing at tissue level is partially independent of geometry or structure of bone. Additionally, by studying the bones' mechanical behavior in the form of complete anatomical units, the contributions of structural characteristics could be identified. Mechanical properties of bone at the two levels presents how bones react *in vivo* forces and can be studied by experiments on sections of bones[7]. Some physical and chemical characteristics that may effect biomechanical quality are shown in Table 2.3 [24].

Table 2.3: Some physical and chemical characteristics of bone that may influence biomechanical bone quality are shown, categorized by physical scale [24].

SCALE (m)	BONE CHARACTERISTICS
$>10^{-3}$	Whole bone morphology (size and shape)
	Bone density spatial distribution
10^{-6} – 10^{-3}	Microarchitecture
	Porosity
	Cortical shell thickness
	Lacunar number/morphology
	Remodeling cavity number, size, and distribution
10^{-9} – 10^{-6}	Mineral and collagen distribution/alignment
	Microdamage type, amount, and distribution
$<10^{-9}$	Collagen structure and cross-linking
	Mineral type and crystal alignment
	Collagen–mineral interfaces

2.5.1. The Hierarchical Structure of Bone

There are several hierarchies of bone which span different length scales. The basic building blocks of the bone are an organic matrix, which is mostly type-I collagen, and a mineral phase (level 1, Figure 2.7). At the next scale length, bone is made up of mineralized collagen fibrils that are 80–100 nm in diameter (level 2, Figure 2.7). Collagen molecules are arranged in a regular, staggered array (level 3, Figure 2.7). The crystals are located within and around the collagen fibrils. They are about 50 nm long, 25 nm wide and 2–3 nm thick. At the later step of hierarchy, the fibrils of mineralized collagen are organized by several patterns. The pattern found most commonly is the lamellar form (level 4, Figure 2.7). Single lamella is 2–3 mm has thickness and is organized in a number of layers, each of which has different fibril orientation. A parallel arrangement could be seen in plywood, therefore it is called as rotated plywood motif. At the next level hierarchy, lamellae are organized

in different ways, with respect to the species and location. For example, the most commonly seen arrangement of layers is concentric type (named as Haversian systems or secondary osteons) in mature bone of horse and dogs. These form cylinders 150–250 mm in diameter and contain a central hollow tube 80 mm in diameter, which contains blood vessels and nerves (level 5, Figure 2.7). Other forms commonly seen are fibrolamellar type (also called as plexiform, as in bovine bone), and lamellar-zonal type (in the reptiles' long bones). At the next stage, structure of bone could be sponge like (cancellous) or generally solid (cortical bone). Cancellous bone has a lot of spaces allocating plates (trabeculae) and struts (level 6, Figure 2.7). This complicated organisation, having three dimensional geometry, finally makes the bone [25] (level 7, Figure 2.7).

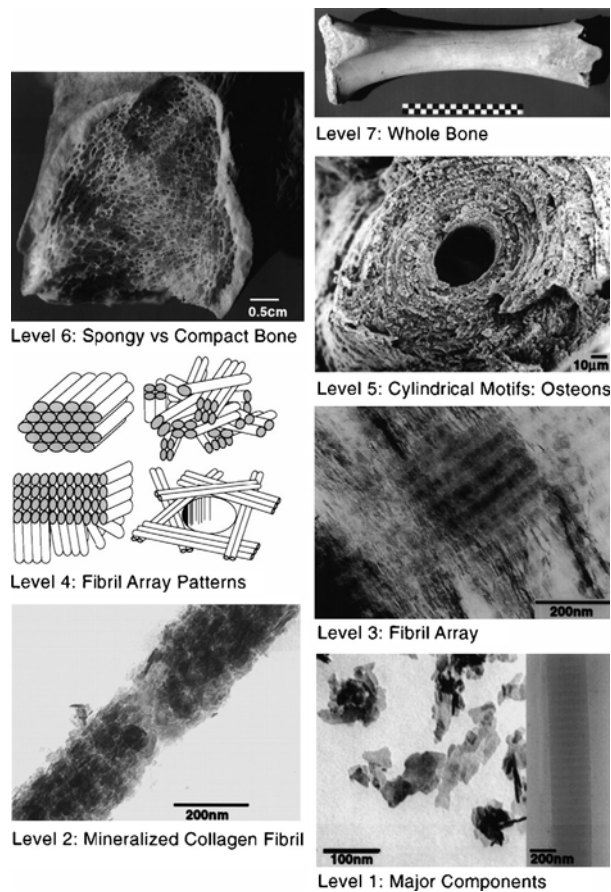


Figure 2.7: The hierarchical levels of structure found in secondary osteonal bone [25].

2.5.2. The Graded Structure of Bone Material

The structure, composition and mechanical properties of a specimen may change either in discrete steps or continuously. The failure resistance and damage properties of surfaces to shear and normal contact or impact forces could be varied by spatial gradients in constituents of a material. Bone is a very good material for a natural material in graded organization [7].

The graded bone organization could be found at some levels. For example, at the level of osteons, mineralization level varies within osteons. Because the younger (inner) lamellae are mineralized less than the older (outer) ones at the beginning, later on inner lamellae contain more mineral. A different instance is the interstitial lamellae that form from residuals of old osteons. They fill areas among osteons, and contain more mineral than osteons. Bone organization in graded building alters the bone's mechanical behaviour, particularly the propagation of crack. Because most cracks tend to propagate until lines of cement. They stop there because of weak interface and turn around the osteon instead of passing through osteon. Another example is the transition between cortical and cancellous bone which is also graded, this can be observed grossly with increased bone porosity from the endosteal to the periosteal surface [7].

2.5.3. Anisotropy of Bone

Biological materials usually have ordered structural units. These provide them quite different mechanical and material characteristics under various circumstances. Therefore, bone's mechanical features change depending not only on the amount of force, but also its rate of application and direction. Materials defined as ideal are homogeneous and always react similarly independent from orientation of load. This is called as *isotropy* and materials have isotropic behaviour [7].

On the other hand, bones show different mechanical features in different directions of loading. This is known as *anisotropy*. Anisotropic behaviour of bone

could be exemplified by the load application to femur bone. Since the femur has vertical orientation, with each step taken during walking, it undergoes to a compressive load. Therefore, it has a capacity to withstand high compressive loads (for example jumping down from a height) without deforming permanently. On the other hand, if it is subjected to a similar load from a transverse direction, it will cause bending stresses that would not be compensated by femur causing fracture. Therefore, the rigidity and strength of bone are normally bigger in the customary loading direction. This works especially in cortical bone, in which osteons are longitudinally oriented [7].

2.5.4. Role of Bone Composition and Microstructure

The mechanical properties of cortical bone are mostly dependent on porosity and the degree of matrix mineralization. More than 80% of the variation in the elastic modulus of cortical bone can be explained by a power-law relationship of the matrix mineralization and porosity. Some studies show that, with increasing age, the mineralization of the matrix increases, causing a stiffer, but more brittle material behavior although other studies show no age-related changes in the degree of mineralization. The strength and modulus of elasticity of trabecular type of bone are effected with BMD very much [7]. Calculation of power-law relationship in bone which takes BMD as a variable shows alterations in strength and modulus of elasticity from 60% to 90% (Figure 2.8).

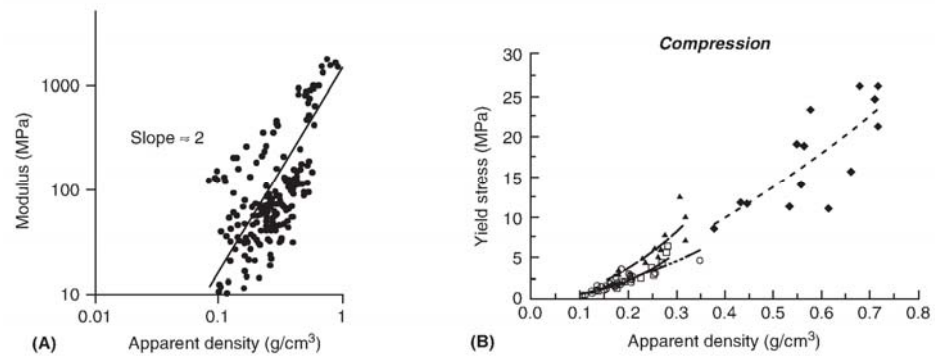


Figure 2.8: Variation in the modulus and strength of trabecular bone with respect to bone density. (a) Modulus of elasticity studied in power law relation as a function of BMD for trabecular bone. (b) Yield stress under compression was studied as a function of BMD in specimens of human trabecular type of bone [7].

The study of power-law relationship taking density as a variable show that minor alterations in BMD could lead to striking variations in mechanical behavior of bone. It was suggested that, a decrease of 25% in BMD that corresponds to some bone loss due to aging for 15 to 20 years, would cause a decrease of strength by 44% in trabecular type of bone [7]. But, strain at yielding and at failure are slightly effected by BMD in trabecular type of bone (Figure 2.9).

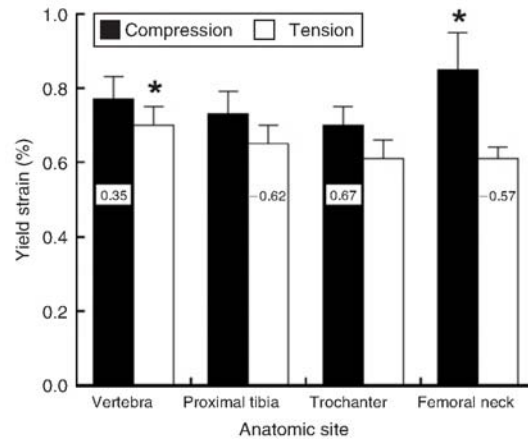


Figure 2.9: Strains for tension, compression and at yield strains of human trabecular type of bone bone in human considering BMD. Error bars show one standard deviation [7].

Cortical and trabecular type of bones have anisotropy. Bone is found to behave generally strongest and stiffest in the vertical loading direction. For instance, if the cortical bone specimen from femoral diaphysis is loaded longitudinally compared the transverse direction it shows a higher strength and modulus of elasticity modulus (Figure 2.10). Trabecular type of bone taken from the vertebra demonstrates a similar anisotropic character. On the other hand, trabecular specimens taken from the iliac crest and centre of head of humerus are almost isotropic. These show that the degree of anisotropy changes with anatomical site of the specimen taken and mode of loading. Therefore, it can be concluded that the anisotropic property of bone gives the bone highest resistance in the direction of principle loading, but causes the bone to resist least out of axis or oblique to the primary loading direction [7].

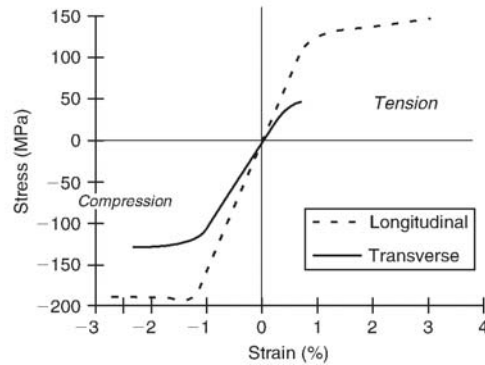


Figure 2.10: Stress versus strain graph for specimens taken from the diaphysis of cortical bone oriented transversely (T) and longitudinally (L). Anisotropic character of bone is shown in specimens tested longitudinally and transversely [7].

Microarchitecture is one of the properties that effects mechanical behavior of bone. The microarchitecture determining factors such as quantity, connections and thickness show strong correlation with BMD and each other. These factors decrease with diminishing BMD on the other hand anisotropy and separation of trabecules increase with diminishing BMD [7].

Other features are the cytological structure (primary versus secondary osteons), constituents of collagen and fiber orientation, the quantity and compositional quality of cement lines, and existance of fatigue microdamage [7].

Transgenic mice expressing abnormal type I collagen gene products have been used for studies for the effect of the collagen on the bone mechanical features. In this way, the matrix of these bones are made abnormal biochemically. The condition in mice might be similar to human collagen diseases, such as osteogenesis imperfecta. It was found that in young animals experiments the decreased production of type I collagen causes a reduction in strength and stiffness in static loading tests [7].

Gradual difference in the mechanical features of bones was detected by increased age. It is proposed that increased fragility of bone by aging is related with

alterations in material properties of collagen. With aging, adaptive changes in bone geometry such as cortical expansion, endosteal resorption, and periosteal bone apposition result in the maintenance of structural level mechanical properties. This is because of the increases in the areal and polar moment of inertia of whole bones. The relationship between composition, structural geometry and biomechanical characteristics of bone demonstrate the significance of the form-function relation in biomechanics of bone [7].

2.6. AGE-RELATED CHANGES IN THE MATERIAL PROPERTIES OF BONE

It was demonstrated in women and men that increasing age causes a decrease in modulus of elasticity and ultimate strength in both trabecular and cortical type of bone. In human cortical bone from the femoral mid-diaphysis, the tensile and compressive strengths and elastic modulus decrease approximately 2% per decade after age 20. Additionally, deformation capacity of bone and energy absorption before fracture occurs is found to decrease about 5% to 12% for per decade. This finding suggests that cortical type of bone becomes less tough and more brittle aging. Fracture toughness diminishes by 4% per decade. Energy to break a specimen from cortical bone by impact loading is found to differ 3 times between 3 and 90 years of age. Increase in porosity with aging could be partially responsible for the elastic modulus and ultimate strength. However, there are possible supplementary causes such as increased mineralization of matrix mineralization and/ or collagen cross-linking alterations by aging [7].

Similar age dependent decrease in material properties may be observed in trabecular bone of human which is mainly a result of the decline in BMD. For instance, BMD of trabecular bone in vertebrae decreases roughly by 50% between ages of 20 to 80. The mechanical properties (compressive elastic modulus, ultimate stress, and energy to failure) decrease approximately 75% to 90%. In trabecular bone of the proximal tibia, an age-related decline in apparent density of 25% is

accompanied by a 30% to 40% reduction in compressive strength and energy absorption properties. In addition, the anisotropy in strength of trabecular bone from human lumbar vertebrae increases with age, as the ratio of compressive strengths of vertically and horizontally loaded specimens increases from about 2 at age 20 to 3.5 at age 80. This observation may reflect age-related changes in the trabecular architecture of vertebral bodies, where horizontally oriented trabeculae are thin and disappear to a greater extent than vertically oriented trabeculae. It is needed to underline that alterations in BMD do not totally describe the age-related decrease in mechanical properties of trabecular type of bone [7].

2.7. MECHANISMS OF BONE FRACTURE

The first bone fracture mechanism occurs when load goes beyond the physiological range accidentally, producing stresses over the strength of bone that has been acquired after growth and development adaptation (for example: traumatic fracture). Two basic reasons for this fracture type are present. An external impact could be generated, e.g., by a fall or by fractures which take place spontaneously without trauma, after a muscle contraction. The second are frequent in osteoporotic older people [7].

Fatigue or creep make up the second type of fracture. Bones usually bear cyclic loads which could generate microdamage and roughly constant loads for long periods of time. If microdamage accumulation is faster than remodelling causing repair, microcracks could become numerous to form macrocracks and make the main fracture. The description defines a stress fracture. It is generally found in people who are subjected to heavy repetitive physical activities as in balet dancers, soldiers and athletes. It is also found in people with low level of activity whose bones are effected by osteoporosis, particularly at advancing ages when remodelling of bone is inactive nearly [7].

However, stress fractures prevention is not only dependent on remodelling causing repair. It is also determined by crack propagation and the initiation process.

The cortical bone microstructure is close to composite materials that are fiber-reinforced. Osteons resemble fibers, interstitial tissue resembles to composite matrix and the cement line functions as a weak interface where cracks might begin [7].

Generally, two fundamental mechanisms cause fractures: when the rate of damage goes beyond the repair/remodelling rate (damage in excess) or when a defective repair/remodelling mechanism does not repair a normal damage (deficient repair). Accumulation of damage in bone is close to synthetic structural materials. It was shown that fatigue damage is similar in vitro and in vivo. The microdamage (related to the load and number of cycles), may appear in different ways at the microstructural level: debonding of the collagen–HA composite, slipping of lamellae along cement lines, cracking along cement lines or lacunae, shear cracking in cross-hatched patterns and progressive failure of the weakest trabeculae. At the macroscopic level damage is hardly visible before there is a large crack and global failure [7].

2.8. MICRO INDENTATION

2.8.1. Structural Organization and Mechanical Properties of Bone

Diseases of bone with a reduced strength and increased risk of fracture would be overcome with the information obtained from mechanical properties of bone from different components of bone and relation between them at the various levels of hierarchical structural organization [26].

1) Cancellous and cortical bone are at the macrostructural level; 2) Haversian systems, osteons, single trabeculae (from 10 to 500 μm) form the microstructural level; 3) lamellae (1–10 μm) are at the sub-microstructural level 4) fibrillar collagen and mineral (from a few hundred nanometers to 1 μm) form the nanostructural level and 5) molecular structures such as mineral, collagen, and non-collagenous proteins (below a few hundred nanometers) are at the subnanostructural level. Irregular but

optimized organization of this hierarchically organized structure makes the bone material heterogenous and anisotropic [27].

Mechanical properties of bone were found to vary at different levels; Young's modulus measured between the 14–20 GPa in large wet cortical specimens but 5.4 GPa in microbending test and 22 GPa by nanoindentation in dry bone [27]. This discrepancy might be due to the testing method or the influence of microstructure.

Cortical bone is composed of Bone Structural Units (BSU) called osteons. Each mature BSU has a fairly uniform mineral content which plays a major role in bone strength. Information about the role of collagen is limited and it may play a role in plastic deformation [26].

2.8.2. Microindentation

Micro indentation has been used as a method to investigate the deformation properties of bone [28]. The load is applied onto the material by the indenter stylus for a determined duration of time. The point that contacts the specimen could be pyramidal, spherical, or another shape. Vickers indentation has a diagonal shape, whereas Knoop indenter has an elongated rhombohedral shape which enables investigation of in plane anisotropy [29] (Figure 2.11).

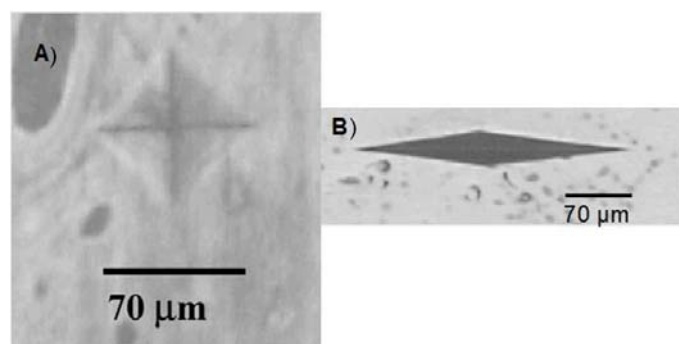


Figure 2.11: A) Image of a microindentation by Vickers technique from bovine bone in wet state, B) Knoop microindentation image obtained from bovine bone in wet state [30].

Microindentation has been used as a method for obtaining the elastic modulus and hardness of bone, dentin, tooth and enamel. Dry cortical bone was shown to have plastic, viscoelastic and brittle properties [30].

Most biomechanical tests made on bone gave attention to fracture at macroscopic size which resulted in lack of visualization of submicroscopic damage. Micro indentation helps to evaluate some contact-related features, especially phenomena of surface-damage under compression of sharp-particle. Additionally, imaging of microindentations facilitating SEM could give information about the response of material to micro-scale mechanical loads to determine the behavior of micro structural components in damage [28].

2.8.3. Hardness

Hardness is the materials resistance against deformation. Microindentation has been used to estimate the hardness of bone microstructure in studies [31]. As an advantage, hardness tests can be done on small sized specimen [28]. Microhardness makes microscopic sized imprints, thus helps to determine hardness in small areas of the sample. The dimensions of the indentation are measured which are used to calculate hardness at the site of indentation. Hardness unit is kg/mm^2 which presents load per unit area of projection [30].

Contact Hardness (H_c) is to the ratio between indentation load and the contact area of the indentation print. Since indentation causes elasto-plastic deformations, H_c is related with both elastic and plastic properties of a material. In bone, H_c was found to be linearly dependent on E. Therefore, H_c cannot be used to distinguish only the plastic behavior of the material [26].

2.8.4. Factors Effecting Microindentation Test Results in Bone

Elastic modulus and hardness of bone are directly affected from both composition and microstructure of bone at the site of indentation. Bone is a

heterogeneous and anisotropic composite material at the scale of nano and micrometers. Amount of anisotropy could change and was described basically as orthotropic or transversely isotropic [30].

Appropriate the independent microindentation variables must be chosen to assure reproducibility and precision of measurement. Variability among measurement sets on the same specimen can result from for example creep and relaxation representing time domain phenomena and from pores representing example the spatial domain. Calibration, setup and compliance of testing machine is important at values of low applied load. Machine compliance is in series with the sample. If the compliance of the machine is low, it could contribute to the compliance of the sample thus causing an error of measurement [30].

There are studies in the literature that investigate the effect of applied mass on variation of hardness. A report showed that there is not any hardness variation with applied mass. Another study found 50 g as a level of applied load below which measurements of microhardness were not safe [30]. Since wet state represent a more physiological state of bone, duration time of a sample standing out of a waterbased liquid is vital. It is reported that hardness increases with time out of liquid [30].

The predetermined microindentation different variables such as applied mass, length of indentation, time needed for drying, time period passing between indentation and measurement; and length of distance between the pores and indentation site was studied [30].

2.9. TOUGHNESS

2.9.1. Strength vs. Toughness

Toughness is described as a resistance of a material to fracture. Strength is the resistance to permanent (plastic) deformation. High strength goes with low toughness and vice versa for many of the ductile materials. On the other hand, in brittle materials as in the case of ceramics in which visible plastic deformation is almost not

present, the strength does not depend on only the strain or stress the material could resist but it is related with the defect distribution, e.g. microcracks [32].

As a measure of toughness, work to fracture, is measured by breaking an unnotched sample, then the strength and toughness would measure the same feature of the material. Since the pre-existing distribution of microcracks is barely clarified, toughness is measured by first precracking the test sample by worst-case flaw, and then determining the stress intensity or energy required to fracture. Bone is a brittle type of material in which microcracks are present and shows inelasticity partially, the bone strength would indicate the stress to deform and fracture it and would be effected by flaw-like defects [32].

Mechanisms inhibiting the motion of dislocations also reduce the materials' ability to relax crack tip stresses. Metallic materials have an inverse relationship between strength and toughness. On the other hand, most of the composite materials have a positive relation between toughness and strength. These materials have a heterogenous structure and would bear diffuse microstructural damage without breaking. As the prefracture damage becomes greater, the postyield deformation becomes greater so the material becomes tougher [33].

Bone generates microcrack type of damage that initiate at yielding. With respect to the amount, size of microcracks and their interaction, bone becomes tough to some degree, by its ability to extend postyield deformation. Aging bone has a less degree of capacity to resist prefailure or postyield damage therefore less tough [33].

2.9.2. K_{Ic} and G_{Ic} Fracture Toughness Measurements

Load displacement curve area that was obtained during the failure of an uncracked specimen is divided by twice area of crack-surface to calculate work of fracture to find the toughness of cortical bone. Results obtained by this method could demonstrated to be dependent of size and geometry [34].

Linear-elastic fracture mechanics can help to define the fracture features of cortical bone. For a material with linear-elastic property where inelastic property such

as yielding is constrained to a small area close to the tip. Displacement fields stress fields close to a previously formed crack tip are defined by the stress-intensity factor, abbreviated by K. K can be described for mode I loading (tensile-opening), mode II loading (shear) or mode III loading (tearing or anti-plane shear) with respect to geometrical crack configuration, (Equation 2.1) where σ is applied stress, and a is crack size, Q represents a constant without a dimension. Q depends on mode of loading (such as I, II or III) and geometry of the material sample (Figure 2.12). Fracture toughness which represents resistance of a material to fracture, in case of a specific mode of loading is defined as the stress intensity (K_{Ic}) at a critical value at the beginning of unstable fracture and it is calculated from peak stress [34].

$$K_{(I,II,III)} = Q\sigma_{app} (\pi a)^{1/2} \quad (2.1)$$

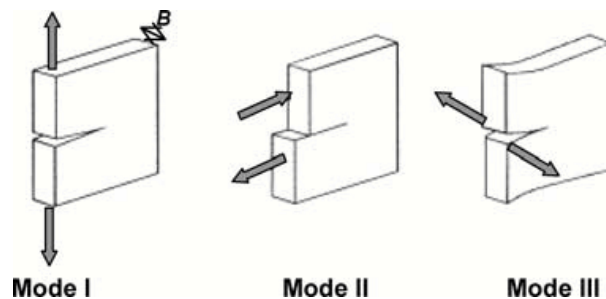


Figure 2.12: Illustrations for different modes of loading. Mode I loading was shown in the first figure to demonstrate tensile-opening type, mode II loading was shown in the second figure to demonstrate for shear type and mode III loading was shown in the third figure for anti-plane shear or tearing. Loading in vivo can be related with one or more than one of the modes [34].

Standard measuring methods for mode I plane-strain fracture toughness were developed by ASTM for metals (ASTM E399-90). Compact-tension specimens and single notched three-point bend are widely utilized for bone [32].

Alternatively, toughness could be defined in terms of a critical value of the strain-energy release rate G_c , which is the change in potential energy per unit increase in crack area at fracture that could be expressed as Equation 2.2 where specimen

thickness is shown by B, applied load is shown by P, and sample compliance with respect to crack extension is shown by dC/da (C represents compliance obtained from the load–displacement curve). G and K are related with Equation 2.3 for linear elastic materials. E stands for the elastic modulus (E′=E in plane stress, E/(1-ν²) in plane strain, where ν stands for the Poisson’s ratio, E stands for the Young’s modulus and μ′ stands for the shear modulus. If conditions for linear elastic exist, both G_c and K_c should give a measure of toughness that is independent of geometry, if plain-strain conditions are met. Table 2.4 shows single value of K and G for bone cortex to demonstrate toughness, comparing with some widely used materials [34].

$$G_c = \frac{P^2}{2B} \cdot \frac{dC}{da} \quad (2.2)$$

$$G = \frac{K_I^2}{E'} + \frac{K_{II}^2}{E'} + \frac{K_{III}^2}{2\mu'} \quad (2.3)$$

Table 2.4: Range of single value K and G (mode I) for cortical bone to demonstrate toughness, comparing with some widely used materials [34].

MATERIAL	E (GPa)	K _c (MPa√m)	G _c (kJ/m ²)
Cortical bone	15-25	2-7	0.15-3.25
Dentin	20-25	1-2	0.05-0.2
Titanium alloy (Ti-6Al-4V)	110	65-100	40-90
High Strength Steel (4340)	210	50-100	10-45
Commercial Silicon Carbide	400	3	0.02
Silicon	110	1	0.01

2.9.3. Crack-Resistance Curve

Fracture instability occurs after crack initiation that was because of the presence of subcritical crack growth in ductile materials and brittle materials that are extrinsically toughened. Bone behaves similar to this and generates its primary cause of toughness while crack grows. Crack-resistance curve, namely R-curve, to evaluate

crack growth is related to the measurement of the crack driving force (K or G) as a function of stable crack extension, Δa [32].

Although most reports on bone fracture studying with LEFM determined a fracture toughness with single-value (e.g., K_{Ic} , G_c), it is understood that the toughness belonging to bone is very well described by a resistance-curve (R-curve). Increasing crack extension was taken into consideration for bone toughness as in the case of composite materials or ceramics. The intrinsic and extrinsic factors affecting toughness can be separated by R-curve. ‘Intrinsic mechanisms’ are protective mechanisms that work mainly in the crack wake. Toughening mechanisms working extrinsically works as in the case of bone in which resistance to fracture increases with extension of crack. A resistance curve (R-curve) approach to fracture-mechanics can describe this fracture behaviour better [34].

2.9.4. Nonlinear-Elastic Fracture Mechanics

J-integral measurements

If extensive plastic deformation exists, non-LEFM might be better for evaluating toughness. If a material satisfies a nonlinear-elastic constitutive law which relates stress (σ) to strain (ϵ) as $\epsilon/\epsilon_0 = \alpha (\sigma/\sigma_0)^n$, where σ_0 and ϵ_0 are reference values, α is a constant, and n is the strain hardening coefficient, the local stresses, σ_{ij} , at distance r and angle θ to a crack tip can be written by an asymptotic solution (Equation 2.4) where angular function of θ and n is shown by $f_{ij}(\theta, n)$, integration constant is by I_n an, and J-integral by J . J is a parameter representing nonlinear-elastic (HRR) singularity. It uniquely describes stress and strain fields of the crack tip [32].

$$r \rightarrow 0, \sigma_{ij}(\theta, n) \rightarrow \alpha \left(\frac{J}{(\alpha \sigma_0 \epsilon_0 I_n r)} \right)^{\frac{1}{n}} f_{ij}(\theta, n) \quad (2.4)$$

2.9.5. Calculation of Toughness from Crack Length Measurements Directly

Vickers indents were developed as a method for calculation of the fracture toughness of ceramic materials. It measures lengths of cracks emanating from the indent the directly. It is reported in the literature as being the most extensively used technique [35] (Figure 2.13).

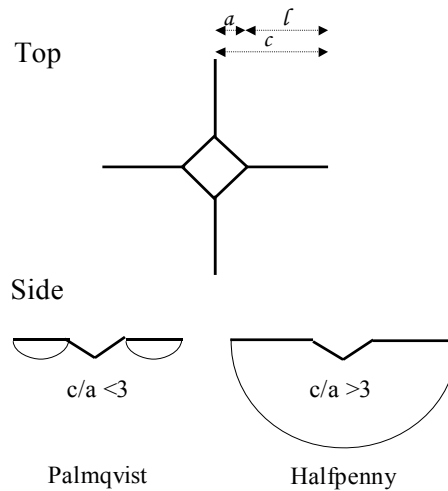


Figure 2.13: Schematic diagram for indentation fracture. Development of a radial crack of length a after loading. After loading and unloading cracks with overall size of c grows.

Indentation fracture method was put forward by Palmqvist first and developed by Evans et al. for the quantification of ceramics' the microstructural toughness. There are two types of shapes of crack formations. In the Halfpenny shape of crack “ c/a ” ratio is greater than 3. To determine the fracture toughness, the Evans and Charles equation can be used where P stands for the load applied by indentation (N), c stands for the length of the crack (m) (Equation 2.5).

$$K_{Ic} = 0,824 \cdot P / c^2 \quad (2.5)$$

Palmqvist shape crack is observed when the “c/a” ratio is smaller than 3. To determine the fracture toughness, the Palmqvist equation can be used where, H: Hardness, E: Young’s Modulus, Φ : the coefficient related to the material constraint ($\Phi \cong 3$) (Equation 2.6).

$$K_{Ic} = 0,035 \cdot \left(\frac{H^{0,6} \cdot E^{0,4}}{\phi^{0,6}} \right) \cdot \left(\frac{a}{(c-a)^{0,5}} \right) \quad (2.6)$$

Lawn et al. made an assumption that a median/radial crack system is formed because of tensile stresses in the unloading part of indentation, they made a model of the elastic-plastic behavior of the material with the effect of indent [35]. They derived Equation 2.7 where the hardness is shown by H, applied load is shown by P is the, Young’s modulus is shown by E, and length of the crack on the surface trace of half penny shaped crack which is measured from the indent center is shown by c. α stands for a calibration constant. It is determined empirically and its value is used as 0.016 ± 0.004 . This value represents a fit to data obtained experimentally [35].

$$K_c = \alpha \sqrt{\frac{E}{H}} \cdot \frac{P}{c^{3/2}} \quad (2.7)$$

There are numerous equations (more than 30) in the literature on this method to make formulations for the calculation of fracture toughness by the use of the length of the cracks on the indented sample surface. Many of these formula are found by curve fitting but not from physical models. Equation 2.7 is the most widely referred and used in measurements. There are some concerns about these formula. Standard deviation (SD) for the calculation of calibration constant on the data fit curve is high, about $\pm 25\%$ which may cause large errors, exceeding $\pm 50\%$ in some cases [35].

Accurate measurement of fracture toughness of materials in brittle character could be difficult. Making sharp preformed cracks might fail the specimen to a great extend or data obtained from notched specimens and toughness is measured at macroscale can give erroneously high values. Measurements of cracks made directly by impressing a sharp diamond indenter, could be considered as another method for

the measurement of toughness. Knoop, Vickers, Berkovich, and cube corner indentations are the examples of this method [35].

This measurement method could be quick and easy to make. It also needs specialized equipment less in number and experience. It makes it possible to make numerous measurements on a small amount of material [35]. In addition, it makes possible studying fracture properties both locally at microscale and at macroscale. Cracks produced in the bone are of the same scale of size seen in vivo, and may give an insight into the damage nature in bone. It was proposed that “in situ” bone matrix toughness measurement at the microscale is the next step in the bone quality and microcracks examination [36]. However, such techniques have been barely reported to give correct fracture toughness results compared with other methods [36].

Techniques related with direct measurements of indent cracks were proposed to be unsuccessful in quantifying the fracture toughness accurately to be able to compare with results obtained from other techniques and other studies. Another aim of using this method may be obtaining a semi-quantitative result quickly to rank toughness of various materials. It is proposed that this method needs large differences in toughness values make reliable conclusions [35].

VIF and Cube corner indentation fracture methods are found to be limited for measuring toughness and for comparing techniques because of the large errors ($\sim \pm 50\%$). Indentation toughness data are suggested to have a difference of at least three to four times to indicate a significant difference in actual toughness. Some new studies report that formation of cracking is difficult by this technique and the cracks located in the plastic zone of the indentation makes the utilization of linear elastic fracture mechanics invalid [35].

2.9.6. Factors Effecting Toughness

2.9.6.1. Effect of Loading Mode

Cortical bone is proven to show the least fracture resistance under mode I (tensile) loading, thus it has been widely studied. For instance, average proportion of G_{IIc}/G_{Ic} is 4.6 and 12.7 in human femurs and tibia, respectively. Likewise, higher G_{IIc} values compared to G_{Ic} was stated in the neck of human femur. G_{IIIc}/G_{Ic} and G_{IIc}/G_{Ic} were found to be 2.6 and 3.8 for longitudinal fracture and 2.9 and 3.4, for transverse fracture respectively in bones from bovine femur [34].

2.9.6.2. Plane Stress versus Plane Strain

If the thickness of specimen has a significantly larger scale than that of local inelasticity, G_c and K_c could be independent of geometry, thickness, and size thus plane strain condition is assumed to exist. On the other hand, the values of toughness could be significantly higher and may be effected by these factors in thinner samples. The ASTM standard (ASTM E-399) requires that Equation 2.8 for plane strain conditions exist for fracture toughness testing in mode I where B represents thickness of the material, σ_y represents the stress at yield. K_I and σ_y may vary with factors such as location, species and orientation, the condition in Equation 2.8 may not be always met for cortical bone, particularly for human bone. For example, a thickness of sample from ~1 to 10 mm could be needed to satisfy conditions of plane-strain in cortical bone in human. Contradictory results are available in the literature on fracture data of bone from different specimen thicknesses [34].

$$B \geq 2,5 \left(\frac{K_I}{\sigma_y} \right)^2 \quad (2.8)$$

2.9.6.3. Effect of Anatomical Location and Microstructural Orientation

The orientation relation between the bone and the crack has a significant effect on the resistance to fracture in cortical bone. Especially, cracking in transverse directions (for example L-R and L-C) in which the crack break through bone osteons, toughness was detected to be higher than cracking longitudinally (for example R-L and C-L), where the crack break osteons longitudinally (Figure 2.14). It was found that toughness increased progressively (from 3.2 to 6.5 MPa \sqrt{m}) in bovine tibia as the sample orientation was changed when the specimen measurements were made beginning from longitudinal direction, ending up with transverse direction. K_{Ic} for obtained from cracks made in transverse direction was found to be twice higher than cracks made in longitudinal direction tibia and femur of cows. If one tries to make cracks in the transversally in human humerus bone, similar results were found with cracks bending $\sim 90^\circ$ towards proximal-distal (longitudinal) direction anatomically [34].

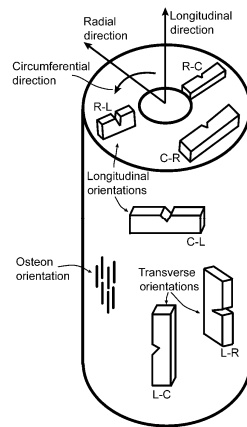


Figure 2.14: Fracture toughness standard suggested by ASTM E399 for the orientation code is shown by the illustration. The first letter represents normal direction to the crack plane whereas second letter denotes direction of crack propagation [37].

Bone location might effect fracture toughness. On the othe hand, it might be hard to differentiate from other variables. For equal sized specimens in C-L orientation, material from shaft of femur showed notably higher mean G_{1c} results compared to specimens from tibial shaft (520 vs. 400 J/m²). Microstructural differences associated with factor of location is not yet clear [34].

2.9.6.4. Effects of Microstructural Factors

Factors such as age, location and orientation could have an effect on the fracture properties of bone. They might be effected by microstructural differences which may be due to architectural alterations in the bone microstructure, or changes in constituents of bone (e.g., collagen). Osteoporosis cannot be considered just as a bone mass loss, but it is related with important alterations in the physical and biochemical features of the collagen network [38]. Variations in mineral content and BMD could be related with alterations in the bone toughness. The idea that increasing wet and dry density of bone increases its toughness and increasing porosity or mineral content decreases its toughness was suggested in some studies made on bovine and human bone. On the other hand, there are studies showing the fracture toughness was not effected from BMD or content of mineral, even it might decrease with aging [34].

Tissue remodelling process made in excess was proposed as a factor for increased fracture risk by aging which can cause loss in bone mass, and also other morphological changes of the microstructure of bone. Fracture occurs easily in bone obtained from human. Human bone contains smaller and fewer osteons. This is in contrast to in vitro findings. The cement line that is between secondary osteons, the lamellar matrix and orientation of the collagen fiber as being microstructural elements are considered to play an important role in the bone fracture. Micro and macro-cracks were detected to deflect alongside the cement lines as soon as meeting osteons. It suggests that the cement line would give the fracture a weak path. This may explain the strong orientation effects that is the bending of transverse cracks longitudinally [34].

Changes in the mechanical properties of the microstructural constituents, such as collagen, may also have an important effect on fracture resistance. Thermal and chemical denaturation of collagen was found to cause gradual attenuation in work of fracture obtained from specimens of human femur [34].

2.9.6.5. Effect of Age

Studies implied a significant decrease of the fracture toughness by aging as in Figure 2.15. Alterations in mineralization and diminished integrity of collagen network were associated with aging, leading to a reduction in the elastic deformability and toughness [34].

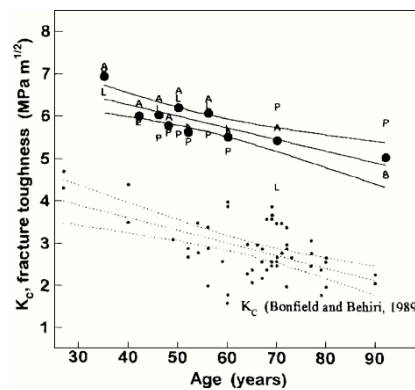


Figure 2.15: Variation in fracture toughness by aging in bone obtained from human cortex. Crack growth in L-C direction in femur (top) and for crack growth in C-L direction in tibia (bottom) are shown [33].

There are only a few reports in the literature studying the collagen changes with respect to the aging and their relation with bone toughness. Although these reports showed the collagen incorporation in age related alterations in quality of bone, mechanisms underlying this are still not identified [38].

2.10. MICROFRACTURE MECHANISMS OF BONE

2.10.1. How Fracture Occurs?

In terms of σ/ε behaviour, failure of bone is divided in three regions as shown in Figure 2.16. In phase I, the material deforms reversibly, but in phase II (the elastic-continuum damage mechanics domain) the material absorbs energy by developing diffuse microcracking damage. In phase III, the fracture mechanics (FM) occurs, energy is absorbed at the final fracture surface.

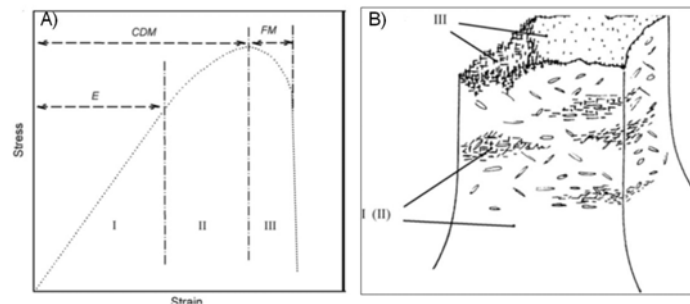


Figure 2.16: A) Stages of fracture behaviour: the elastic range E: the continuum damage mechanics range (CDM), and B) the fracture mechanics [39], [40].

Experiments with composite specimens demonstrate that damage starts as diffuse but at certain strain localizations distributed depending on the heterogeneity of structure. They could be in the form of damage bands which transfer stress into material or in the form of microcracks, that are traction-free. Sometimes, distributed damage end up with dominant single crack, at the tip crack-growing process. Macroscopic characterization of this process by toughness of bone uses LEFM analyses, including fracture toughness with single value, K_{Ic} . Because of the related scales of sizes, LEFM might not be a correct approach [41]

Crack growing can be classified basically into 3 groups in the K_{IC} - J fracture toughness tests. Brittle: In this type, crack propagates roughly straight and travelled with minor deviation from the plane of main fracture. This kind of crack would be the form that consumes least energy since the total length of the crack is shorter in a brittle and isotropic material. On the other hand, it is very energy absorbing process to cut through several bone elements. Deflected: In this type, the crack deviates to a side and grows with an angle. It is higher in length compared to a brittle crack it is relatively flat macroscopically. Looking at microscopically, it is made up of a number of small deviations down and up at interfaces of a material. It consumes little amount of energy than the “brittle” type of crack. Zigzag: direction of crack changes down and up by sharp angles as it met different structural elements. These types of cracks also consume less amount of energy when compared to brittle ones [33].

2.10.2. Microdamage as a Manifestation of Bone Fragility

Recurrent mechanical loading may cause ultrastructural damage which can be detected as microcracks in bone extracellular matrix seen by light microscopy. People at younger ages are exposed to more repetitive loading with higher magnitude and direction and can resist this with greater capacity of remodelling which is impaired with pathologic states and/or aging. Accumulated ultrastructural-level damage takes place in the etiology of fractures due to stress and osteoporosis [42].

Number of microcracks whose length can be up to 300mm can increase exponentially with age and contribute to fatigue fracture in bone. Most microcracks are found at inter-lamellar boundaries and cement lines, possible planes of weakness. It was shown that the main element that fractures is a fibril of mineralized collagen. Therefore, a relationship exists among loading that causes fatigue of bone, accumulation of microdamage, repair and remodeling of bone matrix and fracture. If damage process overcomes remodelling, fracture takes place [42].

2.10.3. Mechanistic Aspects of Microfracture

Microcracks appearing after cyclic tension are found to have diminished growth rate with increased length of crack and to be arrested typically in less than 10,000 cycles. Correspondingly, resistance to crack growth increases with extension of crack. Strain rate makes an influence on the magnitude of damage and attenuation of modulus, and could be as substantial as peak strain. Microdamage caused by fatigue could accumulate and ends up with fracture. While microdamage collects and unites, energy to failure, ultimate strength and stiffness are effected, causing decreased fracture resistance. Fatigue damage together with loss of stiffness causes reduced tensile strength in bone. Microdamage could attenuate fracture toughness and mechanical energy-absorbing capacity [42].

For example, microdamage may cause toughening in bone since network of microcracks (Figure 2.17) can absorb energy, distribute stress and slows crack advancement. Therefore fatigue life can be augmented. Vashishth et al. [43] studied the advancement of a main crack under tensile fatigue in bone and found out that increased number of microcracks causes increased fracture toughness. Based on this, microcrack-based toughening mechanism was proposed [42].

Crack bridging (Figure 2.17) is the occurrence of unbroken bone regions in the crack wake. These bridges span the wake of the crack and counteract opening more. In bone, this is proposed to be the dominant toughening mechanism [44]. It is complicating that while some studies has found useful and others show harmful effects of microdamage. Despite the fact that microcracking could increase fatigue life, microcracks that go beyond a critical crack length will enlarge and finally cause bone failure [42].

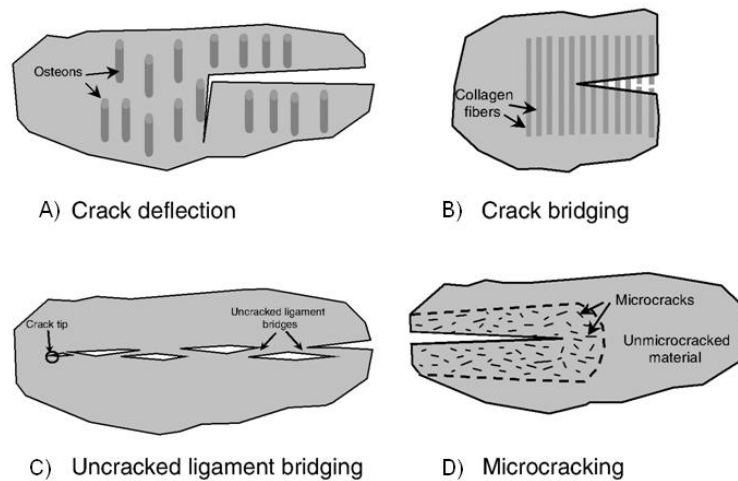


Figure 2.17: Illustrations for some types of toughening mechanisms in cortical bone: A) Crack deflection; B) crack bridging; C) uncracked ligament bridging; D) diffuse microcracking [2].

2.10.3.1. Microindentation Induced Microcracking

In the study of Yin et al., indentation deformation of the dry cortical bone is found to have a viscoelastic recovery at lower loads of indentation and a plastic behavior at any applied indentation loads [28]. Microcracks with a maximum length of about 20 μm were seen with increased applied loads. At 4.9N and higher loads, it was observed that most microcracks form at the Haversian canals boundaries, lacunae and canaliculi of osteocytes. Some microcracks were seen to propagate parallel to the alignment of the interstitial lamellae longitudinally. Visible microcracks were not detected by loads of 0.45N and less. Crack ligament bridging and crack deflection were identified as toughening mechanisms in the dry cortical bone by microindentation [28].

2.10.3.2. Microdamage Analysis utilizing SEM

In order to evaluate surface properties of bone, direct observation of microdamage and fracture mechanisms by microscopic techniques is required. SEM is an efficacious microscope to study composite structures' surface since it has high resolution capacity and great depth of field. It also allows obtaining 3D image of specimen. Bone damage at ultrastructural level which could not be detected by light microscope could be detected by SEM [42].

Cracks imaging with high-resolution in cortical human bone demonstrated that the crack propagates as a mother–daughter crack system of microcracks distributed around the primary crack and with lands of intact material (Figure 2.18). Region of intact lands and microcracks can be described as a bridging. The bridging is formed by uncracked ligaments, that convey stress across the damage zone and shield crack tip from the load. Bridges size could vary up to hundreds of micrometers. Patterns of bridges are essentially dependent on the bone heterogeneity, for instance, microcracks are seen to be related with the structures of osteons. Zone of bridging could be very large in human cortical bone i.e., ~5 mm [41].

Since zones of bridging (or zones of nonlinear process) could be as wide as cortical layer thickness, at the validity of LEFM becomes questionable. When large scale bridging or yielding occurs, the fracture toughness is not considered as a material constant. For a single main crack in a process zone, the toughness K_{Ic} is dependent on extrinsic factors e.g., the loading configuration and specimen shape, since the contribution of bridging to toughening depends on the length of the crack [41].

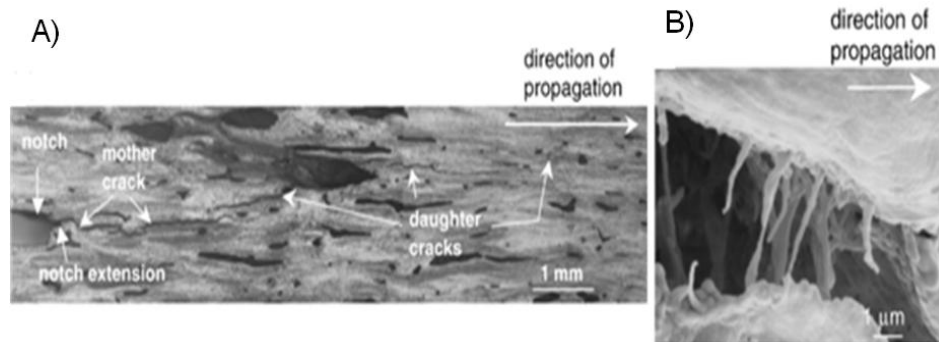


Figure 2.18: A) An image from a crack in cortical bone of 61-year-old human obtained by optical micrography. Notice the development of uncracked ligaments and daughter cracks. B) Collagen fibrils making up bridging in a crack wake in bone from human cortex [44].

Nalla et al. studied effect of cracks on bone microstructure by SEM [44]. It is observed that crack bridging formed by fibers of collagen, and microcracks play a role in the bone fracture toughness. Microcracks are seen to form close to osteons usually, causing pullout of osteon or debonding of matrix. Crack bridging, is related with the generation of unbroken regions which extend across the wake of the tip of crack and withstand opening of crack. Bridging forms by “unbroken collagen fibers” and “uncracked ligaments” [44].

The most frequently detected images on the surface of fracture are layered morphology and inter-lamellar delamination. This is related to microcracking for lamellar type of bones (e.g. Figure 2.19(a)). Protruded fiber bundles are associated with crack bridging by collagen fibers and/or uncracked ligaments (e.g. Figure 2.19(b)), and osteon pullout result from shear microcracks (e.g. Figure 2.19(c)).

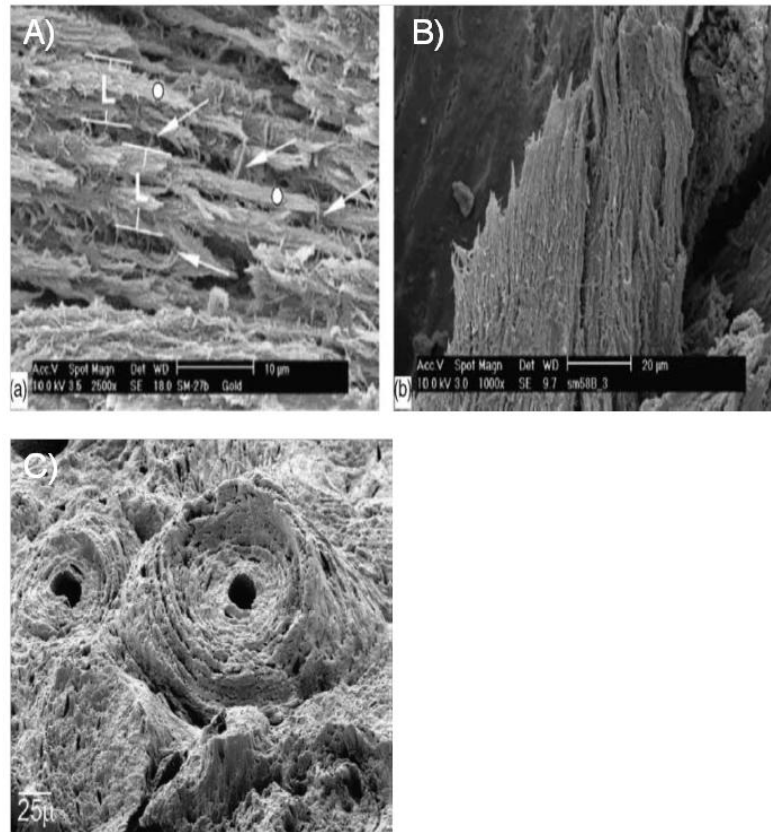


Figure 2.19: Fracture surface details from bovine bone: (a) intra-lamellar bundles of fibers (dots) represent lamellae which are pulled apart (L), lamellae are linked by inter-lamellar fibers (arrows), and; (b) pulled-out bundles of fibers (c). Transverse fracture surface image of an osteon by SEM. Rupture of cement line and interlamellar interfaces shows concentric shape of lamellae and the outer borders of “pulled out” osteons [42],[45],[46].

2.10.3.3. Compositional Parameters Affecting Bone Quality

Composition has an important effect both on mechanical features and damage accumulation. Bone can be considered as a composite material whose mechanical properties can be affected by changes in constituting elements such as e.g. mineral crystalline shape, size, orientation and original ratios for mineral to matrix and mineral to mineral components; organization and orientation of collagen fibers; collagen and

mineral bonding. These factors also change with age which might be related with age-related fragility of bone [42].

Typical structure of mineralized collagen fibrils at the nano scale is very important for its capacity to handle large amount of deformation and for its strength. Mineralized collagen fibrils fascilitate from staggered arrangement since it help to dissipates energy effectively and contributes to toughening [28].

2.10.3.4. R-curve Analysis

Compliance measurements give a method for differentiating the mechanism causing the rising R-curve behavior in bone: microcracking or bridging as being the predominant mechanism [43]. Otherwise the two mechanisms are expected to demonstrate a contrary effect. Bridging is expected to lower the compliance whereas microcracking is expected to increase, being just opposite effect of the other materials [47].

Rising R curve pattern is caused directly by extrinsic toughening mechanisms, that indicate crack-size dependent property of fracture toughness. For extrinsic mechanisms, extension of crack starts at *a crack initiation toughness* designated as K_0 . Stronger driving forces are necessary till a state of 'plateau' is achieved in toughness. The R-curve gradient could be thought as a *crack growth toughness* measure. R-curve analysis is both important to understand the fracture behaviour of bone an to differentiate the intrinsic and extrinsic mechanisms [34].

2.10.3.5. Intrinsic-Extrinsic Mechanisms of Fracture

Mechanisms that induce toughness can be classified as intrinsic and extrinsic. Intrinsic mechanism operates ahead of the crack tip and is the material's resistance to microstructural damage. It is important in ductile materials. It increases resistance to crack initiation. Extrinsic mechanism operates primarily behind the crack tip to reduce the driving force (for example, the local intensity of stres) at tip of the crack

(ie., shielding of crack tip). Crack bridging or microcracking are the most important examples of toughening in brittle materials and composites. It effects crack growth toughness which is detected as increased toughness by increasing crack extension that is also known as R-curve (rising resistance curve) behavior [44].

2.10.3.5.1. Intrinsic Mechanisms of Fracture

Assuming the presence of inelasticity, maximum amount of stresses make a top in front of the notch close to elastic plastic interface area, but maximum amount of strains make a top at the root of the notch. Cracks are observed to initiate at maximum strain points, such as at the notch root [34],[48]. If bones are exposed to bending, diffuse type of microdamage are found in zones of tension, while linear microcracks are found in areas of compressive strains [42],[49]. Growth of crack is shown to be self-limited in tension, but less constrained in compression in bone, which shows extension of crack is dependent on strain [42],[49].

Most microdamage is found in interstitial bone. Microdamage rarely passes across osteons and lines of cement, indicating that cement lines halts growth of crack. Ultrastructural and micro properties of bone could form stress concentrations that start crack formation such as osteocyte lacunae and vascular canals. Higher degree of mineralization could increase formation possibility of microcracking since the bone becomes more brittle. Lines of cement are considered to give a frailing intrinsic root for the fracture. They take part a role in the orientation effect of fracture in bone. Cortical bone bears lower amount of intrinsic toughness where the crack could extend along the lines of cement [34].

2.10.3.5.2. Dominant Extrinsic Mechanism

Predominant role of the extrinsic toughening mechanisms in mineralized tissues is still discussed. Constrained microcracking has been considered to be responsible from rising toughness behaviour of bone [45]. Nowadays it is discussed

that the primary mechanism causing rising behaviour of R curve is crack bridging [44].

Some studies on the cortical bone proposed that a microcracking causes the rising R-curve behavior for toughness which was close to that model proposed first by Evans and Faber for ceramics [44],[50]. Although microcracks ahead of the crack tip act to lower the intrinsic toughness, extrinsic toughening can occur due to the formation of a “frontal process zone” ahead of the growing crack with the consequent formation of a microcracking zone in the crack wake. If it is restrained by embracing rigid material resulting dilation and reduction in modulus, it can cause to protect the crack tip and thus help toughening the material extrinsically. Microcracks should be stable and restrained to give toughening, otherwise they may be harmful for the toughness of the material. Microcracking could lead to heavy microstructural damage to the material, depending on degree of constraint and microcrack distribution [44].

Crack bridging has been found out by SEM and X-ray tomography as an important extrinsic toughening mechanism in dentin and cortex of bone. It is caused mainly by uncracked ligaments and secondarily from intact fibrils of collagen. While the length of major crack increases, the specimen becomes less stiff that is more compliant [44]. Crack bridging involves regions sustaining the applied load. Uncracked areas are formed in the wake of crack. Their formation is either due to non-uniform propagation of tip of crack and/or due to insufficient connection of microcracks. Crack bridging reduces the intensity of stress at the tip of crack shown as K_{tip} , relative to the intensity of applied stress, shown as K_{app} . Because bridges in the crack wake resist to applied load. Bridges form with extension of crack, K_{br} increases with extension of crack, causing rising R-curve behaviour. When bridges are formed and destructed at the same rate, a steady-state making up the ‘plateau’ toughness may be reached [34].

Uncracked-ligament bridges are assumed to contribute as the major extrinsic toughening mechanism with rising R-curve pattern in cortical type of bone. Since collagen fibre bridging might resist the microcrack advancement. Bridging of crack

decreases the specimen compliance (i.e., stiffness increases), on the other hand a zone of diffuse microcracking increases the compliance (stiffness decrease) (Figure 2.20a). Nalla et al. showed experimentally, the compliance is reduced and (Figure 2.20b), crack bridging works as the primary extrinsic toughening mechanism in cortical bone in human [44],[47].

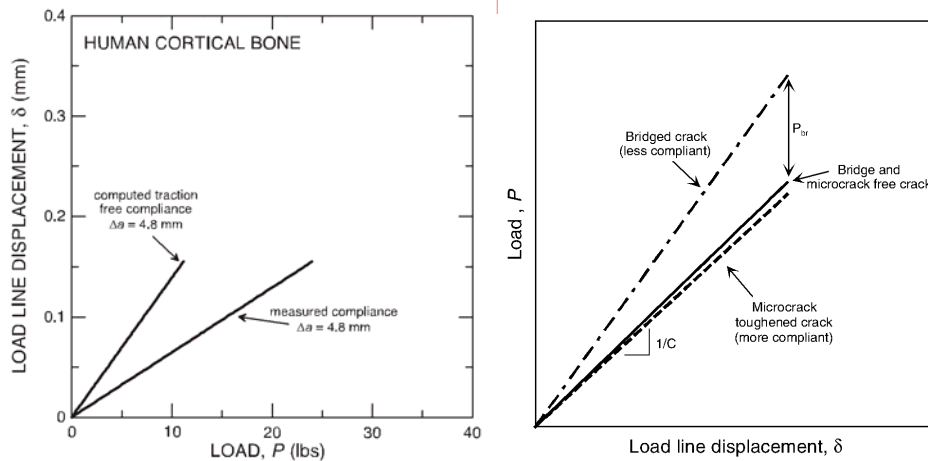


Figure 2.20: (a) Comparison of theoretical (microcrack-free and bridge-free) and experimental curves for compliance. Notice that the measured compliance is lower than the theoretical compliance, that gives an important clue about the function of crack bridging in the mechanism of toughening in cortical bone of human. (b) Change in compliance of a sample with a crack working with the mechanism of toughening [44],[47].

For microcrack toughening mechanism, there is a related decrease in modulus of elasticity in microcracked area, so a related increase in compliance of material is anticipated. Microcrack volume surrounding a macroscopic crack is small, therefore the reduction in elastic modulus is minor. For instance, a reduction of 4% in elastic modulus is caused by a 3% of microcracks volume fraction. Compliance of sample is affected to a minor degree by microcracking. Opposite to this, bridging formed in the crack wake counteracts the opening of the crack, causing an increased stiffness or lower compliance [44].

Crack deflection could take a part in the toughening mechanisms due to the fact that greatest toughness value has been found in the transverse (L-C) orientation. The path of crack deflects perpendicular to the plane of maximum tensile stress [34]. This deflection increases the fracture resistance.

2.10.3.6. Aging Effects on Crack Bridging

In older bone, R-curve shows a noticeable decrease in the contribution of extrinsic toughening (i.e K_{br}), as given in Figures 2.21 and 2.22. From mechanical point of view, increased remodelling levels with age might lead to the presence of greater density of secondarily formed osteons thus, frail cement lines which could fail easily. This might cause a more widespread bridging zone formed by ligaments. Additionally, formation of bridging might be easier because of increased branching of cracks along the higher number of cement lines. Though formation of bridging can be easier, zones of bridging are possible to form smaller bridges. Experimental observations demonstrate high number of smaller bridges, lead to decreased extrinsic toughening.

The quality of the collagen in the formation of bridges are important. Poor collagen quality might cause weaker bridges. Bridges that are fewer and smaller are detected by two-dimensional tomographic images of cracks obtained through-thickness format in older bone [34].

Vashishth et al, and Wu and Vashishth [43],[51], suggest on tibia and femur bone of human that toughness of bone decreases with aging (Figure 2.21). Importantly, not only a decrease in the crack initiation toughness, but also in the crack growth toughness was found by aging (Figure 2.22).

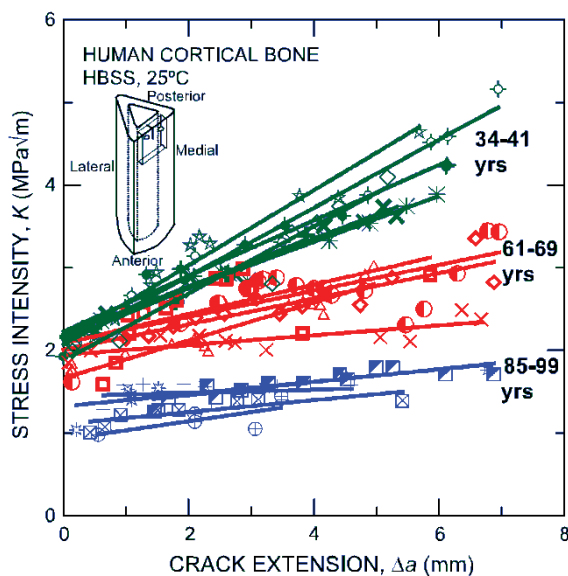
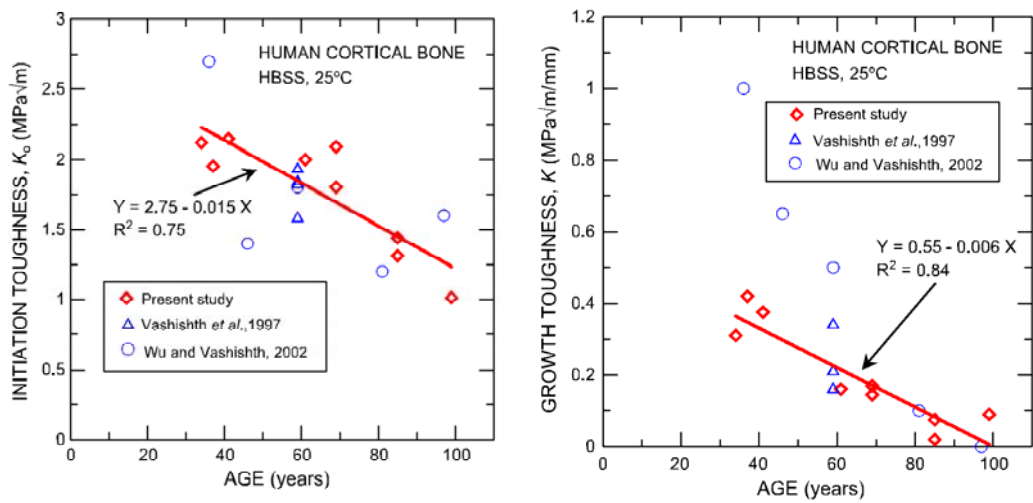


Figure 2.21: $KR(\Delta a)$ resistance curves in vitro in cortical bone of human for extension of stable crack with respect to age. Notice rising R-curve behavior is linear [52].

As the crack initiation toughness decreases, the aging effect is visible mostly on the crack growth toughness that decreases to almost zero in the very elderly. Figure 2.22 gives evident clearly for these tendencies where the crack initiation toughness decreases ~40% from 40 to 100 years over six decades, while the crack growth toughness is mainly diminished in the same range of age. Such derangement in the resistance to fracture by aging is compatible with the tendencies seen in reports that studied single-value toughness (Figure 2.22).



F

figure 2.22: Change in the (a) crack-initiation toughness (K_0), and (b) crack growth toughness (R-curve gradient) in cortical bone from human being by aging [43],[51].

2.11 MECHANISMS OF BONE AGING

2.11.1 Effects of Aging on Bone Ultrastructure

Changes in the bone constituents, such as the organic and mineral phases cause an increase in fracture of bone [54]. Bone is a hierarchical material system that could be effected mechanically by changes at each level. Collagen, plays a role at the nano-scale in which fibrils of collagen and mineralized collagen fibrils can be thought as a composite of collagen, mineral, and water [55]. Therefore, age-related changes in both the collagen (i.e. cross-links and re-orientation) and mineral phases (i.e. crystallinity and mineral content) and water distribution in bone were described [56]. The mechanical properties of bone is effected by mineral density, bone mass, and microarchitecture [55]. Although decreased BMD was demonstrated to be an important fracture risk factor, bone mass and mineral density are inconsistent predictors of bone strength [57] and effect of collagen on the post-yield and pre-yield properties of bone are less studied [55]. The mineral portion is found to be related

with stiffness of tissue, whereas collagen has an influence on post-yield properties such as absorption of energy.

Biomechanical properties of collagen are effected by a variety of molecular level alterations. Cross-linking which results from the reaction of reducing sugar with collagen is either enzymatically or non-enzymatically mediated. The enzymatic process, which is dependent on intracellular and extracellular posttranslational modification of collagen [58], and are mediated by lysyl oxidase, causes the formation of trivalent collagen cross-links deoxypyridinoline and pyridinoline. Contrary to the increasing number of mature cross-links, number of immature enzymatic cross-links was found to decrease until the 28 years of age in human which might reflect age related changes in bone remodeling activity [56]. Non-enzymatic collagen crosslinking producing molecules such as pentosidine as advanced glycation end products (AGE) take place by spontaneous condensation of lysine, arginine, and free sugars.

Both in vivo and in vitro experiments showed that increases in cross-linking are related with increases in some mechanical features such as stiffness and strength and reductions in others such as absorption of energy [55]. Formation of a stiffer collagen network by cross-links, would result in age-related increased fragility and diseases such as diabetes [58].

2.11.2. Effect of Cross-Links to the Mechanical Properties of Bone

Age-related reduction in the ability of bone to absorb energy prior to failure is clinically important since it makes osteoporotic bone prone to failure from any impact load. Collagen changes reduce bone's energy absorption capability, may be a factor increasing the risk of fracture in older women with low bone mass.

In cyclic load tests performed in vitro, cracks were initiated in specimens from older women but not from younger women. This suggests that microdamage accumulation in bone from elderly results from some inherent fragility in the tissue. In studies on baboon model, the percentage of denatured collagen content was related

to failure energy and to the fracture toughness of the tissue. The finding indicates that collagen is a primary arrestor of cracks in bone. This could explain why aging has a more profound effect on the plastic deformation than it has on elastic deformation of bone. The role of collagen may be related either to the amount of collagen or to its molecular stability and cross-linking [59].

One of the alterations in bone quality due to aging is by the production and accumulation of AGEs due to NEG. Although other alterations including porosity take place by aging and effect fragility of bone, the relative effect of AGEs on the resistance to fracture of aging bone is unknown [60].

There are two possible collagen crosslinks types altered by aging. One type is produced by an enzymatic pathway where reducible crosslinks are made between the tail and head of following molecules of collagen that mature to trivalent, stable bonds. The other type is non-enzymatic or glycation-mediated pathway in which intermolecular bonds (including pentosidine, imidazolone, vesperlysine, furosine and Ne-carboxymethyllysine known as AGEs) are produced by spontaneous condensation of lysine, arginine and ribose [55].

The bone specimens are analyzed to determine the effects of age on the concentration of mature, enzymatic crosslinks (hydroxylysyl-pyridinoline—HP and lysyl-pyridinoline—LP) and a non-enzymatic crosslink (pentosidine—PE) using high performance liquid chromatography. Mature cross-links aggregate in human bone until 10–15 years of age, then they are found to be constant or decline slightly. An increased pyridinoline/deoxypyridinoline ratio was proposed to increase compressive strength and stiffness in bone, but has no effect on toughness or ductility. Formation of immature collagen cross-links takes over many years, therefore proteins like collagen with long half-lives, could collect important NEG cross-links by aging. In addition, crosslinks concentration in the secondary osteons is found to be significantly different from that in the interstitial bone. The findings show that the non-enzymatic crosslinking might increase on the other hand, crosslinking by mature enzymatic pathway might decrease with aging. These changes in collagen structure could decrease the bone tissue quality in the skeleton of elderly [55].

In addition, the bone collagen stability reduces by aging as measured by thermal techniques (i.e., contraction rate and shrinkage) and biochemical (i.e., extractability). Decrease in stability of bone collagen is related with a decrease in bone toughness. A few study did not detect a correlation among shrinkage temperature and mature enzymatic crosslink concentrations, stability of collagen or age. However, stability of collagen and concentrations of immature crosslink were found to be lower in bone with osteoporosis compared to healthy bone[61].

The effect of non-enzymatic collagen modifications on the mechanical properties of bone was studied in diabetes mellitus and aging [38]. Additionally, the proportion of mature to immature crosslinks was large close to surfaces forming new bone in osteoporotic bone. It can be considered that an enzymatic crosslinking imbalance could happen in remodelling of bone such as the osteoporosis. However, enzymatic crosslinks do not build up with age in collagen which may be because of the limited lysine residue hydroxylation and the lysyl hydroxylase activity [61].

It has been found that the mechanical properties of the network of collagen depend on age. Modulus of elasticity, failure strength, strain to fracture, work to fracture are shown to decrease by 30%, 35%, 10% and 50% with increasing age, respectively [33] (Figure 2.23). In another study, age-dependent changes in bone such as decreased strength, work to fracture, and fracture toughness of bone; the decreased strength, elastic modulus, and work to fracture of the collagen network; as well as in the increased concentration of pentosidine (a marker of nonenzymatic glycation) and increased bone porosity were also detected [38].

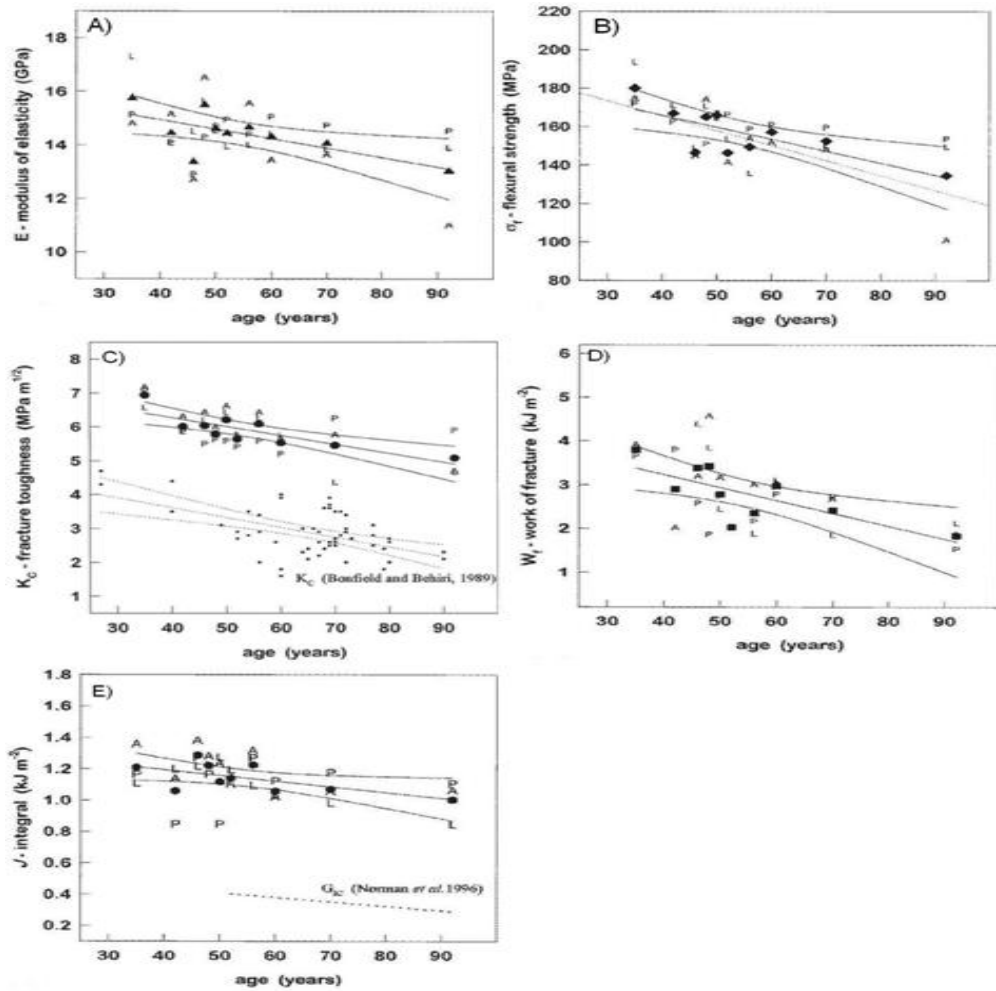


Figure 2.23: Graphs for age vs (E , K_C , sf , J , W_f). L, A, P show lateral, anterior and posterior aspects, respectively. The filled dots show the mean of three values at an age group. The lines represent linear regressions of least squares by confidence intervals of 95% [33]. (A) Results of Zioupos et al. for modulus of elasticity. (B) Dotted line shows the study results of Yamada on a bone from human femur that is relatively wet at RT [62]. In (C), the dotted data and lines are results from wet specimens of human tibia obtained at RT on CT specimens longitudinally by Bonfield and Behiri [63]. (D) Results of Zioupos et al. for work of fracture. (E) dotted line represents results for a rate of critical strain energy release in mode-I from tibia at RT on CT specimens in the longitudinal direction, by Norman et al.[64].

NEG cross linking is proposed to be a process related with age, especially in collagenous tissues with slowly metabolism [61] and was shown to reduce bone quality [60]. Non-enzymatic crosslinks contribution to mechanistic quality of bone is still not clarified. Studies indicate that accumulation of intermolecular crosslinks causes a more brittle bone. For instance, formaldehyde fixation is found to decrease impact energy absorption. Bone incubation with ribose for 38 days reduced the initial modulus of elasticity to the modulus of failure ratio. This reduction shows a loss in the capacity of bone to produce microdamage, that is considered as toughening mechanism of bone NEGs are found to be inversely correlated to creep rate, bone toughness, and strain to failure. Increased pentosidine concentration in bone has been shown to reduce the ultimate strain, and amount of post-yield deformation [55]. On the other hand, a few in vitro experiments that studied ribose or glucose incubated bone did not find any important differences in mineralized bone between stiffness, strength or toughness [61].

Bone derives its resistance to fracture from the extrinsic and intrinsic mechanisms during propagation of crack, opposite to the classical brittle materials and it shows a toughening behavior characterized by a increasing resistance with increasing length of crack. Human bone shows a steady decrease in R-curve behavior by aging. Increased porosity and a decrease in quality of bone matrix might increase the fragility. However, these factors' relative contributions is not clear [60].

Toughness is an important parameter in relation to fracture. It was found that fatigue strength and two parameters of older bone for measurement of toughness namely, W_f representing work of fracture and absorption of energy during impact reduce with increased age. In impact tests and some tests made in un-notched form of bone where fracture and microfractures are nonlocalized, toughness depends on the extend of prefailure damage the specimen can withstand before macrocrack causing fracture forms. As prefracture damage becomes greater, postyield deformation becomes greater and thus the material becomes tougher [33]. Fracture tendency of a brittle microcracking material such as bone can be studied directly by its post-yield

characteristics. Extracted organic matrix from ribosylated bones demonstrated poor energy distribution features [57].

Aging bone can be considered to be tough to less degree since it can hold a less amount of prefailure or postyield damage. Toughness is related with some other causes. For example, in tougher bones: (i) before formation of the macrocrack the damage build up at quite a moderate rate; (ii) the crack is resisted to fracture with respect to its stress intensity factor K_C or the energy related with crack growth, (iii) the energy to create a unit of fractured area increases disproportionately with the strain rate [33].

Bone fracture toughness might change because of the the alteration in organic phase and the osteon morphology without important alterations in porosity and bone mineral phase [54]. Toughness decrease by aging can be influenced by non-enzymatic crosslinking. Process mediated by NEG (i.e, the Maillard reaction) increases the intermolecular crosslinks number in bone [61]. Increased concentrations of pentosidine, a biomarker for glycation induced (NEG) crosslinks is related with a decrease in toughness and strength of demineralized bone from cortex and a decrease in individual trabeculae ductility [38],[61]. Alteration in any of the components of bone their arrangement in space might effect the bone fracture toughness. In a study, it was found that fracture toughness decreases with age in bone and it is correlated with increased bone microhardness [54].

2.11.3. Age-Related Changes in Biochemical Properties of Collagen

2.11.3.1. Collagen Biosynthesis and Fibril Formation

As a biopolymer, collagen provides structural support for load-bearing tissues. Because the maturation and mechanical properties of collagen is dependent on the formation of enzymatic crosslinks, derangements can arise if formation of mature crosslinks is inadequate.

During the biosynthesis of type I procollagen intracellular post-translational reactions occur. These steps are lysyl and prolyl residue hydroxylation, hydroxylysine glycosylation with glucosylgalactose and galactose. Specific enzymes catalyses reactions until the protein folds into the triple-helix configuration (Figure 2.24).

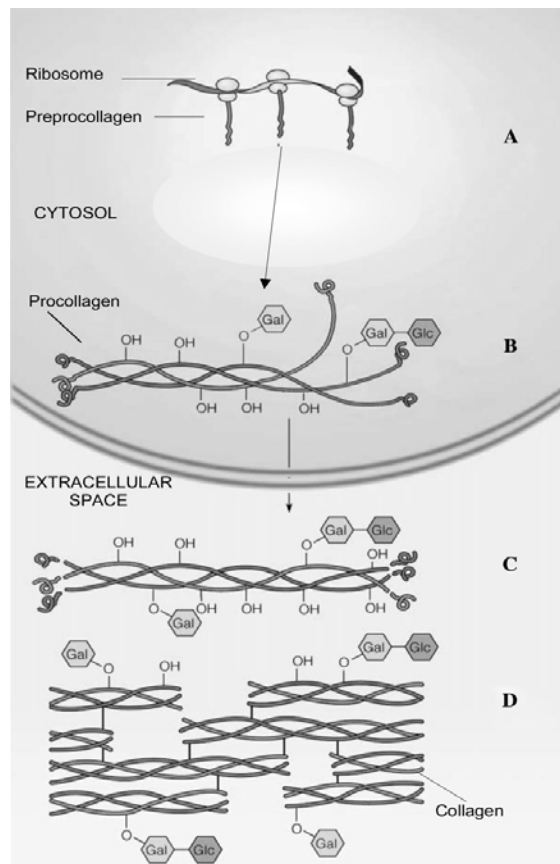


Figure 2.24: Collagen molecule biosynthesis. Collagen synthesis steps are schematized. (A) and (B) occurs intracellularly while (C) and (D) occur extracellularly.

Mature molecules assemble into fibrils. Fibrils are formed by collagen molecules that are parallel to each other, triple helix form. Crystals of HA fill the gaps among collagen fibrils in bone. It was concluded that the amount of glycosylation

effect orientation, diameter, organisation of fibrils and its resistance to mechanical stress [65].

2.11.3.2. Enzymatically Formed Intermolecular Cross-Linking

An important factor for mechanical resistance is the cross-linking number and type within collagen molecules and between collagen molecules making fibril. The last posttranslational modification of the collagen molecule in the extracellular space is the oxidative deamination of hydroxylysines and lysines, which is catalysed by the ϵ -amino lysyl-hydroxylysyl deaminase enzyme. This step is the only enzymatic step required for production of the mature or nonreducible cross-links named as deoxypyridinoline and pyridinoline. Further reactions occur spontaneously until the ring of pyridinium is produced. However, the hydroxylysines bound to a sugar moiety are weak deaminase substrates. Thus, the higher the amount of glycosylation, the less the number of pyridinium cross-links which result in lower the tensile strength of the collagen fibril. Thus, overglycosylation of the collagen causes in a smaller diameter and a lower number of cross-links, consequently stabilisation of the fibril becomes less and resistance is impaired [65]. Enzymatic crosslinks play an important role in mechanical competence of adult skeletal system. Accumulation of enzymatic crosslinks make a plateau with skeletal maturity, and is not correlated with the age-related fragility of skeletal tissues [66].

2.11.3.3. Non-Enzymatic Cross-Linking (Glycation)

The other way for collagen cross-linking between molecules that increases by aging occurs by the non-enzymatic reaction with glucose, named as glycation. Glycation effects on collagen molecule has a main role in the etiopathogenesis of aging [67].

2.11.3.3.1. Reaction of Collagen with Glucose

The aldehyde of open chain glucose goes into reaction with the free o-amino group of a lysine bound to a peptide to make a glucosyl-lysine. This is called as the “Maillard reaction”. This is stabilised by “Amadori rearrangement” that occurs spontaneously to end up with a keto-imine (Figure 2.25). The Amadori complex amount may be quantified by its product reduced by borohydride and by its acid hydrolysis to pyridosine and furosine.

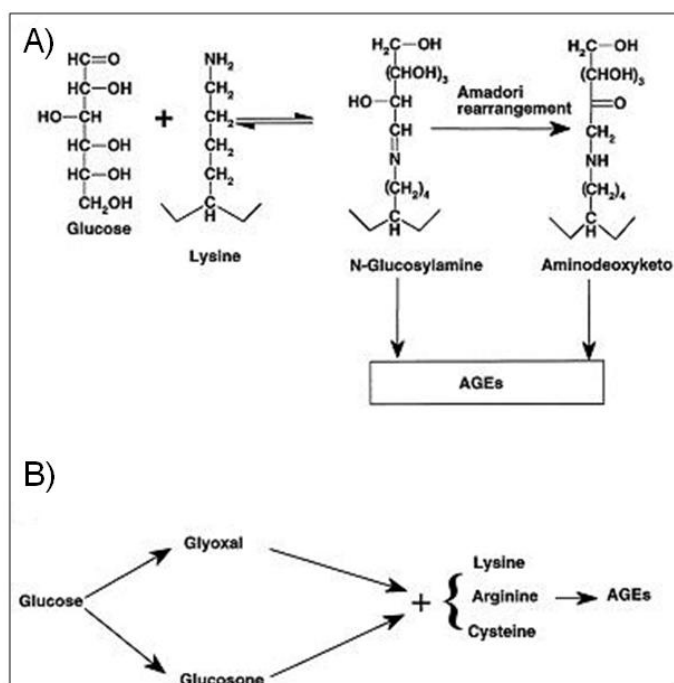


Figure 2.25: Formation of Schiff base and AGE. A) Reaction of glucose and lysine bound to peptide to make up a Schiff base that undergoes rearrangement of Amadori spontaneously to give the Amadori product, an aminodeoxyketose. Both ketose and Schiff base are supposed to undergo further reaction to form AGEs. B) Break down of glucose to glyoxal and glucosone oxidatively, which react later with side-chains of protein to form AGEs [67].

2.11.3.3.2. Advanced Glycation End-Products

Both the keto-imine and the adduct of Schiff base react with residues of other amino acids, or after oxidative breakdown induced by metal-ions to make AGEs. “AGE” defines any moiety bound to protein that is measured after the Schiff base formation. Amadori product is the final molecule (Figure 2.26).

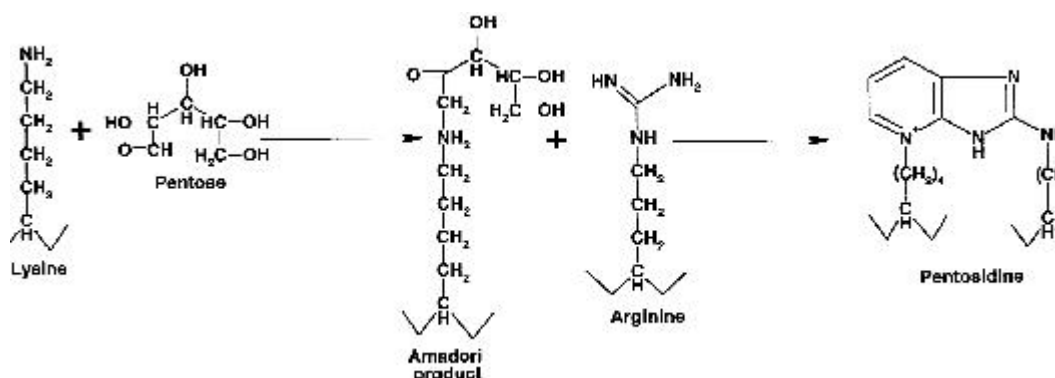


Figure 2.26: Formation of pentosidine [67].

Furthermore, oxidative breakdown could cause the formation of reactive sugars; glyoxals and 3-deoxyglucosone that make a complex with other lysines to make AGEs. They make up a heterogeneous class of molecules characterized by a brown color, fluorescence, and a tendency to polymerize [38].

Collagen molecules in bone have a long lifetime, which cause AGE modification. Thus generation and accumulation of AGEs in bone could be a reason for deterioration of quality (e.g. increased stiffness). Significantly higher levels of the AGE pentosidine as well as of carboxymethyl lysine (CML) were found in the serum of patients with osteoporosis. In another study, concentration of cortical pentosidine showed not a significant exponential increase with age and also negatively correlated to bone density and mineralization (Singh score) [38].

2.11.3.3.3. Intermolecular Glycation Cross-links

Aging causes glycation of fibrous collagen in the long term in vivo, makes it more resistant to enzymes, less soluble and less flexible. Resembling reactions happen after glucose incubation in vitro. Mentioned effects on the characteristics of collagen molecule are compatible with the presence of cross-links between the collagen molecules (intermolecular cross linking). Reaction involves o-amino groups of lysine in the triple helical parts of the collagen molecule rather than the globular tips of molecules and causes enzyme resistance and stiffening rapidly and causes [67].

Pentosidine: It is an imidazo pyridinium product, made up of arginine, lysine and ribose. It was detected as the Maillard reaction's end-product. It is formed by pentoses, hexoses, ascorbate and various Amadori compounds in vitro. Pentosidine show a linear increase with age [67].

2.11.3.3.4. Glycation Cross-link Sites

Inter-helical cross-linking of collagen molecule causes increased temperature for thermal denaturation and increase the resistance of the collagen to enzymes in proportion to the glycation, that could involve arginines and lysine (Figure 2.27).

2.11.3.3.5. The Model of Diabetes

Type 2 diabetes is determined by high concentrations of glucose in blood (hyperglycemia), is associated with increased risk of fracture of the hip, proximal humerus, and foot. Studies on diabetes find that bone has poorer quality, that is not accounted for lower density. Increased concentration of AGEs was related with decreased strength in femurs of human cadaver [68] .

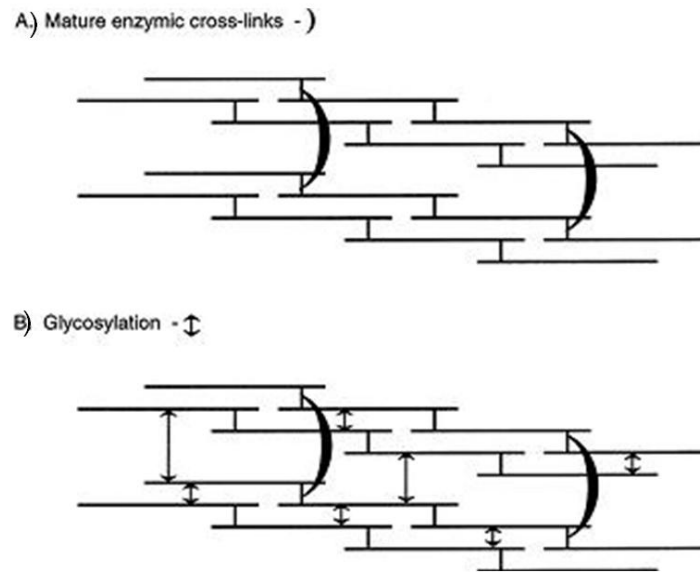


Figure 2.27: Cross-linking location. Mature,(M); Immature, (I); and (†) cross-links of the collagen fibre by aging [67].

Glycation could change the collagen properties in many ways. Biomechanical functioning, supramolecular aggregate formation, the change of its charge can be affected. Additionally, it may act as an oxidising agent [67]. In diabetes, overglycosylation results from hyperglycaemia. With respect to the law of mass-action, lysine and hydroxylysine residues could be glycosylated by nonenzymatic glucose binding to their e-amino acid. The stable nonenzymatically formed Amadori early glycated products makes some further re-arrangements, causing formation of irreversible AGEs which build up over the protein's life span. Thus fibril diameter becomes smaller and a lower amount of of cross-links occur [65].

CHAPTER 3

MATERIALS AND METHODS

3.1. PREPARATION OF SPECIMENS

Two pairs of (bilateral) femur bones belonging to 2 different cows were obtained from a slaughterhouse. Ages of the animals were 1.5 and 6 years old to study the effect of aging in young and old bone, respectively. They are estimated to correspond to 12 and 48 years of human age, respectively. All specimens were kept frozen at -20 °C wrapped by a gauze soaked with phosphate buffered saline solution until experimental preparation. One of 2 femurs from the same animal was kept for macro-mechanical testing. The other cortical bone from the central femurs is cut into slices transversally (perpendicular to the main loading axis) for the micro-mechanical testing. Samples were of 5-10 mm thick and cut using a diamond saw machine (Isomed low speed saw, Buehler) at a low rotary speed. The samples were washed with tap water to extract any abrasives remnant from cutting. After fat and marrow were removed from slices mechanically, they were kept in a mixture of methanol and chloroform (v:3/1) overnight at room temperature (RT) for fine dissolution.

3.2. POLISHING

Bone samples were polished using metallographic polishing techniques. All of the samples were polished by Metaserv 2000 grinder/polisher by a standard protocol using non-adhesive silicon carbide abrasive disk papers with the sequential granulometry of 180, 240, 320, 400, 600, 800, 1000 and 1200, respectively. The specimens were washed before passing to the next finer polishing level. Finally, an

industrial diamond solution was used to reach a final surface roughness below 0.05 μm on a polishing cloth.

All of the polished slices from 2 bovine bones were cut into 6 pieces to parallel to the loading axis by an Isomed low speed saw, Buehler using a diamond cut off wheel 102mmx0.3mmx12.7mm in diameter.

3.3. DENSITY

Density of bones were determined by measurement of mass in air and in water using Precisa Density determination set 320 XT/XB/XR, Precisa Gravimetrics AG, CH-Dietiken. Archimedes' principle states that the buoyancy force on an object is going to be equal to the weight of the fluid displaced by the object, or the density of the fluid multiplied by the submerged volume times the gravitational acceleration, g . Assuming Archimedes' principle to be formulated as follows (Equation 3.1):

$$\text{Density} = \frac{\text{weight in air}}{(\text{weight in air} - \text{weight in water})} \quad (3.1)$$

3.4. NON-ENZYMATIC GLYCATION PROCESS

The solution for ribosylation contains 0.6M ribose, zwitterionic buffers (30 mM HEPES), and protease inhibitors to inhibit reactions of enzymes (5mM benzamidine, 25 mM ϵ -amino-n-caproic acid, 10mM N-ethylmaleimide) in Hanks buffer. The control solution contained the same chemicals as with the ribosylation solution except for ribose [57]. During the process of incubation, solution pH was followed every 24 h and kept between 7.2 and 7.4 by pH meter.

Both young and old groups of bovine cortical bone specimens were grouped into 2 with respect to the state of ribosylation as ribosylated and non-ribosylated. Amount of ribosylation is expected to be proportional to the period of time rested in the solution. It is reported that a 7-day ribosylation in vitro causes formation of an accelerated and increased oxidative stress environment which is approximately equivalent to 2–3 decades of aging [57],[68]. 3 samples of bone species for

microindentation study and cylindrical bone samples obtained along the longitudinal axis of bones for three-point bending configuration from each of the control and ribosylated groups were taken out of the incubation solution which is kept at RT at the beginning and at the ends of 1st, 2nd, 3rd, 4th weeks.

3.5. MICROMECHANICAL TESTING BY MICROINDENTATION

Polished surfaces of bone samples were indented by a Vickers diamond indenter in a microhardness testing machine with an optical microscope (Shimadzu HMV-2 Microhardness, Japan) with various loads for different periods of time according to ASTM E384-99 standard [69]. Indentations were parallel to the loading axis. A distance of at least twice indentation diagonal length was left between the microindentations to stop the interactions between microindentations next to each other. Indentation diagonals lengths were measured by an optical microscope (Figure 3.1).



Figure 3.1: Microhardness tester.

Indentations were made on samples belonging to 8 groups at varying indentation loads and durations both in wet and dry state. Microindenter was applied on 3 different specimens for 5 times from the same group (a total of 15 measurements) for each variable. Indentation was measured in the wet and dry state to determine the factors that may effect result of indentation. Specimens were tested

for about 1h after getting out of the solution to study in wet state. Same specimens were allowed to dry in the laboratory environment for 24h and tested later for dry state (Figure 3.2).

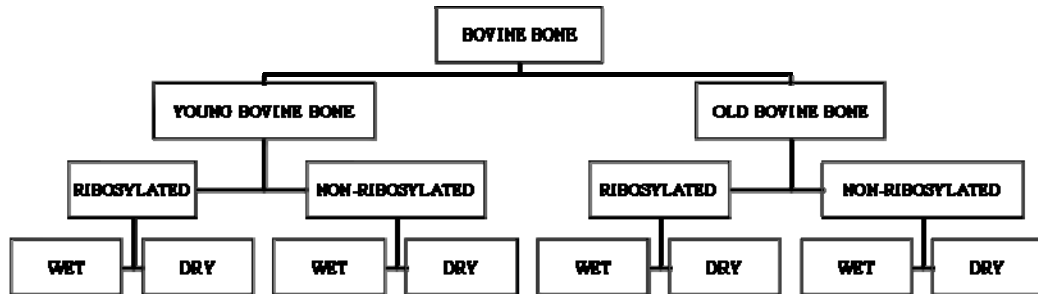


Figure 3.2: Microindentations were made on 3 samples belonging to 8 groups at varying indentation loads and durations both in wet and dry state.

3.5.1. Variation of Hardness with Applied Load

Series of microindentations were made on bone specimen groups for each of five masses namely, 10 g, 25 g, 50 g, 100 g and 200 g for 10 sec. Microcrack formation after indentations was examined and the applied load was increased to 300 g, 500 g, 1000 g and 2000 g for 10 sec to be able to make microcracks.

3.5.2. Hardness Variation with Duration

A series of indentations was made on bone specimen groups for each of five durations of 5 sec, 10 sec, 20 sec, 30 sec for 10 g.

3.5.3. Calculation of Microhardness

Vickers μ -hardness indentation calculation was made with the following formula (Figure 2.13) (Eq. 3.2).

$$HV = 0.001854 \cdot \frac{P}{d^2} \quad (3.2)$$

where HV: Vickers hardness (GPa), P (N): Applied load (g)9.806/1000, d (mm): diagonal indent length (mm)/1000.

3.5.4. Calculation of Fracture Toughness by Micro-Hardness Test

The fracture toughness (K_{Ic}) of the bones was determined using the Vickers micro-hardness test (Figure 2.13). Palmqvist shape crack is observed when the “c/a” ratio is smaller than 3. Then Palmqvist equation is used (Eq. 2.6).

Since cortical bone has anisotropy and isotropy is assumed by the equation, hardness and average modulus values were considered for the calculation of K_{Ic} . Indentations close to or on Volkmann’s and Haversian canals were not included for calculating toughness values. Considering physiological conditions of loading, the transverse cracking is the most related direction. This crack orientation is called as C-L by E399 ASTM Standard for testing of fracture toughness (Figure 2.14) [37].

3.6. MACROMECHANICAL TESTING

3 POINT BENDING TEST

Cylindrical specimens from the cortical wall thickness of long bones from the other extremity of the same animal were prepared. They were cut along the longitudinal axis using an industrial lathe (at Gazi Univ and a Machine shop at Ostim, Ankara) (Figure 3.3). Length and diameter of the bone samples ranged between 4-10mm and 0.2-0.5mm, respectively.

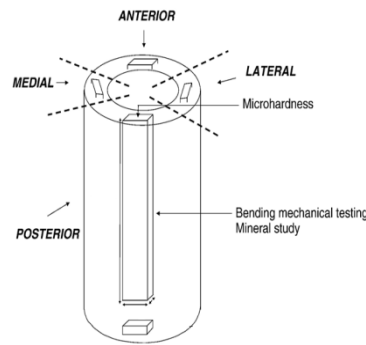


Figure 3.3: Scheme for specimens obtained from the cortical wall thickness of long bones.

Dimensions of the specimens were measured by a caliper for 3 times. Bone properties during bending were measured by bone specimens loading up to failure in testing configuration with a three-point bending by Shimadzu Autograph 100 kN machine (Japan) with the following set-up. The loading rate was 0.5 mm/min. A pre-load was (0.5 N) first held on each hydrated specimen in place on the lower support points of a three-point bending fixture. The span length in between lower supports has been adjusted in proportion to the length of the specimen. The load cell limit was 500N and displacements recorded during a monotonic load-to-failure test. Failure occurred when the load was dropped to 10%.

3 samples of cylindrical specimens from each of control and ribosylated groups were taken out of the incubation solution for macromechanical testing in 0,1st, 2nd, 3rd and 4th weeks. Specimens were tested in a three-point bending configuration in accordance with ASTM D790-10 standard [70].

Elastic modulus of the bones were measured using load vs. deflection curve according to standard beam theory. The length to thickness ratio advised by standards currently is 16:1, on the other hand recent study was showed that ratio of 20:1 is required for bone to make sure that the predicted modulus of elasticity is within 95% range of the actual value of Young's modulus [33].

3.7. SCANNING ELECTRON MICROSCOPY

The effect of microstructural bone properties on crack propagation and deformation were examined using SEM which is capable of producing high-resolution images of a sample surface.

Fracture surfaces of cylindrical samples after 3 point bending test and samples from cross-sections from each group in the dry state were studied in terms of fracture surface and indentations, respectively by an Environmental Scanning Electron Microscope (ESEM) FEI-Quanto 200 FEG.

Samples from bovine humerus cross-sections from each group in the dry state were coated with gold-palladium by Precision Etching Coating System (PECS), Gatan- 682. Images from samples were magnified to 60000-120000 times to observe micrographs of crack initiation and propagation which showed the formation of a frontal process zone and a wake, respectively to support the microcrack-based toughening mechanism in cortical bone.

3.8. STATISTICAL ANALYSIS

All experimental data were expressed as mean \pm SD. General linear model was used to study the effect of load and duration on microhardness in young, old bovine bones of ribosylated and the control of groups. Post-Hoc Tukey test was used to show differences between the 4 groups. Differences in microhardness results between young and old bovine bones were studied by paired sample T test. $P < 0.05$ is accepted as significant.

CHAPTER 4

RESULTS

4.1. MICROHARDNESS

Microhardness test repeated with various indentation loads and durations to study the effect of these parameters on test results were compared between ribosylated (R) and non ribosylated (NR) young and old bovine bone specimens during ribosylation period.

Microhardness test made by 10 g of indentation load for 10 sec did not show any statistically different results between R and NR groups in both the young and old bovine bone for the period of each ribosylation weeks. Except for one measurement in young ribosylated bovine bone in the 3rd week, there was no difference between wet and dry state in two types of bone (Table 4.1). This finding may not be generalized to all of the results obtained by 10 g of indentation load.

Microhardness test made by 25 g of indentation load for 10 sec showed a statistical difference in measurements of R bone form NR bone in young and old bovine. Young wet NR group was also significantly different when compared to young R old, NR old and old R groups. A similar difference was found among young dry NR group and others. Dry state made a significant difference when compared to wet state both in NR and R groups in each week in young and old bovine bone (Table 4.2).

Table 4.1: Microhardness values expressed as mean±SD measured by 10 g of applied force for 10 sec on transverse sections of R and NR young and old bovine bone with respect to duration of NEG in wet and dry state.

DURATION OF NEG (week)	MICROHARDNESS (kg/mm ²)					
	YOUNG BOVINE BONE					
	WET			DRY		
	R	NR	Δ_{mean}	R	NR	Δ_{mean}
1	62.18±16.4	58.83±8.3	3.35	72.7± 7.1	72.64±6.3	0.06
2	71.47±13.7	69.49±10.0	1.98	75.28±13.2	73.39±5.7	1.89
3	71.69±7.8	65.20±5.2	6.49	79.21±7.7 [#]	64.41±12.9	14.8
4	63.98±20.8	55.27±8.6	8.71	70.63±16.1	61.86±9.0	8.77
	OLD BOVINE BONE					
	WET			DRY		
	R	NR	Δ_{mean}	R	NR	Δ_{mean}
1	68.24±10.2	67.59±11.3	0.74	75.97±8.2	73.69±8.9	2.28
2	79.20±9.9	76.91±10.9	2.29	83.55±10.7	81.72±12.5	1.83
3	75.05±10.3	68.58±8.3	6.47	71.81±18.1	75.65±20.4	4.16
4	65.87±11.3	61.86±9.4	4.01	72.67±10.5	65.68±9.9	6.99

[#]: statistical difference between wet and dry ribosylated bone in the same bovine (p<0.05).

Table 4.2: Microhardness values expressed as mean±SD measured by 25 g of applied force for 10 sec on transverse sections of R- and NR- young and old bovine bone with respect to duration of NEG in wet and dry state.

DURATION OF NEG (week)	MICROHARDNESS (kg/mm ²)					
	YOUNG BOVINE BONE					
	WET			DRY		
	R	NR	Δ_{mean}	R	NR	Δ_{mean}
1	67.31±7.3 ^(Δ)	57.02±9.8 ^(*)	10.28	79.94±7.7 ^(#,Δ)	72.34±4.7 ^(&,#)	7.56
2	74.55±6.1 ^(Δ)	58.59±4.9 ^(*)	15.91	82.9±4.8 ^(#,Δ)	78.87±4.4 ^(&,#)	10.03
3	73.09±5.8 ^(Δ)	57.43±6.1 ^(*)	15.57	88.6±7.9 ^(#,Δ)	75.2±8.6 ^(&,#)	12.96
4	79.07±8.1 ^(Δ)	60.97±5.5 ^(*)	18.03	89.25±7.9 ^(#,Δ)	76.48±5.9 ^(&,#)	12.77
	OLD BOVINE BONE					
	WET			DRY		
	R	NR	Δ_{mean}	R	NR	Δ_{mean}
	1	75.44±6.7 ^(Δ)	72.55±6.3	2.69	80.79±7.7 ^(#,Δ)	77.18±8.5 ^(#)
2	81.69±6.5 ^(Δ)	76.45±5.9	5.24	86.03±6.3 ^(#,Δ)	79.55±7.2 ^(#)	6.48
3	77.2±3.4 ^(Δ)	72.74±4.3	4.46	82.17±6.4 ^(#,Δ)	83.31±7.4 ^(#)	11.14
4	79.48±6.9 ^(Δ)	74.0±6.2	5.46	87.42±7.6 ^(#,Δ)	96.13±5.1 ^(#)	8.71

*: statistically different from all other groups in wet state in the same week (p<0.05).

&: statistically different from all other groups in dry state in the same week (p<0.05).

#: statistical difference between wet and dry non-ribosylated bone in the same bovine (p<0.05).

#: statistical difference between wet and dry ribosylated bone in the same bovine (p<0.05).

Δ: statistical difference between ribosylated bone and non-ribosylated bone in the same bovine (p<0.05).

Microhardness measurements made by 50 g indentation load for 10 sec (Table 4.3) showed a statistical difference in measurements of R bone form NR bone in young and old bovine. NR young bovine bone in the wet and dry state was statistically different when compared to R young, R old and NR old bovine bone specimens for each NEG periods. Except for the 2nd week NR dry and 4th week R

wet young bovine bone specimen measurements, all other measurements between wet and dry state were found to be statistically different.

Table 4.3: Microhardness values expressed as mean±SD measured by 50 g of applied force for 10 sec on transverse sections of R- and NR- young and old bovine bone with respect to duration of NEG in wet and dry state.

DURATION OF NEG (week)	MICROHARDNESS (kg/mm ²)					
	YOUNG BOVINE BONE					
	WET			DRY		
	R	NR	Δ_{mean}	R	NR	Δ_{mean}
1	73.04± 2.7 ^(Δ)	60.9± 4.2 ^(*)	12.14	74.6± 9.6 ^(#,Δ)	68.80± 5.6 ^(#,§)	5.8
2	75.73± 4.0 ^(Δ)	62.1± 6.2 ^(*)	13.63	80.1± 7.8 ^(#,Δ)	71.52± 6.6 ^(#,§)	8.58
3	76.87± 3.1 ^(Δ)	61.4± 4.4 ^(*)	15.47	76.9± 3.9 ^(#,Δ)	67.35± 5.3 ^(#,§)	9.55
4	77.09± 7.9 ^(Δ)	59.2± 4.5 ^(*)	17.89	78.7± 6.5 ^(#,Δ)	67.21± 8.2 ^(#,§)	11.49
	OLD BOVINE BONE					
	WET			DRY		
	R	NR	Δ_{mean}	R	NR	Δ_{mean}
	1	69.9± 8.1 ^(Δ)	63.02± 6.4	6.88	84.8± 4.8 ^(#,Δ)	76.6± 5.6 ^(§)
2	73.1± 5.2 ^(Δ)	65.79± 4.0	7.31	86.3± 7.4 ^(#,Δ)	77.4± 6.4 ^(§)	8.9
3	75.1± 5.2 ^(Δ)	66.88± 6.27	8.22	89.0± 7.2 ^(#,Δ)	79.3± 7.6 ^(§)	9.7
4	79.49± 5.7 ^(Δ)	67.39± 5.5	9.1	90.5± 6.6 ^(#,Δ)	78.37± 6.4 ^(§)	12.1

*: statistically different from all other groups in wet state in the same week (p<0.05).

&: statistically different from all other groups in dry state in the same week (p<0.05).

§: statistical difference between wet and dry non-ribosylated bone in the same bovine (p<0.05).

#: statistical difference between wet and dry ribosylated bone in the same bovine (p<0.05).

Δ: statistical difference between ribosylated bone and non-ribosylated bone in the same bovine (p<0.05).

NR wet and dry young bovine bone specimens made by 100 g for 10 sec (Table 4.4) were found to be statistically different from R young and NR old and R old bone specimen measurements in the wet and dry state, respectively. NR and R dry state measurements both in the young and old bovine bone specimens were significantly higher than wet state measurements. Microhardness measurements

showed a statistical difference in measurements of R-bone form NR-bone in young and old bovine.

Table 4.4: Microhardness values expressed as mean±SD measured by 100 g of applied force for 10 sec on transverse sections of R- and NR- young and old bovine bone with respect to duration of NEG in wet and dry state.

DURATION OF NEG (week)	MICROHARDNESS (kg/mm ²)					
	YOUNG BOVINE BONE					
	WET			DRY		
	R	NR	Δ_{mean}	R	NR	Δ_{mean}
1	64.53±6.7 ^(Δ)	61.2±4.6 ^(*)	3.36	76.07±6.8 ^(#,Δ)	68.24±3.6 ^(&,#,Δ)	7.83
2	69.57±5.0 ^(Δ)	63.8±6.2 ^(*)	5.77	77.73±6.7 ^(#,Δ)	67.76±3.9 ^(&,#,Δ)	9.97
3	70.34±3.8 ^(Δ)	62.43±3.8 ^(*)	7.91	78.74±4.8 ^(#,Δ)	66.99±6.0 ^(&,#,Δ)	11.75
4	72.41±7.2 ^(Δ)	63.59±3.4 ^(*)	8.82	81.88±6.8 ^(#,Δ)	68.18±4.9 ^(&,#,Δ)	13.7
	OLD BOVINE BONE					
	WET			DRY		
	R	NR	Δ_{mean}	R	NR	Δ_{mean}
	1	70.85±6.5 ^(Δ)	66.82±7.2	4.03	81.61±5.9 ^(#,Δ)	77.94±6.5 ^(#)
2	74.54±5.2 ^(Δ)	69.53±4.5	5.01	83.92±3.6 ^(#,Δ)	77.21±5.6 ^(#)	6.71
3	75.24±6.5 ^(Δ)	68.12±5.1	6.12	86.5±7.5 ^(#,Δ)	78.75±6.2 ^(#)	7.75
4	78.05±4.8 ^(Δ)	69.80 ± 5.4	8.25	87.75±5.9 ^(#,Δ)	79.41±6.3 ^(#)	8.34

*: statistically different from all other groups in wet state in the same week (p<0.05).

&: statistically different from all other groups in dry state in the same week (p<0.05).

#: statistical difference between wet and dry non-ribosylated bone in the same bovine (p<0.05).

#: statistical difference between wet and dry ribosylated bone in the same bovine (p<0.05).

Δ: statistical difference between ribosylated bone and non-ribosylated bone in the same bovine (p<0.05).

Microhardness measurement made by 200 g for 10 sec in young and old bovine bone (Table 4.5) showed a statistical difference in measurements of R-bone form NR-bone in young and old bovine. NR-young specimen measurements were statistically lower than other 3 groups in the wet and dry state. Dry state in R and

NR groups of young and old bovine bone was significantly higher during ribosylation weeks.

Table 4.5: Microhardness values expressed as mean±SD measured by 200 g of applied force for 10 sec on transverse sections of R and NR young and old bovine bone with respect to duration of NEG in wet and dry state.

DURATION OF NEG (week)	MICROHARDNESS (kg/mm ²)					
	YOUNG BOVINE BONE					
	WET			DRY		
	R	NR	Δ_{mean}	R	NR	Δ_{mean}
1	65,31±4,9 ^(Δ)	61,64± 6,0 ^(*)	3.7	73,14± 5,2 ^(#,Δ)	66,79±7,0 ^(&,*)	6.31
2	68,32±4,9 ^(Δ)	63,93± 4,9 ^(*)	4.4	74,35± 4,5 ^(#,Δ)	66,78±4,8 ^(&,*)	7.52
3	69,13±2,9 ^(Δ)	62,76± 6,2 ^(*)	6.4	73,37± 3,6 ^(#,Δ)	67,0± 7,6 ^(&,*)	6.3
4	70,33±6,5 ^(Δ)	61,48± 5,0 ^(*)	8.9	71,23± 5,4 ^(#,Δ)	64,37±6,1 ^(&,*)	6.9
	OLD BOVINE BONE					
	WET			DRY		
	R	NR	Δ_{mean}	R	NR	Δ_{mean}
	1	72,36± 5,3 ^(Δ)	66,96± 5,4	5.4	79,25± 4,9 ^(#,Δ)	72,64± 6,6 ^(*)
2	73,24± 5,5 ^(Δ)	65,94± 4,1	7.3	81,32±4,6 ^(#,Δ)	73,93± 7,1 ^(*)	7.39
3	74,78± 2,1 ^(Δ)	66,62± 5,3	8.16	82,72± 9,7 ^(#,Δ)	72,77± 6,6 ^(*)	9.95
4	75,23±4,9 ^(Δ)	64,32±5,3	10.91	85,15±5,5 ^(#,Δ)	73,19±5,8 ^(*)	11.96

*: statistically different from all other groups in wet state in the same week (p<0.05).

&: statistically different from all other groups in dry state in the same week (p<0.05).

#: statistical difference between wet and dry non-ribosylated bone in the same bovine(p<0.05).

#: statistical difference between wet and dry ribosylated bone in the same bovine (p<0.05).

Δ: statistical difference between ribosylated bone and non-ribosylated bone in the same bovine(p<0.05).

Experiment made by 100 g for 5 sec to study indentation time effect on microhardness measurements (Table 4.6) showed a statistical difference in measurements of R-bone form NR-bone in young and old bovine. A statistical difference in measurements of R-bone form NR-bone in young and old bovine was detected. There was a statistical difference for NR-young wet and dry specimen

compared to other 3 group in wet and dry state. Dry bone measurements were found to be significantly higher for R- and NR-young and old bovine bone.

Table 4.6: Microhardness values expressed as mean±SD measured by 100 g of applied force for 5 sec on transverse sections of R and NR young and old bovine bone with respect to duration of NEG in wet and dry state.

DURATION OF NEG (week)	MICROHARDNESS (kg/mm ²)					
	YOUNG BOVINE BONE					
	WET			DRY		
	R	NR	Δ_{mean}	R	NR	Δ_{mean}
1	64.75±4.8 ^(Δ)	60.09±7.9 ^(*)	4.66	70.34±5.6 ^(#,Δ)	66.09± 8.8 ^(&,#)	4.25
2	68.88±3.7 ^(Δ)	63.16±2.9 ^(*)	5.72	72.24±5.4 ^(#,Δ)	67.24± 3.9 ^(&,#)	5
3	71.25±7.9 ^(Δ)	64.33±8.5 ^(*)	6.92	74.93±4.2 ^(#,Δ)	68.0± 4.4 ^(&,#)	6.93
4	70.86±6.7 ^(Δ)	63.78±6.2 ^(*)	7.08	76.96±5.2 ^(#,Δ)	69.66±4.7 ^(&,#)	7.3
	OLD BOVINE BONE					
	WET			DRY		
	R	NR	Δ_{mean}	R	NR	Δ_{mean}
	1	68.38±6.2 ^(Δ)	63.94±5.9	4.44	74.89±5.4 ^(#,Δ)	70.05±4.4 ^(#)
2	70.02±6.7 ^(Δ)	65.05±6.6	4.97	77.23±7.0 ^(#,Δ)	71.83±5.1 ^(#)	5.4
3	71.90±9.8 ^(Δ)	64.17±7.2	7.73	79.73± 7.5 ^(#,Δ)	73.14±5.1 ^(#)	6.59
4	75.75±5.0 ^(Δ)	66.98±7.9	8.77	83.34±4.4 ^(#,Δ)	75.1± 6.3 ^(#)	8.24

*: statistically different from all other groups in wet state in the same week (p<0.05).

&: statistically different from all other groups in dry state in the same week (p<0.05).

#: statistical difference between wet and dry non-ribosylated bone in the same bovine(p<0.05).

#: statistical difference between wet and dry ribosylated bone in the same bovine (p<0.05).

Δ: statistical difference between ribosylated bone and non-ribosylated bone in the same bovine(p<0.05).

Results of microindentation made by 100 g applied load for 10 sec in order to study the effect of indentation duration are given in Table 4.4.

Microhardness measurements made by 100 g indentation load for 20 sec (Table 4.7) showed a statistical difference in measurements of R-bone from NR-bone in young and old bovine. There was a statistical difference in NR- young bovine bone in the wet and dry state compared to R- young, R- old and NR- old bovine bone specimens for each NEG periods. Measurements between wet and dry state were found to be statistically different in R-, NR- young or old bovine bone specimens.

Table 4.7: Microhardness values expressed as mean±SD measured by 100 g of applied force for 20 sec on transverse sections of R- and NR- young and old bovine bone with respect to duration of NEG in wet and dry state.

DURATION OF NEG (week)	MICROHARDNESS (kg/mm ²)					
	YOUNG BOVINE BONE					
	WET			DRY		
	R	NR	Δ_{mean}	R	NR	Δ_{mean}
1	62.66±5.1 ^(Δ)	58.69±6.7 ^(*)	3.97	76.07±6.8 ^(#,Δ)	68.24±3.6 ^(&,#)	5.75
2	65.54±4.5 ^(Δ)	60.66±5.7 ^(*)	4.88	77.73±6.7 ^(#,Δ)	67.76±3.9 ^(&,#)	6.95
3	67.17±4.2 ^(Δ)	62.06±4.5 ^(*)	5.11	78.74±4.8 ^(#,Δ)	66.99±6.0 ^(&,#)	7.57
4	71.12±7.9 ^(Δ)	64.97±3.3 ^(*)	6.15	81.88±6.8 ^(#,Δ)	68.18±4.9 ^(&,#)	10.05
	OLD BOVINE BONE					
	WET			DRY		
	R	NR	Δ_{mean}	R	NR	Δ_{mean}
	1	69.65±6.5 ^(Δ)	66.82±7.2	4.27	79.61±5.9 ^(#,Δ)	77.94±7.5 ^(#)
2	73.54±7.2 ^(Δ)	69.53±4.5	5.56	80.92±3.6 ^(#,Δ)	77.21±5.6 ^(#)	4.44
3	73.24±6.5 ^(Δ)	68.12±5.1	5.69	83.5±7.5 ^(#,Δ)	78.75±6.2 ^(#)	6.3
4	76.05±4.8 ^(Δ)	69.80 ± 7.4	6.44	84.75±4.9 ^(#,Δ)	78.41±7.3 ^(#)	8.18

*: statistically different from all other groups in wet state in the same week (p<0.05).

&: statistically different from all other groups in dry state in the same week (p<0.05).

#: statistical difference between wet and dry non-ribosylated bone in the same bovine(p<0.05).

#: statistical difference between wet and dry ribosylated bone in the same bovine (p<0.05).

Δ: statistical difference between ribosylated bone and non-ribosylated bone in the same bovine(p<0.05).

NR wet and dry young bovine bone specimens were found to be statistically different from R- young and NR- old and R- old bone specimen measurements in the wet and dry state respectively for 100 g microindentation load and 30 sec indentation time (Table 4.8). NR- and R- dry state measurements both in the young and old bovine bone specimens were significantly higher than wet state measurements. A statistical difference in measurements of R-bone form NR-bone in young and old bovine was detected.

Table 4.8: Microhardness values expressed as mean±SD measured by 100 g of applied force for 30 sec on transverse sections of R and NR young and old bovine bone with respect to duration of NEG in wet and dry state.

DURATION OF NEG (week)	MICROHARDNESS (kg/mm ²)					
	YOUNG BOVINE BONE					
	WET			DRY		
	R	NR	Δ_{mean}	R	NR	Δ_{mean}
1	64.71±6.9 ^(Δ)	60.02±6.9 ^(*)	4.71	72.1±4.6 ^(#,Δ)	67.94±6.7 ^(&,#)	4.2
2	68.47±5.2 ^(Δ)	62.74±4.1 ^(*)	5.77	74.15±6.9 ^(#,Δ)	68.61±4.7 ^(&,#)	5.5
3	66.15±3.4 ^(Δ)	60.22±4.4 ^(*)	5.95	76.39±4.7 ^(#,Δ)	69.10±5.1 ^(&,#)	7.2
4	69.34±6.2 ^(Δ)	62.61±6.5 ^(*)	6.73	77.22±5.1 ^(#,Δ)	66.27±5.1 ^(&,#)	10.95
	OLD BOVINE BONE					
	WET			DRY		
	R	NR	Δ_{mean}	R	NR	Δ_{mean}
1	70.70±3.7 ^(Δ)	66.05±6.6	4.65	72.43±6.4 ^(#,Δ)	68.1±6.7 ^(#)	4.33
2	71.25±6.5 ^(Δ)	65.33±6.3	5.92	75.28±5.9 ^(#,Δ)	70.22±5.0 ^(#)	5.06
3	73.29±5.0 ^(Δ)	67.33±4.6	5.96	79.41±6.2 ^(#,Δ)	74.22±5.9 ^(#)	5.19
4	74.34±6.3 ^(Δ)	64.70±6.3	9.64	81.25±5.8 ^(#,Δ)	73.94±6.1 ^(#)	7.31

*: statistically different from all other groups in wet state in the same week (p<0.05).

&: statistically different from all other groups in dry state in the same week (p<0.05).

#: statistical difference between wet and dry non-ribosylated bone in the same bovine (p<0.05).

#: statistical difference between wet and dry ribosylated bone in the same bovine (p<0.05).

Δ: statistical difference between ribosylated bone and non-ribosylated bone in the same bovine (p<0.05).

Microhardness measurement to obtain microfracture made by 300 g for 10 sec in R dry young and old bovine bone (Table 4.9) showed that old bone specimen measurements were statistically higher in 1st, 2nd, 3rd and 4th weeks.

Table 4.9: Microhardness values expressed as mean±SD measured by 300 g of applied force for 10 sec on transverse sections of ribosylated young and old bovine bone with respect to duration of NEG in dry state.

DURATION OF RIBOSYLATION (week)	MICROHARDNESS (kg/mm ²)		
	YOUNG BOVINE BONE	OLD BOVINE BONE	Δ_{mean}
	DRY RIBOSYLATED	DRY RIBOSYLATED	
1	65.00±12.7	68.53±6.8 ^(*)	3.53
2	67.45±7.9	74.78±7.9 ^(*)	4.33
3	69.027±4.0	74.59±7.6 ^(*)	5.32
4	71.25±6.9	77.53±4.9 ^(*)	6.28

^(*): statistically different from other group in dry state in the same week (p<0.05).

Microhardness test made by 500 g of indentation load for 10 sec did not show any statistically different results between R- young and old bone groups for the period of ribosylation (Table 4.10).

Microhardness experiments made by 1000 g load for 10 sec (Table 4.11) in R- old dry bovine bone were found to be significantly higher than R- young dry bone measurements in the 3rd and 4th weeks of ribosylation.

Table 4.10: Microhardness values expressed as mean±SD measured by 500 g of applied force for 10 sec on transverse sections of R- young and old bovine bone with respect to duration of NEG in dry state.

DURATION OF RIBOSYLATION (week)	MICROHARDNESS (kg/mm ²)		
	YOUNG BOVINE BONE	OLD BOVINE BONE	Δ _{mean}
	DRY RIBOSYLATED	DRY RIBOSYLATED	
1	67.27±5.0	68.82±4.2	1.55
2	68.03±5.1	71.03±4.6	3
3	71.65±3.1	75.51±6.8	3.86
4	72.04±2.9	76.84±6.3	4.80

Table 4.11: Microhardness values expressed as mean±SD measured by 1000 g of applied force for 10 sec on transverse sections of R- young and old bovine bone with respect to duration of NEG in wet and dry state.

DURATION OF RIBOSYLATION (week)	MICROHARDNESS (kg/mm ²)		
	YOUNG BOVINE BONE	OLD BOVINE BONE	Δ _{mean}
	DRY RIBOSYLATED	DRY RIBOSYLATED	
1	66.1±5.5	66.27±5.6	0.17
2	67.38±2.8	71.23±8.4	3.85
3	69.14±3.6	73.24±4.8 ^ψ	4.1
4	71.69±4.3	76.87±5.4 ^ψ	5.18

^ψ: statistically different from other group in dry state in the same week (p<0.05).

Microhardness test result made by 2000 g applied load for 10 sec (Table 4.12) in dry state in R- old bovine bone was found to be significantly higher in the 3rd week of ribosylation.

Table 4.12: Microhardness values expressed as mean±SD measured by 2000 g of applied force for 10 sec on transverse sections of R- young and old bovine bone with respect to duration of NEG in wet and dry state.

DURATION OF RIBOSYLATION (week)	MICROHARDNESS (kg/mm ²)		
	YOUNG BOVINE BONE	OLD BOVINE BONE	Δ _{mean}
	DRY RIBOSYLATED	DRY RIBOSYLATED	
1	65.87±7.0	67.89±5.55	2.02
2	67.57±3.6	71.43±7.6	3.86
3	69.41±3.0	73.77±3.4(^Ψ)	4.36
4	71.1±2.5	76.38±6.6	5.28

^Ψ: statistically different from other group in dry state in the same week (p<0.05).

4.2. TOUGHNESS AND MICROCRACKS

Densities of transverse sections obtained from cortical bones are shown in Table 4.13. Mean density of old bovine specimens were found to be lower than that of young bone specimens. A weak negative correlation between density and microhardness results made by 100 g of applied load for 10 sec was found.

Table 4.13: Comparison of density measurement expressed as mean±SD for young and old non ribosylated bovine bone transverse section specimens and their correlation with microhardness measurement made by 100 g of load for 10 sec.

BONE	DENSITY (Mean±SD)	MICROHADRNESS (kg/mm ²)	r (Spearmen Correlation)	P
YOUNG NR BOVINE BONE	1.95±0.52	61.2±4.6	-0.31	<0.05
OLD NR BOVINE BONE	1.84±0.89	66.82±7.2	-0.42	<0.05

The NEG occurrence was observed visually in the ribosylated group for both cylindrical and transverse specimes through an alteration in the coloration from white

as seen in the color of the control group towards a yellow tone as seen in the ribosylated group (Figure 4.1).



Figure 4.1: Alteration of colour from white tone in the control group towards a yellow tone in the ribosylated group as a subjective indicator of NEG.

Average of 3 measurements for modulus of elasticity in 3 point bending test for young and old R and NR cylindrical bone specimens are given in Table 4.14. Old NR specimens have a smaller modulus of elasticity compared to young NR bone specimens. Average measurement for old ribosylated of E were smaller than young ribosylated specimens and young or old non-ribosylated specimens (Figure 4.2).

Table 4.14: Average values for modulus of elasticity determined by 3 point bending test in young and old bovine bone with respect to duration of ribosylation (NEG).

DURATION OF RIBOSYLATION	AVERAGE MODULUS OF ELASTICITY (GPa)			
	WEEKS	YOUNGR	YOUNGR	OLDNR
0	23.3	23.2	15.1	15.1
1	21.5	20.4	16.1	14.0
2	22.9	19.4	15.8	11.5
3	21.9	16.4	-	10.5

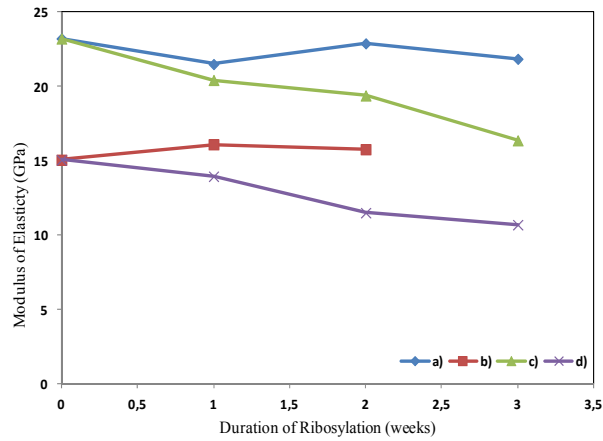


Figure 4.2: Graph for change in elastic modulus measured by 3 point bending test in young and old bovine bone with respect to duration of ribosylation (NEG). (a) young NR-bovine bone; b) old NR-bovine bone; c) young R-bovine bone; d) old NR-old bovine bone).

K_{1c} values calculated by Eq. 2.6 and expressed as mean \pm SD by application of various loads in microindentation testing are given in Table 4.15 for young and old ribosylated dry bovine bone with respect to duration of NEG. Microcrack and K_{1c} obtained by 500 g of load in the 1st week were statistically different than those in the 2nd and 3rd weeks in young bovine bone.

Table 4.15: K_{Ic} values expressed as mean \pm SD and measured by microcrack length in young and old dry bovine bone with respect to various applied load and duration of ribosylation (NEG).

LOAD and DURATION of MICRO-INDENTATION	WEEK	YOUNG BOVINE BONE		OLD BOVINE BONE	
		MICROCRACK LENGTH (μ m) (Mean \pm SD)	K_{Ic} (MPa \sqrt m) (Mean \pm SD)	MICROCRACK LENGTH (μ m) (Mean \pm SD)	K_{Ic} (MPa \sqrt m) (Mean \pm SD)
300g for 10sec	1	55.25 \pm 5.84	4.50 \pm 1.10	57.34 \pm 5.35	3.86 \pm 0.89
	2	54.36 \pm 7.83	5.14 \pm 1.29	-	-
	3	-	-	49.17 \pm 3.051	4.61 \pm 0.31
500g for 10sec	1	70.99 \pm 9.07 [†]	6.20 \pm 3.22 [†]	65.97 \pm 7.57	6.29 \pm 2.18
	2	66.15 \pm 3.80	5.32 \pm 0.66	63.52 \pm 1.26	4.49 \pm 0.77
	3	67.25 \pm 3.84	5.87 \pm 1.51	89.08 \pm 46.04	4.16 \pm 2.04
1000g for 10sec	1	96.90 \pm 6.32	7.41 \pm 1.54	96.57 \pm 14.30	6.48 \pm 1.94
	2	98.70 \pm 11.29	5.32 \pm 0.66	87.38 \pm 5.83	8.73 \pm 5.11
	3	93.70 \pm 7.079	7.38 \pm 2.36	94.05 \pm 46.04	6.12 \pm 21.73
2000g for 10 sec	1	136.80 \pm 10.81 [†]	8.95 \pm 3.74	133.39 \pm 7.85	8.67 \pm 2.40
	2	133.081 \pm 10.36	10.90 \pm 7.22	124.66 \pm 6.75	8.34 \pm 2.81
	3	133.97 \pm 12.05	9.82 \pm 6.20	128.52 \pm 9.48	8.56 \pm 2.54

[†]: Statistically different from 2nd and 3rd week measures (p<0,05).

Effect of indentation load on microcrack length is demonstrated in Figure 4.3A for young ribosylated dry bovine bone, in Figure 4.3B for old ribosylated dry bovine bone, and in Figure 4.3C for comparison of young and old bones. It is evident that microcrack length increases with increasing the microindentation load in microindentation testing.

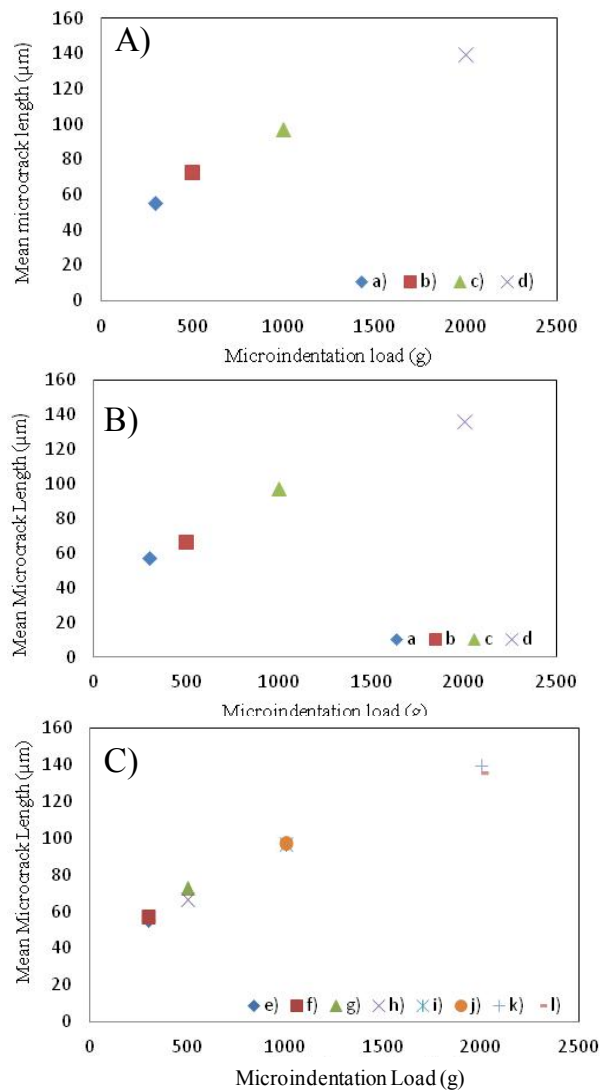


Figure 4.3: Mean microcrack length vs indentation load graph A) for young ribosylated dry bovine bone, B) for old ribosylated dry bovine bone, C) for comparison of young and old bovine bone: a) 300 g for 10 sec; b) 500 g for 10 sec; c) 100 g for 10 sec; d) 2000 g for 10 sec; e) 300 g in young bovine bone for 10 sec; f) 300 g in old bovine bone for 10 sec; g) 500 g in young bovine bone for 10 sec; h) 500 g in old bovine bone for 10 sec; i) 1000 g in young bovine bone for 10 sec; j) 1000 g in old bovine bone for 10 sec; k) 2000 g in young bovine bone for 10 sec; l) 2000 g in old bovine bone for 10 sec.

Mean K_{1c} values measured by different microindentation loads with respect to duration of ribosylation are shown in Figure 4.4 A) in young bovine bone; B) in old bovine bone; C) both. It is apparent that K_{1c} values increase with increased microindentation load. Comparison of young and old bovine bone showed that K_{1c} values are higher in old bovine bone compared to young and this property remained roughly the same during ribosylation weeks.

Mean microcrack length values measured by different microindentation loads with respect to duration of ribosylation were shown in Figure 4.5 A) in young ribosylated dry bovine bone B) in old ribosylated dry bovine bone C) both. Apart from the effect of micro indentation load on microcrack length, it is observed that microcrack length increased in the 3rd week of ribosylation in old bovine bone while it is almost the same for young bovine bone. Older bone has lower microcrack length when compared to young bovine bone by 300, 1000, 2000 g that persisted almost all ribosylation weeks.

Effect of amount of NEG determined by duration of ribosylation on K_{1c} vs microcrack length relation was shown for 300 g indentation load for young bovine bone in Figure 4.6A, for old bovine bone in Figure 4.6B, for comparison of young and old bovine bone in Figure 4.6C. Microcrack did not develop by 300 g in old bovine bone. A prominent difference was not observed between young and old bovine bone during ribosylation period.

Effect of amount of NEG determined by duration of ribosylation on K_{1c} vs microcrack length relation is shown for 500 g indentation load for young bovine bone in Figure 4.7A, for old bovine bone in Figure 4.7B, for comparison of young and old bovine bone in Figure 4.7C. A slight difference of 1st week compared to 2nd and 3rd weeks can be seen for young bovine bone but not in the old bovine bone. Comparison graph does not indicate a prominent difference between the two groups.

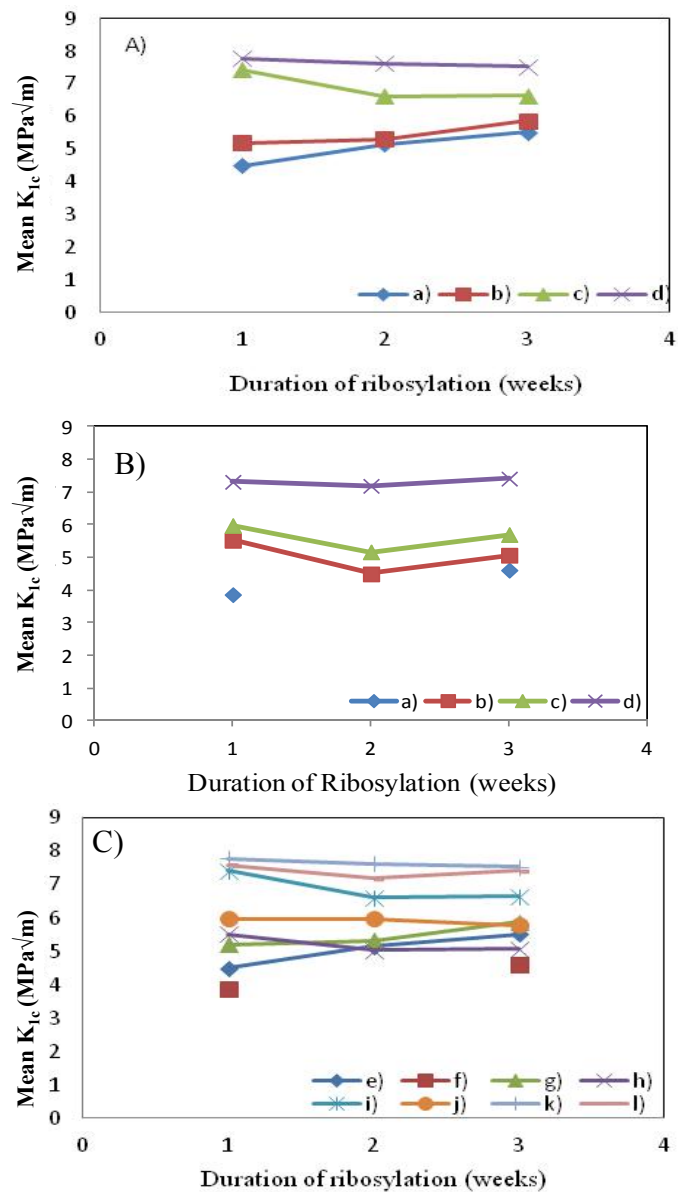


Figure 4.4: Mean K_{Ic} values measured by different microindentation loads with respect to duration of ribosylation A) in young bovine bone B) in old bovine bone C) both: a) 300 g for 10 sec; b) 500 g for 10 sec; c) 100 g for 10 sec; d) 2000 g for 10 sec; e) 300 g in young bovine bone for 10 sec; f) 300 g in old bovine bone for 10 sec; g) 500 g in young bovine bone for 10 sec; h) 500 g in old bovine bone for 10 sec; i) 1000 g in young bovine bone for 10 sec; j) 1000 g in old bovine bone for 10 sec; k) 2000 g in young bovine bone for 10 sec; l) 2000 g in old bovine bone for 10 sec.

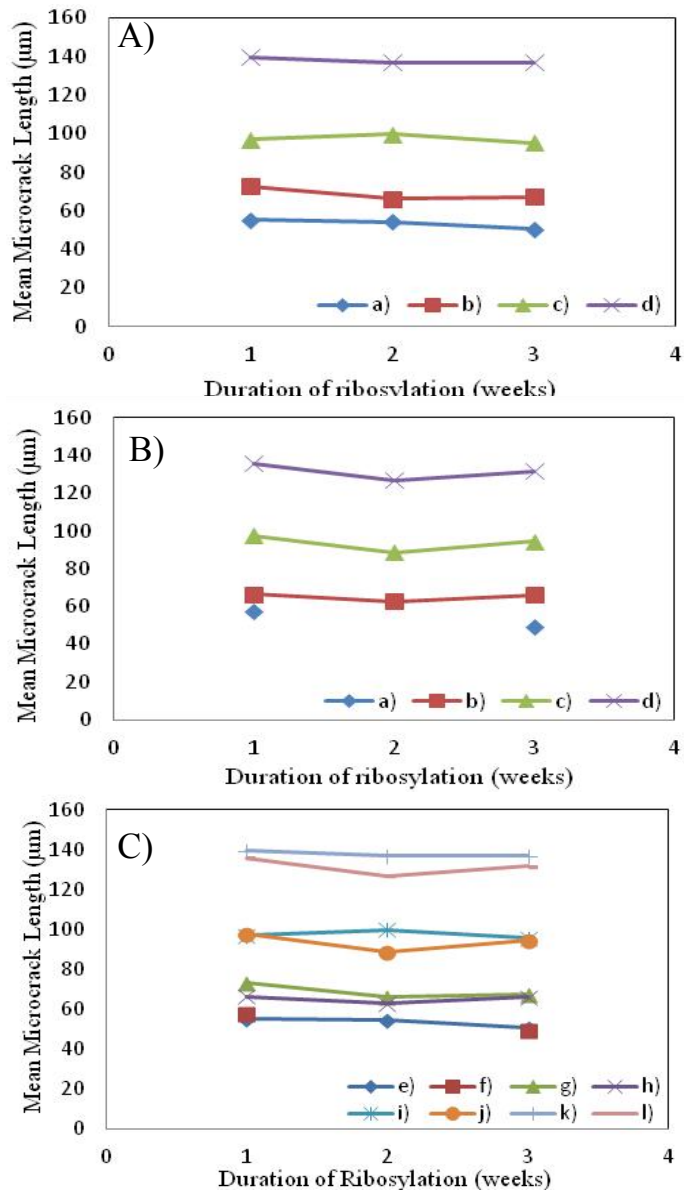


Figure 4.5: Mean microcrack length values measured by different microindentation loads with respect to duration of ribosylation: A) in young ribosylated dry bovine bone; B) in old ribosylated dry bovine bone; C) both: a) 300 g for 10 sec; b) 500 g for 10 sec; c) 100 g for 10 sec; d) 2000 g for 10 sec; e) 300 g in young bovine bone for 10 sec; f) 300 g in old bovine bone for 10 sec; g) 500 g in young bovine bone for 10 sec; h) 500 g in old bovine bone for 10 sec; i) 1000 g in young bovine bone for 10 sec; j) 1000 g in old bovine bone for 10 sec; k) 2000 g in young bovine bone for 10 sec; l) 2000 g in old bovine bone for 10 sec.

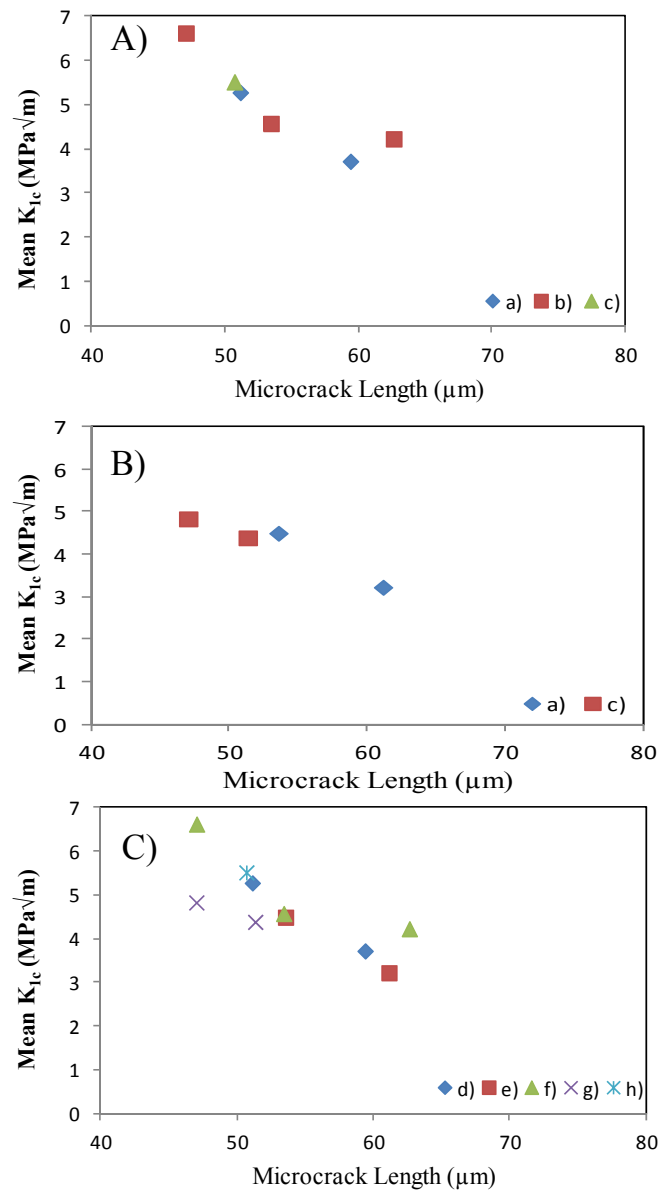


Figure 4.6: Mean K_{Ic} vs mean microcrack length by 300 g for 10 sec microindentation load A) for young ribosylated dry bovine bone; B) for old ribosylated dry bovine bone; C) for comparison of young and old bovine bone with respect to duration of ribosylation (NEG): a) week 1; b) week 2; c) week 3; d) young bovine bone in week 1; e) old bovine bone in week 1; f) young bovine bone in week 2; g) young bovine bone in week 3; h) old bovine bone in week 3.

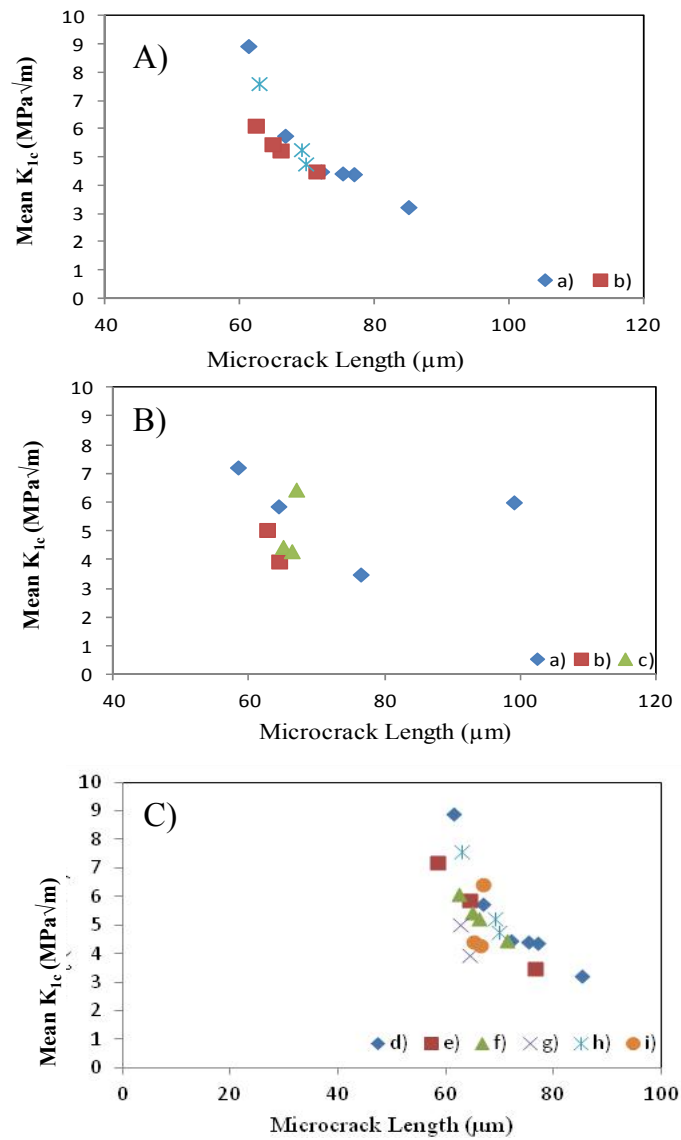


Figure 4.7: Mean K_{Ic} vs mean microcrack length by 500 g for 10 sec microindentation load: A) for young ribosylated dry bovine bone, B) for old ribosylated dry bovine bone, C) for comparison of young and old bovine bone with respect to duration of ribosylation (NEG): a) week 1, b) week 2, c) week 3, d) young bovine bone in week, 1 e) old bovine bone in week 1, f) young bovine bone in week 2, g) old bovine bone in week 2, h) young bovine bone in week 3, i) old bovine bone week in 3.

Effect of amount of NEG determined by duration of ribosylation on K_{1c} vs microcrack length relation is shown for 1000 g indentation load for young bovine bone in Figure 4.8A, for old bovine bone in Figure 4.8B, for comparison of young and old bovine bone in Figure 4.8C. A slight difference between ribosylation weeks can be seen in young bovine bone graph. Old bovine bone showed almost no difference between weeks. K_{1c} vs microcrack length comparing young and old bone was not different with respect to amount of ribosylation.

Effect of amount of NEG determined by duration of ribosylation on K_{1c} vs microcrack length relation is shown for 2000 g indentation load for young bovine bone in Figure 4.9A, for old bovine bone in Figure 4.9B, for comparison of young and old bovine bone in Figure 4.9C. Week 2 and 3 were close to each other with a slight difference in young bone. Week 1 and 2 were slightly different for old bovine bone. On the other hand, comparison of young and old bones did not show a prominent difference with increasing the amount of ribosylation by 2000 g indentation load.

Effect of indentation load in microhardness experiment are studied in Figure 4.10 for K_{1c} vs microcrack length in the 1st week in A) young, B) old ribosylated dry bovine and C) their comparison.

Effect of indentation load in microhardness experiment are studied in Figure 4.11 for K_{1c} vs microcrack length in the 2nd week in A) young, B) old ribosylated dry bovine and C) their comparison. It is clear that K_{1c} vs microcrack length relation is effected from increased indentation load. Younger bone looks tougher than older bone in comparison graph for the 2nd week of ribosylation.

Effect of indentation load in microhardness experiment are studied in Figure 4.12 for K_{1c} vs microcrack length in the 3rd week in A) young, B) old ribosylated dry bovine and C) their comparison. Increased indentation load effected the graph both in young and old bovine bone. Comparison graph did not indicate a prominent difference between young and old bovine bone for the 3rd ribosylation week.

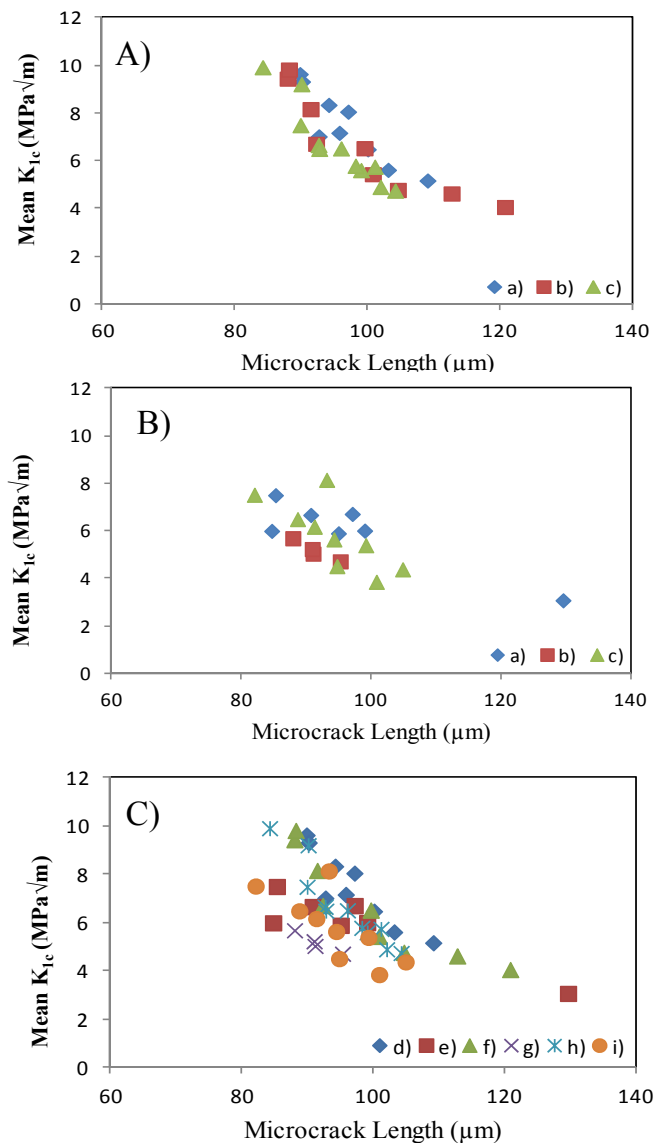


Figure 4.8: Mean K_{Ic} vs mean microcrack length by 1000 g for 10 sec microindentation load: A) for young ribosylated dry bovine bone; B) for old ribosylated dry bovine bone; C) for comparison of young and old bovine bone with respect to duration of ribosylation (NEG): a) week 1; b) week 2; c) week 3; d) young bovine bone in week 1; e) old bovine bone in week 1; f) young bovine bone in week 2; g) old bovine bone in week 2; h) young bovine bone in week 3; i) old bovine bone in week 3.

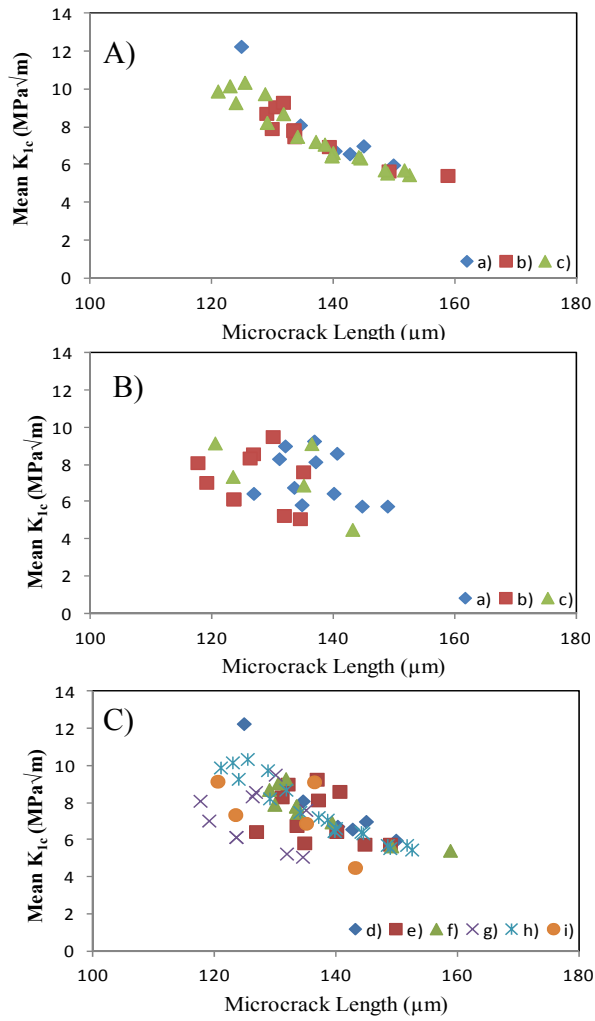


Figure 4.9: Mean K_{Ic} vs mean microcrack length by 2000 g for 10 sec microindentation load: A) for young ribosylated dry bovine bone; B) for old ribosylated dry bovine bone; C) for comparison of young and old bovine bone with respect to duration of ribosylation (NEG): a) week 1; b) week 2; c) week 3; d) young bovine bone in week 1; e) old bovine bone in week 1; f) young bovine bone in week 2; g) old bovine bone in week 2; h) young bovine bone in week 3; i) old bovine bone week in 3.

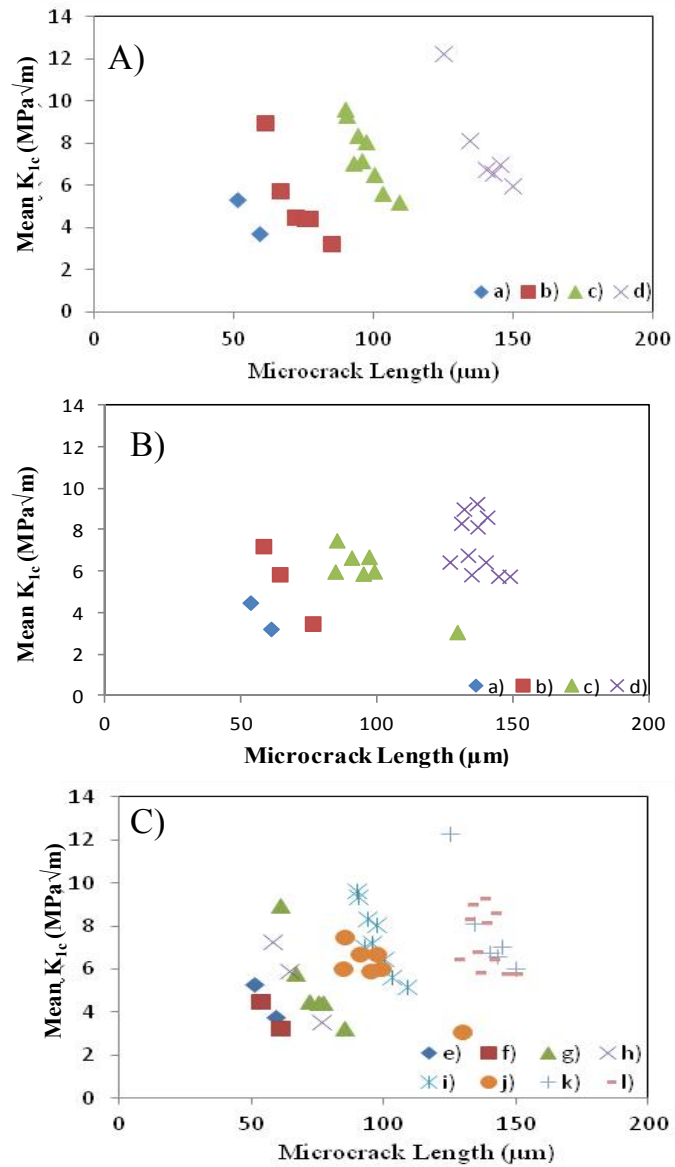


Figure 4.10: K_{Ic} vs microcrack length at various indentation loads in A) young ribosylated dry bovine bone B) old ribosylated dry bovine bone C) for comparison of young and old bovine bone after 1 week of ribosylation (NEG): a) 300 g; b) 500 g; c) 1000 g; d) 2000 g of indentation load; e) 300 g in young bovine bone for 10 sec; f) 300 g in old bovine bone for 10 sec; g) 500 g in young bovine bone for 10 sec; h) 500 g in old bovine bone for 10 sec; i) 1000 g in young bovine bone for 10 sec; j) 1000 g in old bovine bone for 10 sec; k) 2000 g in young bovine bone for 10 sec; l) 2000 g in old bovine bone for 10 sec.

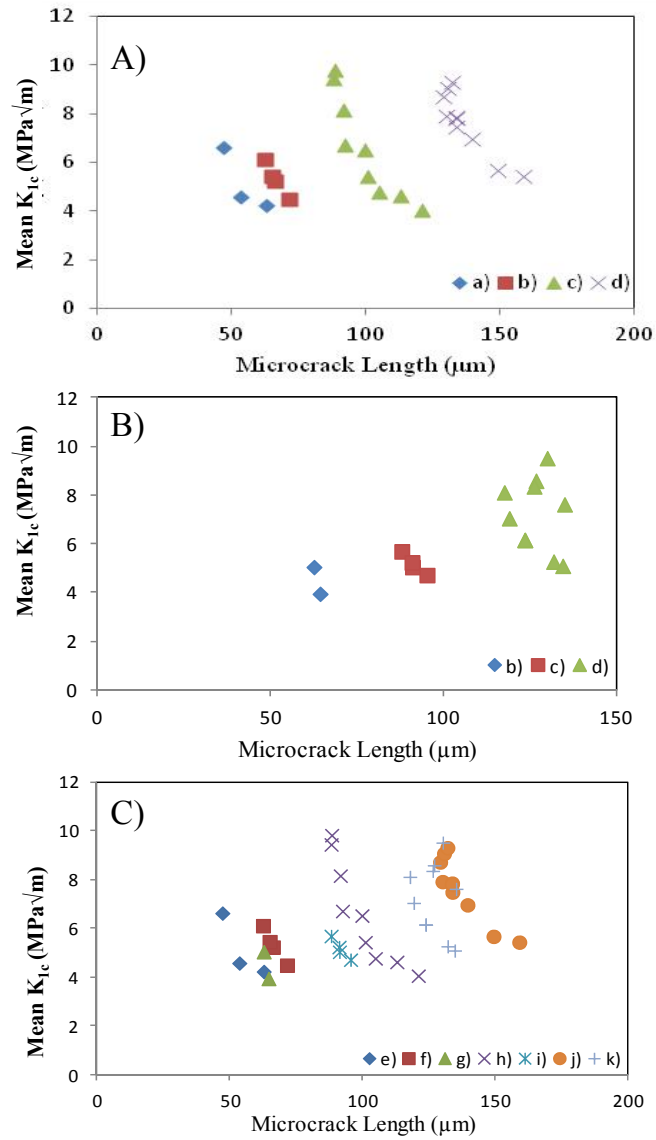


Figure 4.11: K_{Ic} vs microcrack length at various indentation loads in A) young ribosylated dry bovine bone; B) old ribosylated dry bovine bone; C) for comparison of young and old bovine bone after 2 weeks of ribosylation (NEG): a) 300 g; b) 500 g; c) 1000 g; d) 2000 g of indentation load; e) 300 g in young bovine bone for 10 sec; f) 500 g in young bovine bone for 10 sec; g) 500 g in old bovine bone for 10 sec; h) 1000 g in young bovine bone for 10 sec; i) 1000 g in old bovine bone for 10 sec; j) 2000 g in young bovine bone for 10sec; k) 2000 g in old bovine bone for 10 sec.

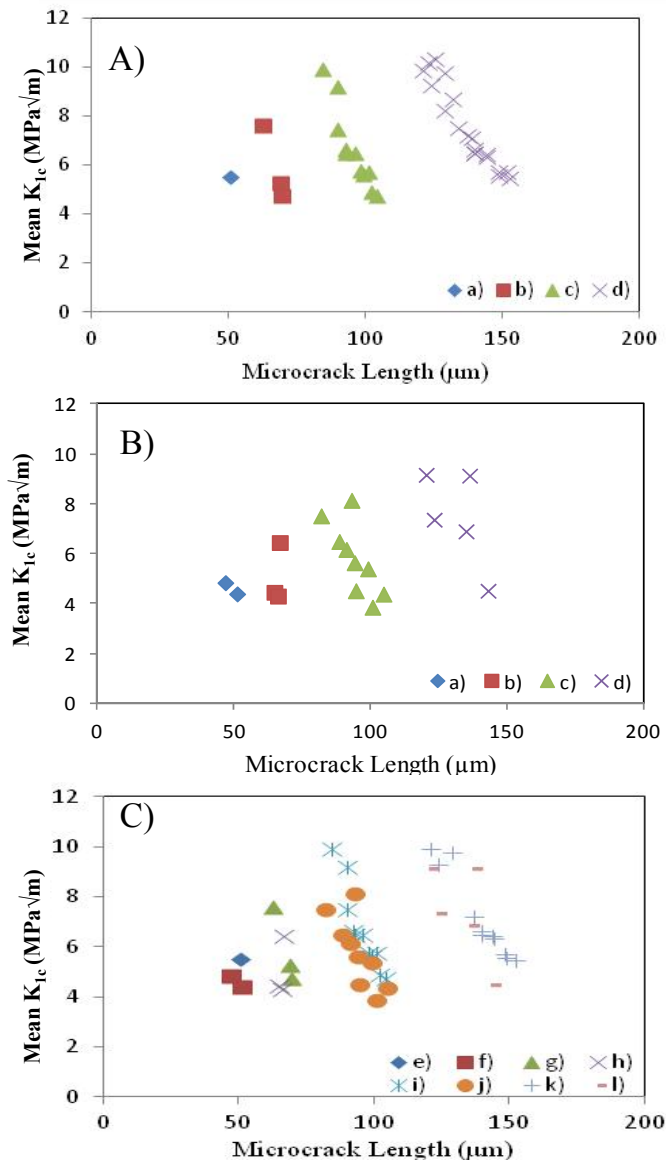


Figure 4.12: K_{Ic} vs microcrack length at various indentation loads in A) young ribosylated dry bovine bone; B) old ribosylated dry bovine bone; C) for comparison of young and old bovine bone after 3 week of ribosylation (NEG): a) 300 g; b) 500 g; c) 1000 g; d) 2000 g of indentation load; e) 300 g in young bovine bone for 10 sec; f) 300 g in old bovine bone for 10 sec; g) 500 g in young bovine bone for 10 sec; h) 500 g in old bovine bone for 10 sec; i) 1000 g in young bovine bone for 10 sec; j) 1000 g in old bovine bone for 10 sec; k) 2000 g in young bovine bone for 10 sec; l) 2000 g in old bovine bone for 10 sec.

Effect of young or old ribosylated bone types on K_{Ic} vs microcrack length graph are shown in Figure 4.13 by 1000 g of applied load after 2 and 3 weeks of ribosylation. Although data for young and old bone were not prominently different, younger bone seems to be tougher for 2nd and 3rd weeks of ribosylation.

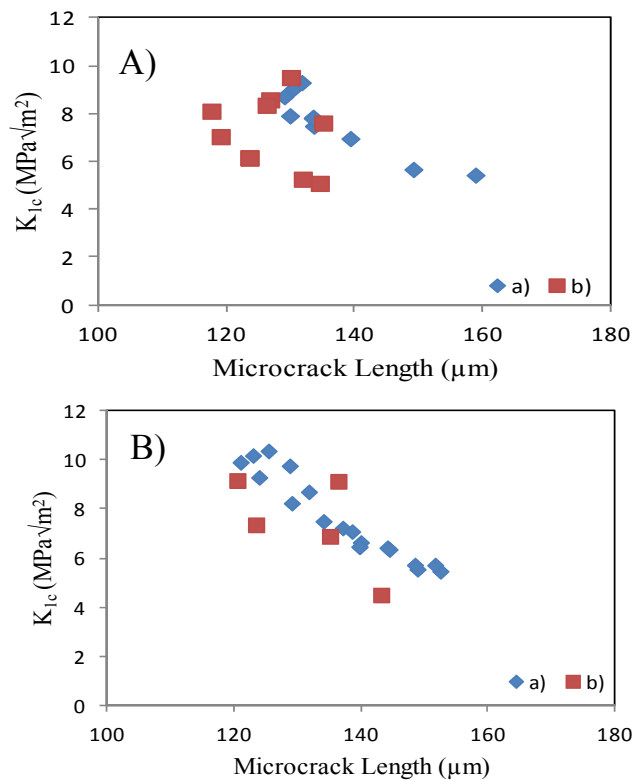


Figure 4.13: K_{Ic} vs microcrack length at 1000 g indentation loads in young and old dry bovine bone after A) 2 weeks of ribosylation; B) 3 weeks of ribosylation (NEG): a) young bovine bone; b) old bovine bone.

Effect of young or old ribosylated bone types on K_{Ic} vs microcrack length graph are shown in Figure 4.14 by 2000 g of applied load after 2 and 3 weeks of ribosylation. Although data for young and old bone were not prominently different, younger bone seems to be tougher for 2nd and 3rd weeks of ribosylation.

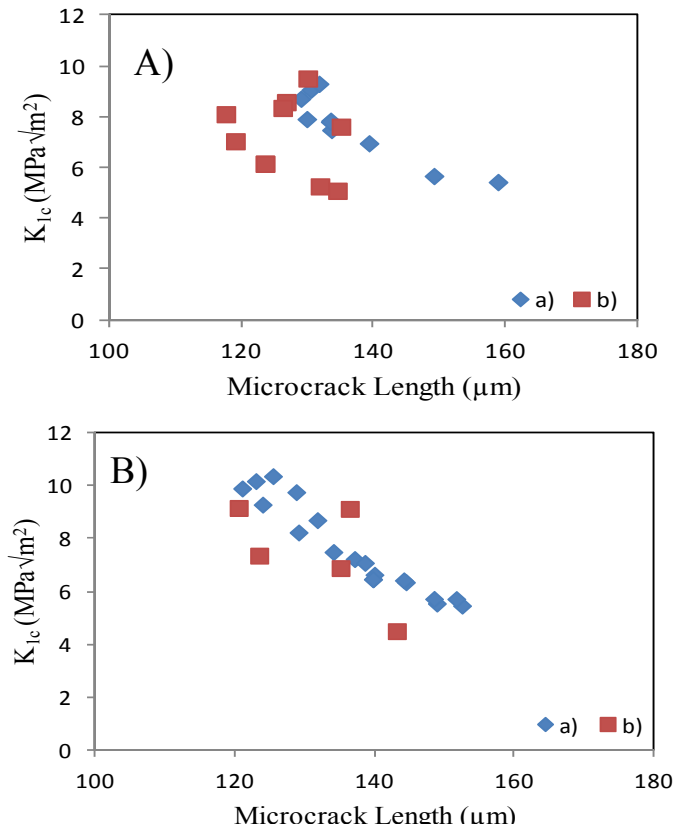


Figure 4.14: K_{Ic} vs microcrack length at 2000 g indentation loads in young and old dry bovine bone after A) 2 weeks of ribosylation; B) 3 weeks of ribosylation (NEG): a) young bovine bone; b) old bovine bone.

4.3. CHARACTERIZATION OF FRACTURE SURFACES BY MICROSCOPY

Fracture surface properties of cylindrical shaped bone material after 3 point bending are given in Figure 4.15. It can be seen that bone has grown a crack at the point where the tensile stress is concentrated. Images are consistent with the information that bone has high compressive strength and low tensile strength. The heterogenous structure of bone due to vascular structures and osteons can be noticed on the surface. The areas work as stress concentrators and may cause a crack to develop during testing.

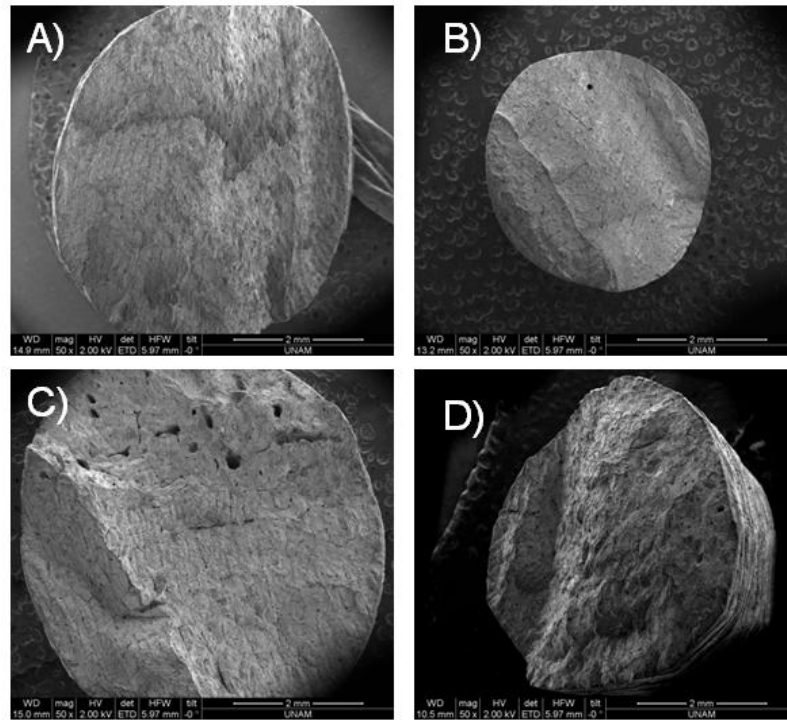


Figure 4.15: SEM images from fracture surface of cylindrical shaped cortical bone specimens after 3 point bending test from different specimens in A,B,C,D.

Hardly few microcracks were identified by indentation loads of 200 g or below. Images from indentations without cracks are shown in Figure 4.16.

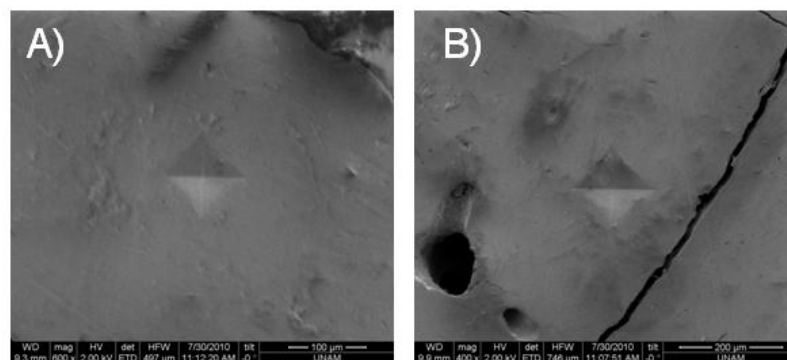


Figure 4.16: Indentations without microcracks at load lower than 200 g A) x600, B) x400 times of magnification. Canals that belong to Haversian system and a line of non-indentation induced crack are also visible.

SEM images were used to identify type of microcracking. Young and old bovine bone specimens were studied considering the duration of ribosylation. A microcrack origination from the corner of a microindentation is shown in Figure 4.17 in young bovine bone 1 week after ribosylation. Crack tip and formation zone can be seen in closer view (Figure 4.17 B, C). Uncracked ligament bridging (Figure 4.17 C, D) and collagen bridging were observed as toughening mechanisms.

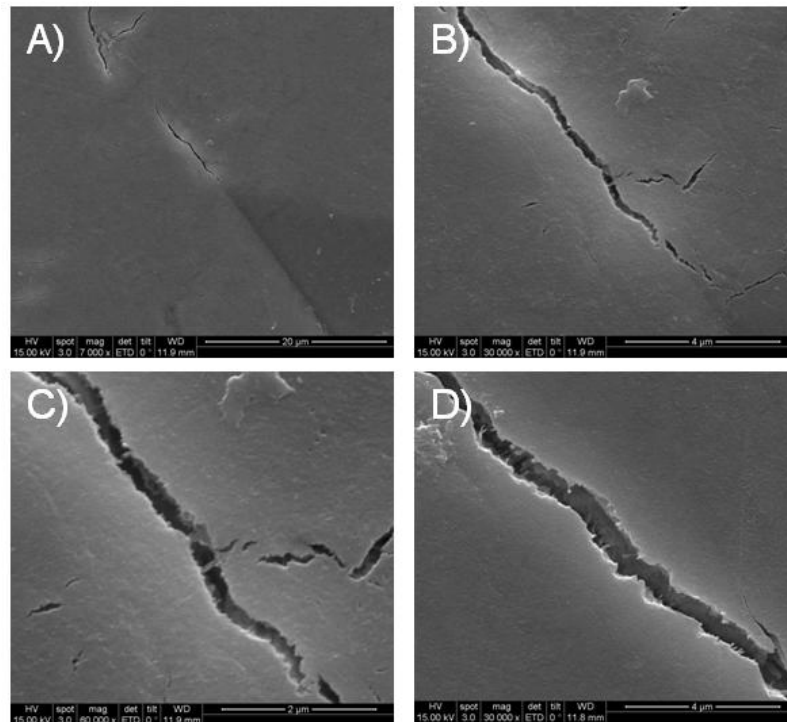


Figure 4.17: SEM images of A) a microcrack originating from the corner of a microcrack formed by microindentation testing in young ribosylated bovine bone 1 week after ribosylation B) and C) closer view of microcrack tip and wake in the same fracture, D) in a different specimen.

Crack bridging is better demonstrated in Figure 4.18 studying closer views of crack wake in young bovine bone 2 weeks after ribosylation. Figure 4.18 A,B demonstrates the collagen fibers that have teared apart ends. Figure 4.18 C,D demonstrates nicely the collagen brige formation with partial preservation of some collagen fibers extending between the 2 edges of the crack wake. These extending

fibers are clearly observed in different specimens in views getting closer and closer to the wake zone in Figure 4.18 E, F, G, H.

SEM images taken from young bovine bone 3 weeks after ribosylation are shown in Figure 4.19 which shows microindentation induced microcracks. Uncracked ligament bridging and bridge formation can be seen in Figure 4.19 A, B and C, D in combination. Collagen bridging is observed in Figure 4.19 E, F, G and uncracked ligament bridging in Figure 4.19 H, I, J as the dominant extrinsic toughening mechanisms. It is noted that the number of collagen bridges were reduced after in vitro ribosylation.

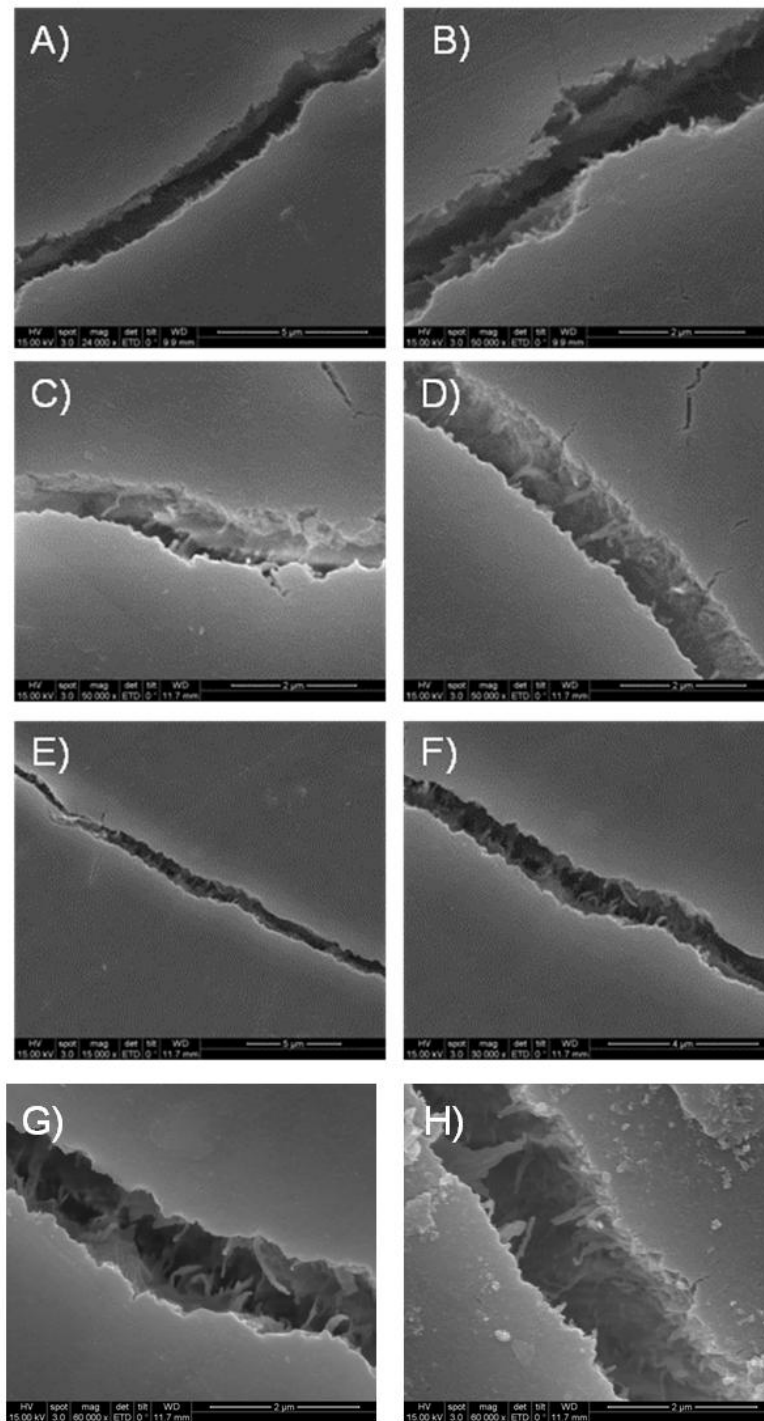


Figure 4.18: SEM image of a microcrack from young bovine bone 2 weeks after ribosylation in views getting closer to the wake zone: (A, B), (C, D), and (E, F, G, H) pairs of images belong to 3 different specimens.

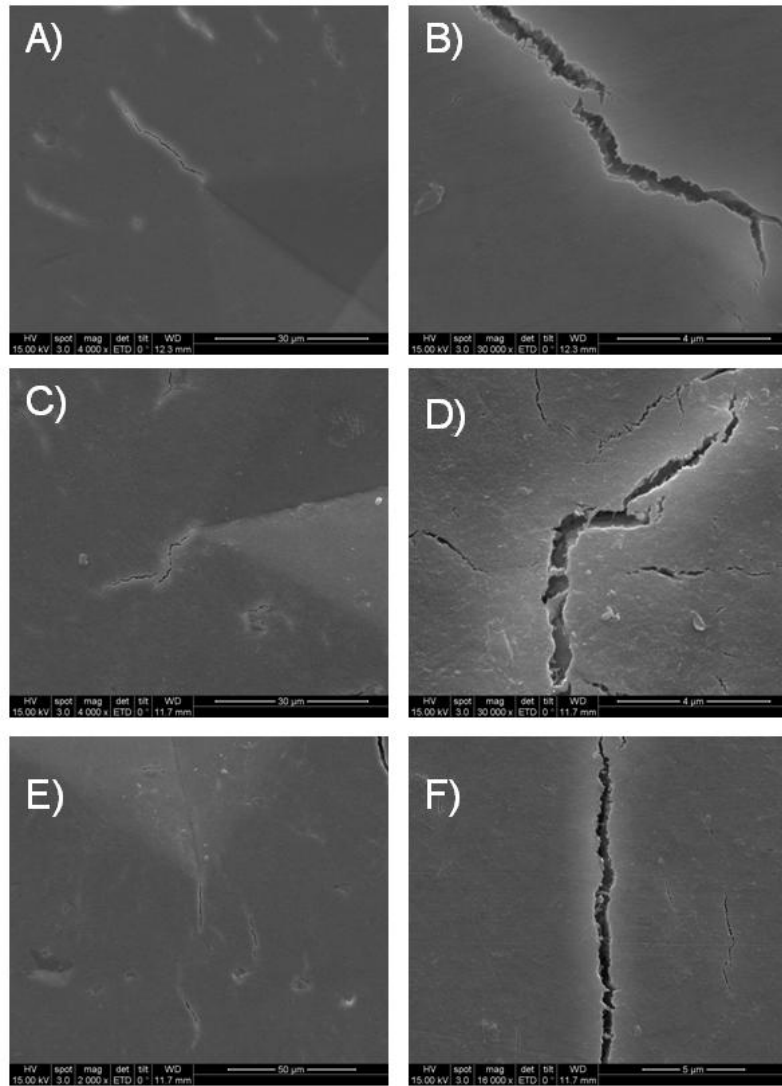


Figure 4.19: SEM images of microindentation induced microcracking from young bovine bone 3 weeks after ribosylation. A, B and C, D and E, F, G and H, I, J, K belong to different specimens or different microcracks.

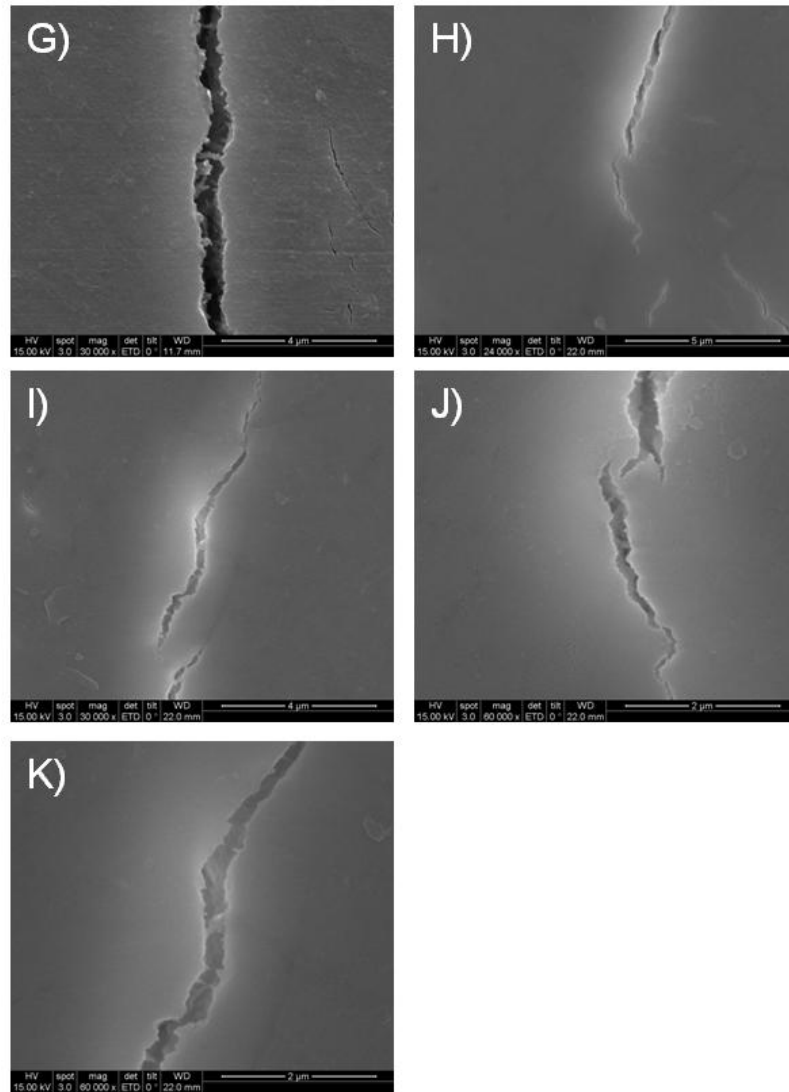


Figure 4.19: (Continued).

CHAPTER 5

DISCUSSION

5.1. VARIABLES THAT EFFECT MICROHARDNESS

Micro indentation test was used to derive the hardness and toughness of bone at the microscale, since these are related to microstructure at the site of indentation. Bone is an anisotropic heterogenous composite material at the scale of micrometers and nanometers which is composed of harder mineral crystals of calcium phosphates and softer collagen. Therefore, tools are needed to reveal the material properties at different scales. Effect of amount of load, dwell time (duration of indentation) and state of bone (wet or dry) were studied on microhardness test to detect the collagen stiffening by means of NEG. These values are selected to find the precision of the measurement in detecting changes in collagen fiber structure and binding caused by NEG.

a) Effect of Applied Load

Microhardness values measured by 10 g of load for 10 sec were indifferent between the ribosylated and non-ribosylated groups in the young and old bovine bone indicating that this load is not indicative of the structural collagen changes. Loads of 25 g, 50 g, 100 g and 200 g for 10 sec were able to differ R from NR young bone, R from NR old bovine bone. It was also able to differ NR young bovine bone from R-young, NR-old and R-old bovine bone. This might point that microhardness test by these loads are able to discriminate non-modified collagen structure from modified collagen. On the other hand, it is not found to discriminate the degree of NEG modification among R young, R and NR old bone [30].

A previous study on bone did not find any change of microhardness with applied load, on the other hand another study found that applied test mass below 50 g were not reliable for hardness measurements. There is a study in which hardness variation with applied load was found to be largest by 10 g but minimal by loads of 50 g and above for bovine bone. They proposed that a minimum load of 100 g is needed for bovine bone to obtain results to reproduce among different machines of microindentation. They demonstrated that hardness decreased with increasing applied mass. This can be explained by the relation of applied load and the indentation size. While microindentation could evaluate small regions, impression is required to be large enough to measure precisely [30].

Domain phenomena for example creep and relaxation could cause variation among measurements sets on the same sample. Additionally variation could also be caused by pores representing the spatial domain. Technically, calibration, set up and compliance of test machine are important at low applied loads. Compliance of test machine are in series with compliance of sample. If the compliance of indentation machine is low, it could add to the specimen compliance causing an error measurement. Vickers and Knoop type of indentations have four-sided pyramids. Vickers point has equal diagonals in contrast to the Knoop point which has indenter diagonals with two distinct lengths. Both indenter points are sensitive to elastic anisotropy. Due to difference in diagonals, Knoop point is reported to be more sensitive than Vickers [30].

Hardness versus load graph is found to be either constant or decreasing with load or transiting to a constant value for materials such as metals or ceramics. Increase in microindentation with increased load was observed in dry embalmed human rib [28]. However, hardness is found to decrease with the applied load in bovine metacarpus microindentation in wet state.

Concept of stress concentration at flaws is not found to be applicable for natural materials due to their many levels of structural hierarchies. At the microstructural level, bone is composed of cylindrical haversian systems. Therefore, one should be cautious comparing the hardness values at different length scales. The

microindentations can solely cover a small osteonal area at lower loads. Hardness values measured by small deformations on the size of the distance among osteocytes could be different than hardness values obtained from indentations on the scale of multiple osteons [28]. In this study various loads from 10 g at the lowest to 2000 g at the highest range were used, indentation sizes varying in a wide range. The indentation area covered different levels of microstructures may contribute to different findings.

b) Effect of Indentaion Duration

It is investigated whether period of time the indenter point makes a contact with the sample effects indentation measurement results. For this, a constant load of 100 g for varying durations of indentations namely 5, 10, 20 and 30 sec were measured. It is found that varying indentation duration did not make a difference in discriminating degree of ribosylation between R young, R and NR old bovine bone in precision of measurement. It was possible to discern NR young bovine bone from 3 other groups with all indentation of duration studied. It was found that measurements differentiate R from NR young bone, R from NR old bovine bone, which were similar to the findings due to effect of applied load. In the support of our findings, a study did not find any significant difference for indentation durations from 5 sec to 60 sec [30].

c) Effect of Hydration

Although many of the literature use dry or dry embalmed bone specimens, wet state of bone represent a more physiological environment. Water content of bone, which typically ranges from 10 and 20%, has a fundamental role in determining its mechanical features [71]. Duration that a sample waited out of a water based liquid is important since the specimen could dry.

It is documented that the mechanical properties of bone show important changes after dehydration. In general, drying increases the Young's modulus of bone, decreases its toughness and reduces the strain to fracture. It was shown that rewetting the dried bone replenish the mechanical properties which are similar to fresh wet

specimens. It was postulated that drying leads to contraction of the individual collagen fibrils with the degree of contraction depending on the level of mineralization in the bone [71]. Thus time the bone specimen waited out of water based liquid can change indentation measurements. The specimens were kept up to 60 min out of solutions at RT for the examination of wet specimens. They are left for drying for 24 hours to study the effect of dry state.

In a study it was shown that drying causes a significant increase in the microhardness of bone. Furthermore, higher drying temperatures were shown to produce greater increases in microhardness [71]. A 9% increase in microhardness after 2 days of drying was found in another study that used microindentation testing [30]. It was also found that drying caused increased elastic modulus and hardness in bone with nanoindentation. This increase was different in interstitial and osteonal regions of bone [72]. Additionally, a material pile-up near the pyramidal indent corners has been detected because of the applied indentation load in embalmed specimens. On the other hand, there was no specimen pile-up detected at the indentation edges in wet specimens [28]. Results of this thesis are consistent with the previous results. Microhardness of dry specimens being either ribosylated or non-ribosylated were statistically higher than that of wet specimens in young and old bone. This difference was detected by all indentation loads and durations except for 10 g for 10 sec.

5.2. MICROCRACK FORMATION BY MICROINDENTATION

While studies to measure toughness of bone and its alteration with extension of crack (rising R-curve behaviour) were at a macroscale, the techniques did not allow a microstructural toughness measurement. Measurement of microscale toughness in the bone matrix could be an important step for the examination of quality of bone and microcracks [35].

Since indentation fracture allows measurement at the microscale, it has a few superiority over toughness testing methods at the macroscale. This technique allows

numerous measurements on a little amount of material. Cracks generated in bone are about the same size as those seen in vivo. This might give an insight into the bone damage nature. The aim of this thesis was to investigate indentation fracture as a method of measuring the cortical bone microstructural toughness. A few cracks were observed by light microscopy at the corners or edges of indentations by 50, 100 and 200 g of load with a marked viscoelastic recovery at low applied loads namely 10, 25 g and any time for indentation. At a load of 300 g, microcracks in greater number were found to develop at the site of indentation.

Microindentation allows evaluating contact related features, especially surface damage under compression by sharp particles. SEM imaging of microindentations could clarify response of material to mechanical loads [28]. Additionally, another point of concern is related with dehydration of the indented material samples to be able to observe by SEM. Dehydration of cortical bone specimens in the presence of a stress concentrator can induce spontaneous cracking at the stress concentration sites [36]. Vacuum used for SEM imaging in dry state in this study would cause additional microcracks on the surface in our study as well. These were identified and were not considered for measurement.

Mode of deformation and crack propagation are also dependent on bone microstructure. Cortical bone has a hierarchical structure. Phase and material direction change and there is a 5% porosity roughly because of living cells and blood vessels. These structural heterogeneities might be responsible for the variability in crack length. Dry cortical bone was shown to have viscoelastic, plastic and brittle behaviors in microindentation.

Tropocollagen molecules are frequently capable of distributing energy by unconnected microcrack formation or viscoplastic flow. The characteristic nanostructure of mineralized collagen fibrils is crucial for its capacity to withstand large deformations and for its strength. Staggered mineralized collagen fibrils provide an effective energy dissipation mechanism which contributes to toughening [28]. Smaller loads of indentation were not observed to produce microcracks even if they were modified structurally by NEG in this thesis.

5.3. MICROINDENTATION TOUGHNESS

Accurate measurement of the fracture toughness of materials in brittle character could be difficult. Making pointed, sharp, exact preformed cracks could fail the specimen. Fracture toughness data obtained by use of notched specimens could end up with inaccurately high values. Toughness measurements from indent cracks are insufficient to quantify and compare the results obtained by other techniques and from other studies. They may help to categorize the toughness of various materials semi-quantitatively. On the other hand they cannot be used indiscriminately. Wide toughness differences are necessary to make conclusions [35].

In this thesis, Vickers microindenter was used to calculate the indentation toughness of the bone with the specified equations. Many number of (more than 30) equations was found in the literature to calculate fracture toughness using the length of the indented cracks. These equations are not found from using physical models but they are found by curve fitting to experimental data. There are several concerns related with these equations. As a first concern, an empirical constant of calibration is utilized. The constant was not proven to be valid by physical models. Additionally standard deviation to obtain the calibration constant is found to be $\pm 25\%$. The toughness is proposed to be $\pm 50\%$ in experimental measurements [35].

There are some probable violations of postulations for the model. This can contribute to large errors. VIF model assumes that two perpendicular half penny cracks in median/radial directions are generated below the indent surface area during unloading part of indentation because of the residual tensile stress field. It is also assumed that the crack is in equilibrium with generated stress field. Palmqvist type indentation cracking is hard to differentiate from half-penny type of crack looking above on the surface in some ceramics. An analysis suggests that fundamental fracture toughness equations are little effected if the cracks formed in indentation are in balance with stress field. Another point of is that cracks are often observed to form along the loading part of the microindentation instead of unloading. This may disturb residual stress field underlying the surface and effect the crack growth in unloading

portion of indentation. Another point is that cone cracks or lateral cracks that are known to disturb the residual stress field may form. These types of cracks are frequently observed with Vickers indentation. These cracks require post indent sectioning to be visible in opaque materials [35]. Formation of lateral cracks were detected by either light microscopy or SEM with Vickers indent. Cone cracks were not detected due to requirement for sectioning.

It is difficult to make an accurate equation that applies to all brittle materials. Because, it was proposed that indentation induced cracking depends on the nature of the material very much. Growth of sub-critical crack could take place after indentation, that end up with extensions of cracks. This can cause an erroneously low toughness calculations. The sub-critical crack growth threshold might be effected by the time length passing between indentation formation and measurement in addition to the testing condition that is presence of water [35].

Materials such as biocomposites and bone, teeth representing hard tissues, and bioceramics demonstrate rising resistance to fracture depending on extension of crack. Then, a fracture resistance curve (*R*-curve) indicating the strength of the material must be drawn to express fracture resistance. In rising *R* curve, fracture resistance rises with increased extension of crack. For materials with rising *R* curve, indentation fracture test allows sampling only one point on the *R*-curve. It is questionable that indentation techniques could quantify K_{Ic} correctly with a single data.

This point would depend on the applied load. Hardness, being one of the variables in toughness equation depends on the load of indentation [35]. In contrast to this, there are two separate studies which found that there is no hardness dependence on load with the Vickers tip [72].

Indentation load vs toughness relation were studied in our study in Table 4.18 and Figure 4.3 which indicated a clear relation. Previously, it has been shown that the fracture toughness calculated by the indentation method is a function of indentation load. It may increase or decrease with indentation force. Therefore, the change cannot be attributed to variations in *H* alone. Thus, even if a well-correlated equation

was used for a given material, it would not be possible to measure an R-curve by varying the indentation force. It can be concluded that the indentation hardness test is unsuitable for measuring the toughness of brittle materials and for making R-curves [36].

It is clear from Figure 4.6 that toughness increased with increased crack length. At 300 g of applied load, mean toughness was 4.5 ± 1.1 MPa $\sqrt{\text{m}}$ with a mean crack length of 55.25 ± 5.8 μm in young NR bovine bone whereas at 2000 g of applied load the mean toughness was 8.95 ± 3.74 MPa $\sqrt{\text{m}}$ with a mean crack length of 136.8 ± 10.81 μm . In another study with 3.0 N (306 g) of load applied which produced an average crack length of 56 μm , the maximum toughness was found as 2.3 MPa $\sqrt{\text{m}}$. Findings of this thesis were close to this study. On the other hand, it was reported that this measurement is at the lower end of the toughness measured by macroscopic methods. The samples' measured toughness values previously reported in literature are between 2.1-6.0 MPa $\sqrt{\text{m}}$ typically [1].

This thesis showed that microcrack length increased with the increased applied load (Table 4.5). The effect of indentation length size could cause a larger toughness measurement results. The size gets larger for higher indent loads producing longer cracks. All of these cause a higher value of toughness although the toughness is not higher in reality. This end up with erroneously rising *R*-curve-like results. This could be true for materials without showing a rising *R*-curve. Literature indicates increases or decreases in toughness with increasing indent size in materials without rising *R*-curve, such as α -SiC and a ceramic glass. *R*-curve obtained with indentation techniques was not comparable to results obtained from conventionally measured *R*-curves. More than 1 of the factors mentioned above can have a role in the variation of toughness depending on indent load. It was advised not to use alternating loads for indentation to obtain *R*-curves with method of VIF [35].

Fracture indentation method by VIF was proposed as unacceptable or inaccurate technique. Critical reviews and original data are in agreement that indentation fracture method generates important errors in the toughness measurement which does not allow comparison of VIF with other techniques. They

also suggest that the effectiveness of the method of VIF is very much limited even for comparing. The calculated toughness was found to be $\pm 50\%$ of the expected value at the 95% confidence interval. It was proposed that findings would be worse in some literature. Two materials having same toughness can produce a difference in toughness by a factor of three by this technique or sometimes error factor would be greater.

In a review it was shown that considering even similar ceramics or ceramic glasses, real toughness obtained by this technique ranks materials incorrectly [35]. Mean and SD were suggested to be used to compare hardness and crack length not only among different materials but also within the same material. They even concluded that VIF test should not be used for measurement of fracture resistance for materials like ceramics or any others. Hard tissues that are known to carry organic component are not similar to the ceramics in terms of indentation fracture testing. It was quoted that this technique introduces larger errors in softer materials when compared to brittle ceramics. If the cracking does not go out of zone of the plastic deformation produced by indentation, mechanic rules for linear elastic fracture would not be applied [35].

5.4. EFFECT OF AGING ON TOUGHNESS

Changes in collagen content, or changes to inter- and intrafibrillar collagen cross-linking, can reduce the energy required to cause bone failure (toughness), and therefore increase fracture risk. Although collagen may have less effect on bone's strength and stiffness than does mineral, it may have an important effect on bone fragility. Collagen changes that occur with age and reduce bone's toughness may be an important factor in the risk of fracture in older women with low bone mass [59]. The risk of bone fracture in human increases with age due to the decrease of bone mass and bone quality. One of the age-related changes in bone quality occurs through the formation and accumulation of advanced glycation end-products (AGEs) due to NEG.

Crack initiation toughness has been found to decrease about ~ 40% over 60 years between 40 to 100 years of age, on the other hand crack growth toughness decreased to much greater degree in a study. These were consistent with the finding of another study which found that not only the crack propagation resistance (designated by the crack-growth toughness), but also the intrinsic fracture resistance (designated by crack initiation toughness) decreases by aging [52]. The results of a study found that NEG caused a decrease in propagation fracture toughness (R-curve slope) by 52%. The combined effects of AGEs and porosity caused a 88% decrease in propagation toughness [60].

Rising R-curve behaviour was shown in some studies using macroscopic techniques in bone. Rising R-curve indicates the presence of extrinsic toughening mechanisms in the crack wake. It was found that the toughness of human and bovine bone specimens increased linearly from 1.6 to 2.5 MPa \sqrt{m} and 3.9 to 7.2 MPa \sqrt{m} , respectively for measured extensions of crack which is ~2.25 mm. Initiation K_0 results were measured to be 1.6 and 3.9 MPa \sqrt{m} for human and bovine bone, respectively. Other authors showed ~3.2 MPa \sqrt{m} and ~5 MPa $\sqrt{m/mm}$ for the crack initiation toughness and the first gradient, respectively. Another study found rising R curve with average K_0 values of ~4.38–4.72 MPa \sqrt{m} and average slopes of 1.06–2.57 MPa $\sqrt{m/m}$. The decrease in toughness of bone with age was presented. Mean crack-initiation toughness K_0 values of 2.07, 1.96 and 1.26 MPa \sqrt{m} , with average gradients of 0.37, 0.16 and 0.06 MPa $\sqrt{m/mm}$, have been detected for the young aged donor (34–41 years), middle aged donor (61-69), aged donor (85-99 years), respectively. It was demonstrated that there is not solely a decline in the crack initiation toughness by aging, but also a decline in the crack growth toughness [2].

The effect of nonenzymatic collagen modifications on the mechanical property was shown as a feature of aging and diabetes mellitus. The findings of a study indicated that nonenzymatic glycation increases with age which correlates with the deterioration of bone. It was speculated that AGE might modify the bone matrices and might take place in the remodeling of old bone tissue. It was also shown

that bone collagen is subjected to changes mediated by glycation by in vitro treatments of ribose which increased the stiffness of the collagen [33].

Pentosidine is the only AGE product that is measurable and is an old cross-link. It was used as an assessment marker for cross-links induced by the NEG [38]. It was also found that mineral does not make a barrier to stiffening effect of glycation-mediated crosslinking [61]. As a limitation of this thesis, we did not quantify the degree of ribosylation, as a measure of cross linking in collagen. Therefore it was not possible to correlate changes in microhardness and toughness with changes in amount of cross links.

Change of colour in proteins with long-life such as crystalline of lens and collagen and was taken as a proof for AGE accumulation [57]. A change from white to yellow colour in the specimens were also observed. The presence NEG and products of AGEs were confirmed by fluorescent biomarkers. It was shown that incubation for 7 days causes AGE accumulation in bone corresponding to 2–3 decades of aging. In a study it is shown that the ribosylated specimen from a 42-year-old donor has a resembling AGE level as specimen from the 74-year-old donor in the control group. Therefore, it was expected that the amount of AGEs accumulation in vitro NEG remains in physiological ranges [57]. Incubation of the specimens for 4 weeks might have caused excessive accumulation of the AGE's or might have even resulted in saturation of the crosslinks. First week changes were reflected as an increase whereas second and third week changes were lower when compared to second week. This finding might be related with the duration of ribose incubation.

Bone take its post-yield characteristics from its organic phase and its stiffness mainly from mineral phase as a composite material [57]. Organic matrix alterations due to posttranslational modifications by NEG would cause changes in post-yield behavior. In studies using a baboon model, the percentage of denatured collagen compared with total collagen content was significantly related to failure energy and to the fracture toughness of the tissue [59].

5.5. TOUGHENING MECHANISMS

Cyclic loading application causes the formation of microdamage morphologies that are prominently strain-dependent. It was demonstrated that young donors (38 ± 9 years) showed a longer fatigue life and made more diffuse damage compared to the older donors (82 ± 5 years). Old donors were found to have a shorter fatigue life and more linear microcracks compared to the younger donors. It was demonstrated that young donors had a tendency to make diffuse damage over interlamellae. Linear microcracks take a critical role in energy dissipation and they can resist a prominent fracture. Damage morphology changes due to age might be an important factor for the increased fragility of bone in the older population [4].

Microcracks were found to be smaller or were not observed at loads smaller than 1.96 N in our study. This was consistent with the results of another study. Indentational deformation recovery was shown at loads below 0.45 N due to viscoelasticity in lamp femur. This behaviour was also observed in wet bovine femur and in R-curve testing of human cortical bone. Crack ligament bridging and crack deflection are well-known toughening mechanisms in ceramics which were also identified in microindentation in the dry cortical bone. Anisotropic behavior in cracking can be ascribed to the weak porosity boundaries. In a study, microcracks were shown to develop at the indentation apex among the lamellar layers [28]. Strict structure-property relationship does not exist for bone. This might be related with multiple hierarchical levels of bone, each of them with typical mechanical properties, toughening and deformation mechanisms.

The crack-growth toughness indicates the effect of extrinsic toughening mechanisms. This mechanism is found to be principally associated with crack bridging [47],[45]. The main source of bridging in is the formation of uncracked ligaments in the crack wake. The assistance from this mechanism is demonstrated to decrease with age [52]. This finding is parallel to our findings that ribosylated young bovine bone had less number of collagen bridging.

Changes in collagen network due to aging could cause weaker collagen bridges and therefore a less crack growth toughness. Age is considered to augment non-enzymatic crosslinking in the structure of collagen [38]. This decreases collagen's postyield deformation. It was proposed that increased turnover has a negative influence on the toughness in older bone since porosity and resorption cavity formation increases. Bone turnover is beneficial in repair of bone. If the turnover is elevated, secondary osteons increase. Cement lines provide weak interfaces for cracking. A study proposed that increased bone turnover is a risk factor alone, independent of BMD [53].

A series of extrinsic toughening mechanisms have been detected in bone. Crack bridging by uncracked ligaments and collagen fibrils, crack deflection, and microcracking are microscopically observed. In this study, all of the above mechanisms were observed but particularly uncracked ligament formation and collagen bridging. Rising R-curve fracture toughness character of bovine cortical bone was not possible to be observed by indentation fracture toughness measurements therefore it is not possible to discuss extrinsic toughening mechanism contribution in the crack wake by this method. The presence of extrinsic toughening mechanisms such as crack bridging formed by collagen fibers and uncracked ligaments were observed directly by SEM [49].

It is accepted that crack bridging decrease the measured compliance (i.e., increase stiffness) whereas microcracking should marginally increase the compliance (decrease stiffness). Uncracked ligament bridging is seemed to be the predominant toughening mechanism for macroscopic crack propagation. Compliance measurement was not made by indentation method. It cannot be concluded whether compliance was decreased or increased and which of the extrinsic toughening mechanisms took place.

The bone's mineral phase is definitely the stronger and stiffer phase, on the other hand, resistance to fracture is not measured by the features of only single phase a composite material e.g., bone. Principal mechanisms, for absorbing energy are deflection of crack, particularly around osteons and along cement lines, collagen

phase plasticity, diffuse microcracking, and the crack bridging by ductile phases [41]. Therefore, it should be kept in mind that quality of bone is dependent not only to mineralization, but also to the collagen character and the morphological organization of the phases and structures in bone.

This thesis used bovine bones to make an estimate on the effects of non-enzymic glycation as a mechanism of aging on micromechanical properties of bovine bone. Further studies involving human bone are needed to show real effect of NEG. Furthermore, micromechanical properties of human bone could be studied on various bone obtained from people belonging to different age groups.

CHAPTER 6

CONCLUSIONS

1. Widely known methods for measurement of indentation toughness such as Vickers take into consideration the cracks emerging from indent. This method is popular for determining the toughness of hard biological tissues and other biomaterials and since it allows microscale evaluation.
2. Neither applied load nor duration of indentation made a difference in identification of degree of ribosylation but able to differ non-ribosylated specimens from ribosylated specimens.
3. Organic component taking part in the structure of hard tissues makes them softer compared to brittle materials and indentation methods might cause even larger errors. State of hydration (wet or dry) also effects the results of measurements. Dry specimens have higher hardness value which was independent of ribosylation.
4. There is an additional risk of formation of unintended cracking due to sample preparation by dehydration in imaging with SEM.
5. Size of the indentation cover smaller or larger areas which contribute to variation in hardness results.
6. Toughness is essentially a measure of the resistance to crack growth in a material. Methods using indentation technique has difficulty in relating the resistance to crack growth to the Mode I fracture toughness.
7. Indentation fracture toughness methods were not considered as sufficient for studying materials that are having rising *R*-curve behavior. They allow sampling only one point on the *R*-curve.
8. Calculated fracture toughness measured by the indentation method is a function of indentation load. Therefore, the changes cannot be attributed to variations in *H* alone.
9. Indentation fracture method by Vickers indentation in bone is found to be roughly useful for measuring the fracture toughness but less for relative toughness ranking.

10. Bridging by collagen fibers and uncracked ligament was observed as external toughening mechanisms with SEM. It was observed that number of collagen fibers might be reduced by NEG induced aging.

11. Aging and bone diseases can result in abnormal cellular and molecular functions in bone, which in turn causes adverse ultra-structural and micro-structural changes in the tissue and leads to deteriorated bone quality.

CHAPTER 7

REFERENCES

- [1] L.P. Mullins, M.S. Bruzzi, P.E. McHugh, Measurement of the microstructural fracture toughness of cortical bone using indentation fracture, *Journal of Biomechanics*, 40 (2007) 3285-3288.
- [2] R.O. Ritchie, J.H. Kinney, J.J. Kruzic, R.K. Nalla, A fracture mechanics and mechanistic approach to the failure of cortical bone, *Fatigue & Fracture of Engineering Materials & Structures*, 28 (2005) 345-371.
- [3] X.D. Wang, N.S. Masilamani, J.D. Mabrey, M.E. Alder, C.M. Agrawal, Changes in the fracture toughness of bone may not be reflected in its mineral density, porosity, and tensile properties, *Bone*, 23 (1998) 67-72.
- [4] T. Diab, K.W. Condon, D.B. Burr, D. Vashishth, Age-related change in the damage morphology of human cortical bone and its role in bone fragility, *Bone*, 38 (2006) 427-431.
- [5] N.D. Nguyen, H.G. Ahlborg, J.R. Center, J.A. Eisman, T.V. Nguyen, Residual lifetime risk of fractures in women and men, *Journal of Bone and Mineral Research*, 22 (2007) 781-788.
- [6] S.R. Cummings, D. Bates, D.M. Black, Clinical use of bone densitometry: scientific review, *Journal of the American Medical Association*, 288 (2002) 1889-1897.
- [7] J.P. Bilezikian, L.G. Raisz, T.J. Martin, *Principles of Bone Biology*, Academic Press. 2008.

- [8] S. Kaptoge, G. Armbrecht, D. Felsenberg, M. Lunt, T.W. O'Neill, A.J. Silman, J. Reeve, EPOS Study Group, Incidence of vertebral fracture in Europe: results from the European Prospective Osteoporosis Study (EPOS), *Journal of Bone and Mineral Research* 17 (2002) 716-724.
- [9] Türkiye İstatistik Kurumu.
http://www.tuik.gov.tr/VeriBilgi.do?tb_id=6&ust_id=1 (last visited on 04.19.2009).
- [10] Türkiye Osteoporoz Derneği.
http://www.osteoporoz.org.tr/sayfalar/Etkinlikler_BilimselFaaliyetler.asp
(last visited on 04.19.2009).
- [11] O. Johnell, J. Kanis, Epidemiology of osteoporotic fractures, *Osteoporosis International*, 16 (2005) 3-7.
- [12] P. Pietschmann, M. Rauner, W. Sipos, K. Kersch-Schindl, Osteoporosis: an age-related and gender-specific disease, *Gerontology*, 55 (2008) 3-12.
- [13] P. Garnero, P.D. Delmas, Contribution of bone mineral density and bone turnover markers to the estimation of risk of osteoporotic fracture in postmenopausal women, *Journal of Musculoskeletal and Neuronal Interactions*, 4 (2004) 50-63.
- [14] M. Cankurtaran, B.B. Yavuz, M. Halil, N. Dagi, S. Ariogul, General characteristics, clinical features and related factors of osteoporosis in a group of elderly Turkish men, *Aging Clinical and Experimental Research*, 17 (2005) 108-115.
- [15] L.C. Junqueira, J. Carneiro, R.O. Kelley, *Basic Histology*, Mc Graw-Hill, 9th Edition, (1998).

- [16] T.S. Leeson, C.R. Leeson, A.A.W.B. Paparo. Text/Atlas of Histology, Saunders Company, (1988) 183-186.
- [17] N.V. Bhagavan, Medical Biochemistry, Harcourt/Academic Press, 173-178 (2002) 585-590.
- [18] Y.C. Fung, Biomechanics: mechanical properties of living tissues, New York: Springer-Verlag, (1993).
- [19] H. Ehrlich, H. Worch, Collagen, a huge matrix in glass sponge flexible spicules of the meter-long *Hyalonema sieboldi*. In: Bäuerlein E., Behrens. P., Epple. M., Handbook of Biomineralization. Weinheim: Wiley-VCH, (2007).
- [20] A. Veis, Collagen fibrillar structure in mineralized and nonmineralized tissues, Current Opinion in Solid State & Materials Science, 2 (1997) 370-378.
- [21] K.E. Kadler, D.F. Holmes, J.A. Trotter, J.A. Chapman, Collagen fibril formation, Biochemical Journal, 316 (1996) 1–11.
- [22] J. Myllyharju, K.I. Kivirikko, Collagens, modifying enzymes and their mutations in humans, flies and worms, Trends in Genetics, 20 (2004) 33–43.
- [23] R.L. Braddom, R.M. Buschbacher, L. Chan, K.J. Kowalske, E.R. Lawkowski, D.J. Matthews, K.T. Ragnarrson, Physical Medicine & Rehabilitation, Saunders Elsevier, 3rd Edition, (2007) 930.
- [24] C.J. Hernandez, T.M. Keaveny, A biomechanical perspective on bone quality, Bone, 39 (2006) 1173-1181.

- [25] S. Weiner, H.D. Wagner, The material bone: structure mechanical function relations, *Annual Review of Materials Science*, 28 (1998) 271–298.
- [26] Y. Bala, B. Depalle, T. Douillard, S. Meille, P. Clément, H. Follet, J. Chevalier, G. Boivin, Respective roles of organic and mineral components of human cortical bone matrix in micromechanical behavior: An instrumented indentation study, *Journal of the Mechanical Behavior of Biomedical Materials*, 4 (2011) 1473-1482.
- [27] J.-Y. Rho, L. Kuhn-Spearing, P. Zioupos, Mechanical properties and the hierarchical structure of bone, *Medical Engineering & Physics*, 20 (1998) 92-102.
- [28] L. Yin, S. Venkatesan, S. Kalyanasundaram, Q.-H. Qin, Effect of microstructure on micromechanical performance of dry cortical bone tissues, *Materials Characterization*, 60 (2009) 1424-1431.
- [29] P.E. Riches, N.M. Everitt, A.R. Heggie, D.S. McNally, Microhardness anisotropy of lamellar bone, *Journal of Biomechanics*, 30 (1997) 1059-1061.
- [30] W.M. Johnson, A.J. Rapoff, Microindentation in bone: Hardness variation with five independent variables. *Journal of Materials Science: Materials in Medicine*, 18 (2007) 591–597.
- [31] E. Dall’Ara, C. Öhman, M. Baleani, M. Viceconti, The effect of tissue condition and applied load on Vickers hardness of human trabecular bone, *Journal of Biomechanics*, 40 (2007) 3267-3270.

- [32] K.J. Ritchie, S. Koester, W. Ionova, N.E. Yao, J.W. Lane, I.I. Ager, Measurement of the toughness of bone: A tutorial with special reference to small animal studies, *Bone*, 43 (2008) 798-812.
- [33] P. Zioupos, J.D. Currey, Changes in the stiffness, strength, and toughness of human cortical bone with age, *Bone*, 22 (1998) 57-66.
- [34] R.O. Ritchie, J.H. Kinney, J.J. Kruzic, R.K. Nalla, A fracture mechanics and mechanistic approach to the failure of cortical bone, *Fatigue & Fracture of Engineering Materials & Structures*, 28 (2005) 345-371.
- [35] J.J. Kruzic, D.K. Kim, K.J. Koester, R.O. Ritchie, Indentation techniques for evaluating the fracture toughness of biomaterials and hard tissues, *Journal of the Mechanical Behavior of Biomedical Materials*, 2 (2009) 384-395.
- [36] L.P. Mullins, M.S. Bruzzi, P.E. McHugh, Measurement of the microstructural fracture toughness of cortical bone using indentation fracture, *Journal of Biomechanics*, 40 (2007) 3285-3288.
- [37] ASTM E399-90, In: Annual Book of ASTM standards, Vol 03.01: Metals mechanical testing; Elevated and Low temperature tests, Metallography. ASTM, West Conshohocken, Pennsylvania, USA, (2002).
- [38] X. Wang, X. Shen, X. Li, C. Mauli Agrawal, Age-related changes in the collagen network and toughness of bone, *Bone*, 31 (2002) 1-7.
- [39] H.S. Gupta, P. Zioupos, Fracture of bone tissue: The 'hows' and the 'whys', *Medical Engineering & Physics*, 30 (2008) 1209-1226.

- [40] P. Zioupos, Recent developments in the study of failure of solid biomaterials and bone. 'fracture' and 'pre-fracture' toughness, *Materials Science & Engineering C: Biomimetic Materials, Sensors & Systems*, 6 (1998) 33–40.
- [41] Q.D. Yang, B.N. Cox, R.K. Nalla, R.O. Ritchie, Re-evaluating the toughness of human cortical bone, *Bone*, 38 (2006) 878-887.
- [42] N.D. Sahar, S.-I. Hong, D.H. Kohn, Micro- and nano-structural analyses of damage in bone, *Micron*, 36 (2005) 617-629.
- [43] D. Vashishth, J.C. Behiri, W. Bonfield, Crack growth resistance in cortical bone: Concept of microcrack toughening, *Journal of Biomechanics*, 30 (1997) 763-769.
- [44] R.K. Nalla, J.J. Kruzic, R.O. Ritchie, On the origin of the toughness of mineralized tissue: microcracking or crack bridging?, *Bone*, 34 (2004) 790-798.
- [45] P. Braidotti, E. Bemporad, T. D'Alessio, S.A. Sciuto, L. Stagni, Tensile experiments and SEM fractography on bovine subchondral bone, *Journal of Biomechanics*, 33 (2000) 1153-1157.
- [46] L.P. Hiller, S.M. Stover, V.A. Gibson, J.C. Gibeling, C.S. Prater, S.J. Hazelwood, O.C. Yeh, R.B. Martin, Osteon pullout in the equine third metacarpal bone: Effects of ex-vivo fatigue, *Journal of Orthopaedic Research*, 21 (2003) 481–488.
- [47] R.K. Nalla, J.J. Kruzic, J.H. Kinney, R.O. Ritchie, Mechanistic aspects of fracture and R-curve behavior in human cortical bone, *Biomaterials*, 26 (2005) 217-231.

- [48] R.K. Nalla, J.S. Stölken, J.H. Kinney, R.O. Ritchie, Fracture in human cortical bone: local fracture criteria and toughening mechanisms, *Journal of Biomechanics*, 38 (2005) 1517-1525.
- [49] D. Vashishth, Hierarchy of bone microdamage at multiple length scales, *International Journal of Fatigue*, 29 (2007) 1024-1033.
- [50] D. Vashishth, K.E. Tanner, W. Bonfield, Contribution, development and morphology of microcracking in cortical bone during crack propagation, *Journal of Biomechanics*, 33 (2000) 1169-1174.
- [51] P.-C. Wu, D. Vashishth, Age related changes in cortical bone toughness: initiation vs. propagation. 2nd Joint EMBS/BMES Conference, vol. 1. Houston, TX7 IEEE; (2002) 425-426.
- [52] R.K. Nalla, J.J. Kruzic, J.H. Kinney, R.O. Ritchie, Effect of aging on the toughness of human cortical bone: evaluation by R-curves, *Bone*, 35 (2004) 1240-1246.
- [53] R.K. Nalla, J.J. Kruzic, J.H. Kinney, M. Balooch, J.W. Ager III, R.O. Ritchie, Role of microstructure in the aging-related deterioration of the toughness of human cortical bone, *Materials Science and Engineering C*, 26 (2006) 1251-1260.
- [54] X.D. Wang, N.S. Masilamani, J.D. Mabrey, M.E. Alder, C.M. Agrawal, Changes in the fracture toughness of bone may not be reflected in its mineral density, porosity, and tensile properties, *Bone*, 23 (1998) 67-72.
- [55] T. Siegmund, M.R. Allen, D.B. Burr, Failure of mineralized collagen fibrils: Modeling the role of collagen cross-linking, *Journal of Biomechanics*, 41 (2008) 1427-1435.

- [56] J.S. Nyman, M. Reyes, X. Wang, Effect of ultrastructural changes on the toughness of bone, *Micron*, 36 (2005) 566-582.
- [57] S.Y. Tang, U. Zeenath, D. Vashishth, Effects of non-enzymatic glycation on cancellous bone fragility, *Bone*, 40 (2007) 1144-1151.
- [58] D. Vashishth, G.J. Gibson, J.I. Khoury, M.B. Schaffler, J. Kimura, D.P. Fyhrie, Influence of nonenzymatic glycation on biomechanical properties of cortical bone, *Bone*, 28 (2001) 195-201.
- [59] D.B. Burr, The contribution of the organic matrix to bone's material properties, *Bone*, 31 (2002) 8-11.
- [60] S.Y. Tang, D. Vashishth, The relative contributions of non-enzymatic glycation and cortical porosity on the fracture toughness of aging bone, *Journal of Biomechanics*, 44 (2011) 330-336.
- [61] J.S. Nyman, A. Roy, R.L. Acuna, H.J. Gayle, M.J. Reyes, J.H. Tyler, D.D. Dean, X. Wang, Age-related effect on the concentration of collagen crosslinks in human osteonal and interstitial bone tissue, *Bone*, 39 (2006) 1210-1217.
- [62] H. Yamada, *Strength of Biological Materials*. In: Evans, F.G., Ed. Baltimore, MD: William & Wilkins, (1970) 20.
- [63] W. Bonfield, J.C. Behiri, Fracture toughness of natural composites with reference to cortical bone. In: Friedrich K., Ed. *Application of Fracture Mechanics to Composite Materials*. Amsterdam: Elsevier Science, (1989) 615-635.

- [64] T.L. Norman, S.V. Nivargikar, D.B. Burr, Resistance to crack growth in human cortical bone is greater in shear than in tension, *Journal of Biomechanics*, 29 (1996) 1023–1031.
- [65] L.J. Dominguez, M. Barbagallo, L. Moro, Collagen overglycosylation: A biochemical feature that may contribute to bone quality, *Biochemical and Biophysical Research Communications*, 330 (2005) 1-4.
- [66] S.Y. Tang, A.D. Sharan, D. Vashishth, Effects of collagen crosslinking on tissue fragility, *Clinical Biomechanics*, 23 (2008) 122-123.
- [67] L. Knott, A.J. Bailey, Collagen cross-links in mineralizing tissues: A review of their chemistry, function, and clinical relevance, *Bone*, 22 (1998) 181-187.
- [68] J. III. Catanese, R.A. Bank, J.M. TeKoppele, T.M. Keaveny, Increased crosslinking by non-enzymatic glycation reduces the ductility of bone and bone collagen, *ASME Bioengineering Conference*, 42 (1999) 267–268.
- [69] ASTM E384-99, Standard Test Method for Microindentation Hardness of Materials. <http://www.astm.org/DATABASE.CART/HISTORICAL/E384-99.htm>, (last visited 03.04.2012).
- [70] ASTM D790 – 10 Standard Test Methods for Flexural Properties of Unreinforced and Reinforced Plastics and Electrical Insulating Materials. <http://www.astm.org/Standards/D790.htm>, (last visited 03.04.2012).
- [71] J.Y. Rho, G.M. Pharr, Effects of drying on the mechanical properties of bovine femur measured by nanoindentation, *Journal of Materials Science: Materials in Medicine*, 10 (1999) 485-488.

- [72] L.P. Mullins, M.S. Bruzzi, P.E. McHugh, Authors' Response to 'Comments on 'measurement of the microstructural fracture toughness of cortical bone using indentation fracture'', *Journal of Biomechanics*, 41 (2008) 2602–2603.

CURRICULUM VITAE

GÜLİN FINDIKOĞLU

Contact information:

University of Pamukkale
Department of Physical Medicine and Rehabilitation
Denizli, 21100, Turkey
Tel: 090-258-2118129 (work)
Fax: 090-258-2118129
E-mail: gulinfdk@gmail.com, gulin_f@yahoo.com

Education:

Degree	Department	University	Year
Doctor Of Medicine	Faculty of Medicine	University of Hacettepe, Turkey	1999
Specialist	Physical Medicine and Rehabilitation	SB Ankara Eğitim ve Araştırma Hastanesi, Turkey	2005
Ph.D.	Engineering Science	Middle East Technical University, Turkey	2012

Academic positions:

Position	Department, University	Year
Research Assistant	1 st Physical Medicine and Rehabilitation Clinic, SB Ankara Eğitim ve Araştırma Hastanesi	2001-2005
Specialist	Physical Medicine and Rehabilitation Clinic, Çankırı Devlet Hastanesi	2005-2007
Instructor	Department Physical Medicine and Rehabilitation, University of Pamukkale	2007-2008
Assist. Prof. Dr.	Department Physical Medicine and Rehabilitation, University of Pamukkale	2008-.....

PUBLICATIONS

Journal Articles (SCI, SCI EXP):

1. **G. Findikoglu**, B. Gunduz, H. Uzun, B. Erhan, S. Rota, F. Ardic, Investigation of cartilage degradation in patients with spinal cord injury by CTX-II, *Spinal Cord*, 50(2) (2012) 136-1340.
2. G. Günkut, F. Ardic, **G. Findikoğlu**, S. Rota, The effect of mud pack therapy on serum YKL-40 and hsCRP levels in patients with knee osteoarthritis, *Rheumatology International*, 32(5) (2012) 1235-1244.
3. A. Goren, N. Yildiz, O. Topuz, **G. Findikoglu**, Ardic. F, Efficacy of exercise and ultrasound in patients with lumbar spinal stenosis: a prospective randomized controlled trial, *Clinical Rehabilitation*, 24(7) (2010) 623-631. (doi:10.1177/0269215510367539)
4. S. Deniz, O. Topuz, N.S. Atalay, A. Sarsan, N. Yildiz, **G Findikoglu**, O Karaca, F Ardic, Comparison of the Effectiveness of Pulsed and Continuous Diclofenac Phonophoresis in Treatment of Knee Osteoarthritis, *Journal of Physical Therapy Science*, 21(4) (2009) 331-336.
5. F. Ardic, Y. Kahraman, M. Kacar, C. Mehmet, **G. Findikoglu**, Z.R. Yorgancioglu, The relationship between clinical, functional and radiological findings in shoulder impingement syndrome, *American Journal of Physical Medicine & Rehabilitation*, 85(1) (2006) 53-60.
6. F. Gökoğlu, **G. Findikoğlu**, Z. Yorgancioglu, M. Okumuş, E.Ceceli, S. Kocaoğlu, Evaluation of iontophoresis and local corticosteroid injection in treatment of carpal tunnel syndrome, *American Journal of Physical Medicine & Rehabilitation*, 84(2) (2005) 92-96.

Journal Articles Published in Other Indexes:

1. **G. Findikoğlu**, U. Alemdaroğlu, Y. Köklü, F. Ünver Koçak, A.E. Erol, Isokinetic Analysis Of Hamstrings And Quadriceps Muscles In Turkish Second Division Basketball Player, *Ovidius University Annals, Series Physical Education And Sport Science, Movement And Health*, 11(1) (2011) 5-7.
2. **G. Findikoğlu**, E. Ceceli, Z.R. Yorgancioglu, Y. Demir, Geriatrik ve orta yaşlı kadınlarda farklı tip egzersizlere kardiyak otonom cevap: Yaşlılarda egzersiz fiziolojisi, *Turkish Journal of Geriatrics*; 9(1) (2006) 8-12.

Journal Articles Published in National Journals With Peer Review:

1. S. Akkaya, N. Akkaya, N. Yıldız, N.Ş. Atalay, **G. Fındıkoğlu**, A. Sarsan, F. Şahin, Plantar Topuk Ağrısında Muayene Bulguları Ve Fonksiyonel Durumun Radyolojik Ve Klinik Değişkenlerle İlişkisi, Romatoloji ve Tıbbi Rehabilitasyon Dergisi, 21(1) (2010)1-10.
2. N. Yıldız, N. Çatalbaş, N. Akkaya, **G. Fındıkoğlu**, O. Topuz, Omurilik Yaralanmalı Hastalarda idrar Yolu Enfeksiyonu ile ilişkili Faktörler, FTR Bil Der (J PMR Sci), 13, (2010)41-78.
3. N. Akkaya, S. Akkaya, N.Ş. Atalay, N. Yıldız, **G. Fındıkoğlu**, A. Sarsan, Şahin F, Menisküs Lezyonu Tanısında Fizik Muayene Bulgularının Manyetik Rezonans Görüntüleme Bulguları Ve Fonksiyonel Durum İle İlişkisinin Retrospektif İncelenmesi, Romatoloji ve Tıbbi Rehabilitasyon Dergisi, (2009) 20(4), 126-131.
4. F. Gökoğlu, **G. Fındıkoğlu**, N. Üstün, Z.R. Yorgancıoğlu, Generalize osteoartrit hastalarında sauna ve stanger bath (hidroelektrik banyo) tedavisinin karşılaştırılması, FTR Bilimleri Dergisi (J PMR Sci), 1 (2008) 1-7.
5. **G. Fındıkoğlu**, E. Ceceli, Z.R. Yorgancıoğlu, Y. Demir, Geriatrik ve orta yaşlı kadınlarda farklı tip egzersizlere kardiyak otonom cevap: Yaşlılarda egzersiz fizyolojisi, Turkish Journal of Geriatrics 9(1) (2006) 8-12.
6. F. Ardiç, M. Köybaşı, **G. Fındıkoğlu**, Z.R. Yorgancıoğlu, Derleme: Romatoid artrit patogenezinde T hücrelerinin rolü, Fiziksel Tıp Dergisi, 8(3) (2005) 173-178.
7. F. Ardiç, **G. Fındıkoğlu**, M. Köybaşı, Z.R. Yorgancıoğlu, Derleme: Romatoid artritte biyolojik tedaviler, Fiziksel Tıp Dergisi, 8(1) (2005) 59-61.
8. **G. Fındıkoğlu**, Z.R. Yorgancıoğlu, Fiziksel Tıp Dergisi, Derleme: Kas iskelet sistemi ve kardiovasküler otonom fonksiyonlar, 7(3) (2004) 151-155.
9. F. Ardiç, Z.R. Yorgancıoğlu, Y. Kahraman, **G. Fındıkoğlu**, Artrogripozisde değerlendirme ve rehabilitatif yaklaşım, Acta Rheumatologica Turcica, 18(2), (2003) 65-69.

Conference Presentations:

1. **G. Fındıkoğlu**, B. Gündüz, H. Uzun, B. Erhan, S. Rota, F. Ardiç, Spinal kord yaralanmalı hastalarda kıkırdak yıkımının CTX-II düzeyi ile belirlenmesi, S-024, 23rd National Congress of Physical Medicine and Rehabilitation, Antalya,Turkey, 2011.

2. **G. Fındıkoğlu**, A. Özlü, E. Toprak, F. Ardıç, Obez hastalarda kombine aerobik ve progresif dirençli egzersizlerin aerobik kapasite üzerine etkisi, P-200, 23rd National Congress of Physical Medicine and Rehabilitation Antalya, Turkey, 2011.
3. **G. Fındıkoğlu**, A. Özlü, E. Toprak, F. Ardıç. Obez hastalarda kombine aerobik ve progresif dirençli egzersizlerin vücut kompozisyonu üzerine etkisi, P-201, 23rd National Congress of Physical Medicine and Rehabilitation Antalya, Turkey, 2011.
4. **G. Fındıkoğlu**, E.N. Çetin, A. Sarsan, C. Yıldırım, F. Ardıç, Genç sağlıklı erişkinlerde tek termal kaplıca seansının göz içi basıncına etkileri, P-207. 23rd National Congress of Physical Medicine and Rehabilitation, Antalya, Turkey, 2011.
5. H. Alkan, N. Yıldız, A. Sarsan, N. Akaya, **G. Fındıkoğlu**, O. Topuz, F. Ardıç, Altmışbeş yaş üstü bireylerde postürografik düşme riski ile klinik denge testleri arasındaki ilişki, P-220, 23rd National Congress of Physical Medicine and Rehabilitation Antalya, Turkey, 2011.
6. **G. Fındıkoğlu**, N. Akaya, B. Çırak, N. Sabir, F. Şahin, Spontan Odontoid fraktürü olan romatoid artritli bir olgu sunumu, P-321, 23rd National Congress of Physical Medicine and Rehabilitation, Antalya, Turkey, 2011.
7. N. Akaya, **G. Fındıkoğlu**, S. Akaya, U. Alemdaroğlu, Posturografi ile yüksek düşme riski saptanan Marfan Sendromlu Basketbol Oyuncusu, P-358, 23rd National Congress of Physical Medicine and Rehabilitation, Antalya, 2011.
8. N. Akkaya, S. Akkaya, N. Atalay Şimşir, H. Alkan, **G. Fındıkoğlu**, A. Ardıç, Alt ekstremité amputasyonu olan hastalarımızda fonksiyonel durum ve yaşam kalitesi, P-104, 23rd National Congress of Physical Medicine and Rehabilitation, Antalya, 2011.
9. **G. Fındıkoğlu**, A. Özlü, E. Kılıç Toprak, F. Ardıç, Effect of combined aerobic and progressive resistive exercise on aerobic capacities of obese people, Turkish-FEPS (Federation of European Physiological Societies) Physiology Congress, İstanbul, Turkey, 2011.
10. **G. Fındıkoğlu**, A. Özlü, E. Kılıç Toprak, F. Ardıç, Effect of combined aerobic and progressive resistive exercise on body composition of obese people, Turkish-FEPS (Federation of European Physiological Societies) Physiology Congress, İstanbul, Turkey, 2011.
11. Ö. Ercidoğan, **G. Fındıkoğlu**, H. Alkan, H. Akca, O. Topuz, Yaşlı osteoporozlu kadınlarda D vitamini eksikliğinin kas kuvveti üzerine etkisi, PP:36, 4th National Osteoporosis Congress, Antalya, Turkey, 2011.

12. U. Alemdarođlu, Y. Kkl, **G. Fındıkođlu**, F. nver Koçak, E. Erol, Isokinetic analysis of hamstrings and quadriceps muscles in Turkish first division basketball players, The Wingate Congress of Exercise and Sport Sciences, Netenya, Israel, 2010.
13. **G. Fındıkođlu**, U. Alemdarođlu, Y. Kkl, F. nver Koçak, E. Erol, Isokinetic analysis of hamstrings and quadriceps muscles in Turkish second division basketball players, 10th Annual International Scientific Conference Perspectives In Physical Education and Sport, Constanta,Romania, 2010.
14. **G. Fındıkođlu**, Z. Evis, Enzimatik olmayan glikasyon ile deđiřtirilen kemik mikro yapısının mikrosertlik zerine etkisi, PS:51, 5th National Biomechanical Congress, İzmir, Turkey, 2010.
15. N. Akkaya, S. Akkaya, N. Atalay, N. Yıldız, **G. Fındıkođlu**, A. Sarsan, F. řahin, Menisks yırtıđı tanısında fizik muayene bulgularının manyetik rezonans grntleme ve fonksiyonel durum ile iliřkisi, PS: 82, 4th Turkish Rheumatology Congress, Antalya, Turkey, 2010.
16. N. Akkaya, S. Akkaya, N. řimřir Atalay, A. Sarsan, N. Yıldız, **G. Fındıkođlu**, F. řahin, Plantar topuk ađrısında muayene bulguları ve fonksiyonel durumun radyolojik ve klinik deđiřkenlerle iliřkisi, PS:5, 4th Turkish Rheumatology Congress, Antalya, Turkey, 2010.
17. **G. Fındıkođlu**, O. Ercidogan, E. Nevin Cetin, O. Topuz, F. Ardic, Harlequin face in a patient with spinal cord injury, P:1164, 5th International Society of Physical Medicine and Rehabilitation Medicine, Istanbul, Turkey, 2009.
18. E. řanal, F. Ardiç, S. Kırac, A. Sarsan, N. Yıldız, N. řimřir Atalay, O. Topuz, **G. Fındıkođlu**, Differences between men and women in response to aerobic and combined aerobic resistance training, P: 1052, 5th World Congress of the International Society of Physical Medicine and Rehabilitation, Istanbul, Turkey, 2009.
19. G. Odemis Gungen, F. Ardic, S. Rota, N. Yildiz, A. Sarsan, N. Simsir Atalay, O. Topuz, **G. Fındıkođlu**, Effects of mud compress on serum levels of YKL-40 and hsCRP in patients with knee osteoarthritis, P: 0740, 5th World Congress of the International Society of Physical Medicine and Rehabilitation, Istanbul, Turkey, 2009.
20. S. Deniz, O. Topuz, A. Sarsan, N. Yildiz, N. řimřir Atalay, **G. Fındıkođlu**, F. Ardic, Comparison of the effectiveness of pulsed and continuous diclofenac phonophoresis treatment in knee osteoarthritis, P: 0728, 5th World Congress of the International Society of Physical and Rehabilitation Medicine, Istanbul, Turkey, 2009.

21. **G. Fındıkoğlu**, Z.R. Yorgancıoğlu, Herediter sensorial ve otonomik nöropatili (HSAN) vakalara rehabilitasyon yaklaşımı, PA:103, 21st National Congress of Physical Medicine and Rehabilitation, Antalya, Turkey, 2007.
22. **G. Fındıkoğlu**, Z.R. Yorgancıoğlu, E. Ceceli, M. Sani, C. Çulha, Koroner arter hastalığı riski taşıyan bayanlarda farklı üst ekstremitelerde egzersizlerine kardiyak otonom cevap, SS-16, 20th National Congress of Physical Medicine and Rehabilitation, Bodrum, Turkey, 2005.
23. **G. Fındıkoğlu**, Z.R. Yorgancıoğlu, F. Gökoğlu, S. Kocaoğlu, M. Yılmaz, Normal ve obez postmenopozal kadınlarda vücut kitle indeksi ve kemik mineral yoğunluğu ilişkisi, PS:226, 20th National Congress of Physical Medicine and Rehabilitation, Bodrum, Turkey, 2005.
24. S. Kocaoğlu, Z.R. Yorgancıoğlu, **G. Fındıkoğlu**, E. Ceceli, M. Yılmaz, M. Okumuş, F. Gökoğlu, Geriatrik hastalarda osteoporoz, PS:210, 20th National Congress of Physical Medicine and Rehabilitation, Bodrum, Turkey, 2005.
25. F. Ardiç, E. Şensoy, B. Tönük, **G. Fındıkoğlu**, Z.R. Yorgancıoğlu, Atipik göğüs ağrılı hastalarda kardiyovasküler egzersiz tolerans testi sonuçlarının analizi, PS:120, 20th National Congress of Physical Medicine and Rehabilitation, Bodrum, Turkey, 2005.
26. M. Okumuş, Z.R. Yorgancıoğlu, **G. Fındıkoğlu**, N. Üstün, E. Ceceli, Kocaoğlu S, Gökoğlu F, Tönük B, Geriatrik hastalarda postür analizi, PS:051, 20th National Congress of Physical Medicine and Rehabilitation, Bodrum, Turkey, 2005.
27. **G. Fındıkoğlu**, E. Ceceli, Z.R. Yorgancıoğlu, Y. Demir, Geriatrik ve orta yaşlı kadınlarda istirahat sonrası kardiyak otonom fonksiyonların karşılaştırılması, P:33, Geriatri 2005, "Multidisciplinary Approach to Elderly", İstanbul, Turkey, 2005.
28. **G. Fındıkoğlu**, Z.R. Yorgancıoğlu, E. Ceceli, E. Demir, Cardiac autonomic responses before and after isometric exercise in obese women, 7th German-Turkish Meeting for Rheumatology and Rehabilitation with International Participation, Antalya, Turkey, 2005.
29. S. Kocaoğlu, **G. Fındıkoğlu**, E. Ceceli, F. Gökoğlu, M. Okumuş, Z.R. Yorgancıoğlu, Osteoporosis and epidemiological factors, 5th International Mediterranean Congress of Physical&Rehabilitation Medicine, Antalya, Turkey, No: PP 099, 2004.
30. S. Kocaoğlu, **G. Fındıkoğlu**, E. Ceceli, M. Okumuş, F. Gökoğlu, Z.R. Yorgancıoğlu, Medical therapy of osteoporosis, 5th International Mediterranean Congress of Physical&Rehabilitation Medicine, Antalya Turkey, No: PP 098, 2004.

31. F. Gökođlu, R.Z. Yorgancıođlu, N. Üstün, **G. Fındıkođlu**, Evaluation of hand strength and functional ability in patients with generalised osteoarthritis, *Annals of The Rheumatic Diseases* Volume: 62, Pages:260, Supplement: Suppl, 1 EULAR ,2003.
32. M. Okumuş, Z.R. Yorgancıođlu, N. Üstün, **G. Fındıkođlu**, F. Gökođlu, Osteoporozlu hastalarda ađrı analizi P:222, 19th National Congress of Physical Medicine and Rehabilitation, Antalya, Turkey, 2003.
33. F. Gökođlu, Z.R. Yorgancıođlu, **G. Fındıkođlu**, M. Okumuş, Karpal Tünel Sendromlu hastalarda enjeksiyon ve iontoforez tedavisinin etkinliđinin karşılaştırılması, TP:44, 19th National Congress of Physical Medicine and Rehabilitation, Antalya, Turkey, 2003.
34. S. Kocaođlu, **G. Fındıkođlu**, B. Şensoy, F. Soyupek, Z.R. Yorgancıođlu, Diz osteoartritli hastalarda uygulanan intra-artiküler hyalüranik asit enjeksiyonlarının sonuçları, P:206, 19th National Congress of Physical Medicine and Rehabilitation, Antalya, Turkey, 2003.
35. F. Gökođlu, Z.R. Yorgancıođlu, **G. Fındıkođlu**, N. Üstün, Generalize osteoartritli hastalarda sauna ve stangerbat tedavisinin karşılaştırılması, 5th National Balneotherapy Congress, Gönen, Turkey, 2002.